International Journal of Coal Science & Technology (2024) 11:47
https://doi.org/10.1007/s40789-024-00690-0

RESEARCH

Geochemistry of Cenozoic coals from Sarawak Basin, Malaysia: implications for paleoclimate, depositional conditions, and controls on petroleum potential

Lanre Asiwaju[1] · Khairul Azlan Mustapha[1] · Wan Hasiah Abdullah[2] · Say Gee Sia[3] · Mohammed Hail Hakimi[4]

Received: 4 April 2023 / Revised: 4 August 2023 / Accepted: 28 March 2024

Abstract
Forty Tertiary coals from Mukah-Balingian and Merit-Pila coalfields of the Sarawak Basin, Malaysia were investigated using bulk and molecular geochemical techniques such as proximate analysis, gas chromatography-mass spectrometry, elemental analyser, isotope ratio mass spectrometry, and inductively coupled plasma mass spectrometry to reconstruct their paleovegetation, paleoclimate, and environments of deposition. In addition, principal component analysis (PCA) of selected geochemical parameters was carried out to determine the controlling influences on the petroleum potential of the humic coals. $\delta^{13}C$ values and the abundance of terpenoids imply the predominant contribution of angiosperms to the paleoflora. Bimetal proxies (Sr/Ba, Sr/Cu, and C-value), and δD values are generally suggestive of a warm and humid climate during the accumulation of the paleopeats. However, *n*-alkane proxies (P_{wax}, P_{aq}, n-C_{23}/n-C_{29}, etc.) and polycyclic aromatic hydrocarbons (PAHs) distribution suggest that Balingian coals accumulated under relatively drier and strongly seasonal paleoclimate in the Late Pliocene. When compared with published global average abundances, the investigated coals are mostly depleted in major oxides and trace elements, suggesting peat accumulation in freshwater-influenced environments. Nonetheless, higher (> 0.5 wt%) total sulfur content in some Mukah-Balingian coals suggests some degree of epigenetic marine influence. Furthermore, the low to moderately-high ash contents of the Sarawak Basin coals indicate the presence of ombrotrophic and rheotrophic peat deposits. PCA result of selected geochemical proxies suggests that source input, paleoflora, and marine incursions are not major controlling influences on the petroleum potential. However, climatic, and depositional conditions appear to slightly influence the petroleum potential of the studied humic coals.

Keywords Humic coal · Sarawak Basin · Paleoclimate · Paleoflora · Depositional environment · Petroleum potential

1 Introduction

A significant number of oil-prone coal-bearing sequences are found in Australasia and Southeast Asia (Isaksen et al. 1998), and according to Macgregor (1994), these coal-bearing sequences can be classified into two broad paleoclimatic and paleobotanical associations: Tertiary tropical coals and Late Jurassic-Eocene coals. The first group is dominated by coal-bearing basins in Southeast Asia countries, which were reportedly supported by the tropical ever-wet climate in the Tertiary (Macgregor 1994; Thompson et al. 1994). Additionally, a recent review by Friederich et al. (2016) concluded that the combination of humid paleoclimate, depositional settings suitable for peat accumulation, and tectonics settings suitable for the development of extensive basins resulted in the formation of the extensive Cenozoic coal deposits in Indonesia and Malaysia.

Malaysia's Sarawak Basin contains large amounts of low-rank Tertiary coals with excellent petroleum potential (Kiat et al. 1987; Johari et al. 1994; Abdullah 1997; Sia and Abdullah 2012; Hakimi et al. 2013; Sia et al. 2014). This study, however, examines the Balingian Formation and

✉ Khairul Azlan Mustapha
azlan_0401@um.edu.my

1 Department of Geology, Faculty of Science, University of Malaya, 50603 Kuala Lumpur, Malaysia

2 Geological Society of Malaysia, C/O Department of Geology, University of Malaya, 50603 Kuala Lumpur, Malaysia

3 Department of Mineral and Geoscience, Malaysia, 80000 Johor Bahru, Malaysia

4 Geology Department, Faculty of Applied Science, Taiz University, 6803, Taiz, Yemen

Published online: 04 June 2024

Liang Formation coals from the Mukah-Balingian coalfield, and Nyalau Formation coals from the Merit-Pila coalfield (Fig. 1). The Liang Formation, Balingian Formation, and Nyalau Formation coals are commonly referred to as Balingian, Mukah, and Merit-Pila coals, respectively. Whilst no commercial accumulation of petroleum has been discovered onshore, petroleum is currently produced in the offshore areas of the Sarawak Basin and the source rocks are hosted in formations that consist of coals, fluvial and estuarine channel sands, and clays of tidal and coastal plain deposits (Madon and Abolins 1999; Amir Hassan et al. 2017). Furthermore, geochemical analysis of crude oils from offshore Sabah and Sarawak has established that the oils were derived from mature terrigenous source rocks that were deposited in the peatlands environment (Awang Jamil et al. 1991).

Paleoenvironmental interpretations of the Sarawak coal deposits have mostly been based on their petrographic composition (Sia and Abdullah 2012; Sia et al. 2014; Murtaza et al. 2018; Zainal Abidin et al. 2022). However, interpretations based on the exclusive use of petrographic composition can be misleading due to oversimplifications (Moore and Shearer 2003; Sen et al. 2016). This study, therefore, characterizes coals from Mukah-Balingian and Merit-Pila coalfields of the Sarawak Basin using geochemical techniques such as total organic carbon and total sulphur analysis, proximate analysis, elemental analyser isotope ratio mass spectrometry (EA-IRMS), inductively coupled plasma mass spectrometry (ICP-MS), and gas chromatography-mass spectrometry (GC–MS). The obtained analytical results are applied to reconstruct the paleovegetation, paleoclimate and paleodepositional conditions of the Sarawak Basin. Additionally, using statistical analysis techniques, we assess and determine the geochemical controls on the petroleum potential of the coals.

2 Geological setting

The Sarawak Basin is one of Malaysia's prolific hydrocarbon-producing basins, accounting for 80% of coal resources, 23% of known oil reserves, and 51% of its proven natural gas reserves (Madon 1999b). The Basin, which forms the southern margin of the Oligocene-Recent South China Sea, was initiated as a foreland basin and thereafter developed into a passive continental margin (Madon 1999a, b). The development of the Sarawak Basin started in the Late Oligocene and has undergone phases of rifting and sea-floor spreading, evolving from deep foreland basin phase pre-Oligocene to shallow marine shelf progradation phase from post-Oligocene to the present day (Mat-Zin and Swarbrick 1997; Madon et al. 2013). According to Ho (1978), the entire sedimentary succession in Sarawak Basin consists of eight sedimentary cycles that are separated by regressive sequences. Furthermore, seven structural-stratigraphic provinces have been identified in the Sarawak Basin, namely SW Sarawak, Tatau, Balingian, Tinjar, Central Luconia, West Luconia, and North Luconia (Madon 1999a). The onshore Sarawak Basin can also be classified into three zones based on tectonostratigraphic history: Miri, Sibu, and Kuching Zones (Madon 1999b). Detailed information on the tectonic evolution of the Sarawak Basin is provided by Mat-Zin and Swarbrick (1997), Madon (1999a), Mat-Zin and

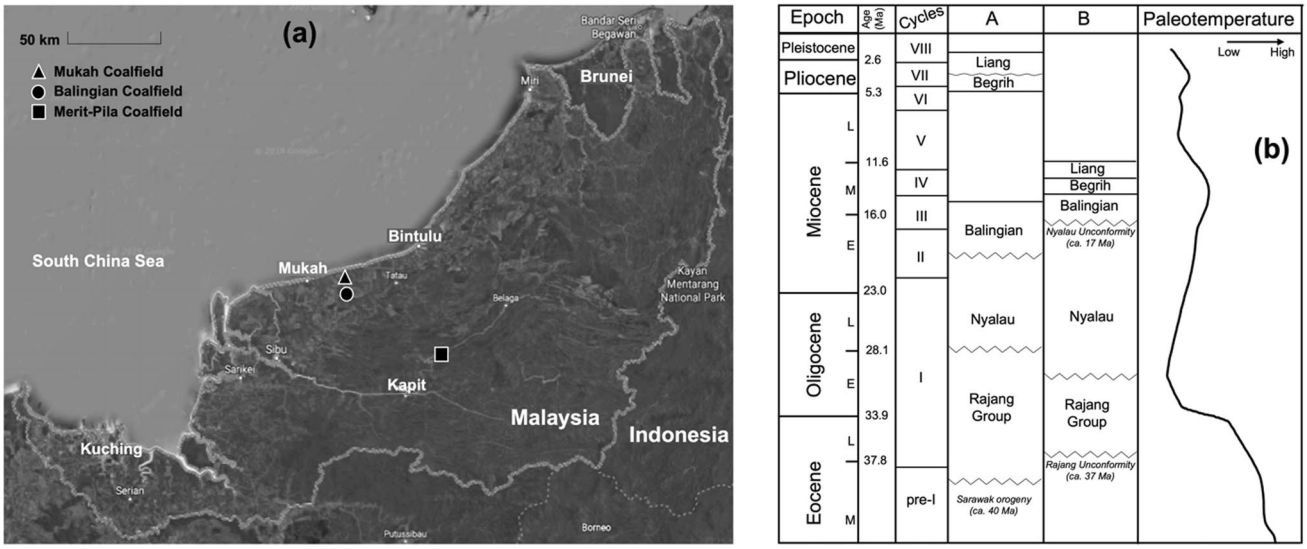

Fig. 1 **a** Regional satellite image showing the location of study areas in onshore Sarawak Basin, and **b** Simplified stratigraphic framework of Mukah-Balingian and Merit-Pila coalfields (after A: Hageman 1987; Madon 1999a; Murtaza et al. 2018; this research, and B: Hennig-Breitfeld et al. 2019)

Tucker (1999), and Lunt and Madon (2017). In addition, recent studies by Hennig-Breitfeld et al. (2019), Breitfeld et al. (2020), and Lunt (2020) offer new viewpoints on the stratigraphy of the Basin.

3 Materials and methods

A total of forty coal samples from the Sarawak Basin were analysed in this study. Fourteen samples are from the Balingian coalfield, six samples from the Mukah coalfield, and twenty samples from the Merit-Pila coalfield.

3.1 Proximate analysis

Proximate analysis was carried out on all forty coal samples to determine their moisture, volatile matter, fixed carbon and ash contents using a PerkinElmer Diamond Thermogravimetric/Differential Thermal Analyzer (TG/DTA) at the organic geochemistry laboratory of the Department of Geology, University of Malaya, Kuala-Lumpur, Malaysia. Approximately, 5–10 mg of the powdered coal samples were heated to 900 °C in the presence of nitrogen. The analytical procedure is described by Donahue and Rais (2009). The temperature was programmed to start at 25 °C, increased to 110 °C at the rate of 85 °C/min and then held at 110 °C for 6 min. Successively, the temperature was increased from 110 to 900 °C at the rate of 80 °C/min and then held for 5 min at 900 °C. Following Donahue and Rais (2009), the instrument software was employed to determine the percentages of moisture, volatile matter and fixed carbon whilst the ash content was obtained by subtracting the sum percentages of moisture, volatile matter and fixed carbon from 100%.

3.2 Total organic carbon and sulfur analyses

Forty coal samples were analysed to determine the total organic carbon (TOC) and total sulfur (S_T) contents. Before the analysis, the powdered coal samples were treated with sufficient 4 M hydrochloric acid to remove carbonates, rinsed with deionized water to remove residual acid, oven-dried at a temperature of 65 °C, and subsequently analysed using a Leco CS832 Carbon–Sulfur analyser at organic geochemistry laboratory of the Department of Geology, University of Malaya, Kuala-Lumpur, Malaysia.

3.3 Inductively coupled plasma mass spectrometry

Twenty-three coal samples were analysed for eleven major and fifty-three trace element concentrations at the Mineral Laboratories of Bureau Veritas (AcmeLabs), Vancouver, Canada. For trace element analysis, 0.5 g of the powdered samples were digested with a modified aqua regia mixture of HCl, HNO_3, and H_2O (1:1:1 v/v/v) and thereafter analysed for 37 elements using inductively coupled plasma mass spectrometry (ICP-MS). To measure the abundances of major element oxides, 5 g of the pulverized samples were dissolved with the lithium borate fusion technique and subsequently investigated with ICP-MS analysis. Analysis of reference materials (DS11 and OREAS262) and duplicate samples were carried out to ensure optimal working conditions and accurate results.

3.4 Elemental analyser-isotope ratio mass spectrometry

Elemental analyser isotope ratio mass spectrometry (EA-IRMS) analysis was performed on twenty-one samples using a flash Elemental Analyzer linked to a Sercon Geo 20-20 continuous flow mass spectrometer. Before analysis, the samples were oven-dried and thereafter stored in a desiccator. The dried samples were finally weighed and wrapped in tin capsules. The reference material, pure Graphite with a carbon isotopic ($\delta^{13}C$) value of $-15.99‰$ on the Vienna Pee Dee Belemnite (VPDB) scale, was used to calibrate the system. The carbon isotopic ratios were measured in triplicates and the average $\delta^{13}C$ values were reported. For hydrogen isotope measurements, the samples were analysed in duplicates and the mean hydrogen isotopic (δD) values were recorded. A reference standard material, polyethylene with a δD value of 100.30‰, was used to calibrate the system. All bulk isotopic measurements were carried out at the Department of Chemistry, Malaysia. The standard deviation of replicate measurements is $<0.3‰$ and $\pm 2‰$ for $\delta^{13}C$ and δD values, respectively.

3.5 Bitumen extraction, hydrocarbon fractionation, and mass spectrometry

All forty samples were extracted with 250 mL of an azeotropic mixture of dichloromethane (DCM) and methanol (93:7, v/v) in a Soxhlet apparatus for a minimum of 72 h. Liquid column chromatography was thereafter employed to fractionate aliquots of the coal extracts into aliphatic, aromatic and polar fractions by using solvents of increasing polarity; petroleum ether (100 mL), DCM (100 mL) and methanol (50 mL), respectively. The aliphatic and aromatic hydrocarbon fractions were further analysed using an Agilent 5890 gas chromatograph coupled to an Agilent 5975B mass selective detector set at electron ionisation energy of 70 eV, 100 mA filament emission current and 230 °C source temperature. The gas chromatograph (GC) was equipped with flexible silica capillary columns (30 m × 0.32 mm I.D. × 0.25 μm) using helium as carrier gas. The GC temperature, which was programmed to start at 40 °C increased to 310 °C at the rate of 4 °C/min and was then held at 310 °C

for 30 min. For aliphatic biomarker analysis, mass chromatograms for *n*-alkanes and isoprenoids (*m/z* 85) and terpenoids (*m/z* 123 and *m/z* 191) were recorded. Aromatic biomarker data were acquired via mass chromatograms for phenanthrene and anthracene (*m/z* 178), methylphenanthrenes (*m/z* 192), dimethylphenanthrenes (*m/z* 206), fluorene (*m/z* 166), methylfluorenes (m/z 180), dibenzofuran (*m/z* 168), methyldibenzofurans (*m/z* 182), naphthalene (*m/z* 128), methylnaphthalenes (*m/z* 142), dimethylnaphthalenes (*m/z* 156), trimethylnaphthalenes (*m/z* 170), tetramethylnaphthalenes and dibenzothiophene (*m/z* 184), methyldibenzothiophenes (*m/z* 198), cadalene (*m/z* 183), 6-*iso*propyl-1-*iso*hexyl-2-methylnaphthalene (*ip*-iHMN; *m/z* 197), and retene (*m/z* 219). Compounds in mass chromatograms were identified by comparing their relative retention times with standard samples and published mass spectra (Noble et al. 1986; Weston et al. 1989; Killops et al. 1995; van Aarssen et al. 1999, 2000; Radke et al. 2000; Weiss et al. 2000; Ahmed et al. 2009; Nakamura et al. 2010; Romero-Sarmiento et al. 2011; Marynowski et al. 2013; Stojanović and Životić, 2013; Escobar et al. 2016; Jiang and George 2018, 2019; Cesar and Grice 2019; Yan et al. 2019; Zakrzewski et al. 2020).

3.6 Statistical analyses

Statistical analyses were carried out to identify the strength of relationships between geochemical parameters and to also identify the principal components. The analyses were performed on JASP 0.16 for macOS. For linear correlation analysis, Pearson's correlation coefficient was employed. Coefficients (r) > ±0.7, ±0.5 to 0.7, ±0.3 to 0.5, and < ±0.3 are accordingly regarded as strong, moderate, weak, and very weak correlations. The above-described geochemical analyses were not carried out on all forty samples and therefore geochemical data were unavailable for all samples. Hence, twenty-five samples were selected for principal component analysis (PCA). The selected samples are asterisked in Table 2. The number of components was auto-derived based on the distribution of components, and up to four principal components were obtained for each PCA run. In addition, the rotation method applied was Promax, an oblique rotation method that allows factors to be correlated.

4 Results

4.1 Basic geochemical characteristics

Bulk geochemical and group composition data of the Mukah, Balingian and Merit-Pila coals are presented in Table 1. The geochemical data (T_{max} < 430 °C, production index < 0.10, *A*-factor > 0.4, and extract yield > 4000 ppm) generally indicate thermal immaturity and excellent potential for the

Table 1 Average geochemical data of the studied Sarawak Basin coals

Coalfield	Rock-Eval pyrolysis										ATR-FTIR				Py-GC		Bitumen	
	T_{max}	*S1*	*S2*	*S3*	GP	PI	BI	HI	OI	QI	*S2*/*S3*	A_F	C_F	CL	I_{AL}	I_{HG}	Type Index	C_8/*xy*	EOM	HC Conc
Balingian	403	3.3	68.0	52.0	71.3	0.04	6.4	131	101	137	1.5	0.57	0.41	0.97	0.54	70	2.0	0.52	37794	4385
Mukah	418	2.4	103.3	23.8	105.7	0.02	5.0	204	44	209	5.2	0.56	0.38	1.05	0.53	111	1.2	0.99	38450	5338
Merit-Pila	412	5.8	129.0	45.5	134.8	0.04	10.2	226	80	236	3.0	0.57	0.42	1.04	0.54	125	1.6	0.67	89073	12373

T_{max}, Temperature at Maximum *S2* (°C); *S1*, Free Hydrocarbons (mg HC/g rock); *S2*, Pyrolysable Hydrocarbons (mg HC/g rock); *S3*, Organic CO_2 (mg CO_2/g rock); GP, Genetic Potential = *S1* + *S2* (mg HC/g rock); PI, Production Index = *S1*/(*S1* + *S2*); BI, Bitumen Index = (*S1*/TOC) × 100 (mg HC/gTOC); HI, Hydrogen Index = (*S2*/TOC) × 100 (mg HC/gTOC); OI, Oxygen Index = (*S3*/TOC) × 100 (mg CO_2/gTOC); QI, Quality Index = (*S1* + *S2*)/TOC × 100 (mg HC/gTOC); ATR-FTIR, Attenuated Total Reflection-Fourier Transform Infrared Spectroscopy; A_F, *A*-factor = (2930 + 2860)/(2930 + 2860 + 1600) cm^{-1}; C_F, *C*-factor = [1710/(1710 + 1600) cm^{-1}]; CL, Aliphatic Chain Length (CH_2/CH_3) = 2850/2955 cm^{-1}; I_{AL}, Aliphaticity index = [(2950 + 2920 + 2850) cm^{-1}]/[(2950 + 2920 + 2850 + 3030 + 1600) cm^{-1}]; I_{HG}, Index for Hydrocarbon Generation = I_{AL} × HI; Py-GC, Pyrolysis–Gas Chromatography; Type Index = m(+p)-xylene/*n*-1-octene; C_8: *n*-1-octene; xy: m(+p)-xylene; EOM, extractable organic matter yield (ppm); HC Conc, hydrocarbons concentration (ppm)

Table 2 Vitrinite reflectance (R_o), total organic carbon (TOC) and total sulfur (S_T) content and proximate analysis data of the studied Cenozoic Sarawak Basin coals

Sample/*coalfield*	R_o (%)	S_T (%)	TOC (wt%)	TOC/S_T	M_{ad} (wt%)	A_d (wt%)	V_d (wt%)	C_d (wt%)	Fuel ratio
Balingian									
B01-1[a]	0.30	0.29	61.0	210	7.9	6.3	54.2	39.5	0.73
B01-4	0.29	0.16	61.6	385	17.6	6.4	45.3	48.3	1.07
B01-5	0.32	0.17	60.3	355	12.2	6.9	44.2	48.9	1.11
B02-4	0.32	0.46	62.8	137	21.2	4.3	42.1	53.6	1.27
B03-2[a]	0.30	0.17	61.4	361	21.0	5.0	49.7	45.2	0.91
B03-3	0.27	0.15	63.9	426	42.3	6.1	53.7	40.2	0.75
B03-6[a]	0.28	0.13	61.5	473	25.3	14.9	46.1	39.0	0.85
E55-2[a]	0.34	0.23	62.4	271	20.4	8.4	46.1	45.5	0.99
L04A-1[a]	0.31	1.48	53.1	36	15.9	19.3	42.1	38.6	0.92
L04B-1	0.32	1.18	58.6	50	40.4	11.1	43.8	45.1	1.03
ML46A-6	0.36	0.18	61.0	339	40.0	5.5	49.5	45.0	0.91
ML46A-7[a]	0.34	0.58	60.8	105	31.1	5.1	47.3	47.6	1.01
BG1[a]	0.36	0.23	65.0	283	7.9	1.0	52.0	47.0	0.90
BG2[a]	0.35	0.13	61.4	472	10.2	1.7	47.2	51.2	1.09
Mukah									
046A[a]	0.40	0.85	65.2	77	–	–	–	–	–
M03-2[a]	0.38	0.20	46.9	235	3.3	37.5	33.3	29.2	0.88
MK1[a]	0.39	0.31	52.1	168	5.4	22.5	37.6	39.8	1.06
MK2[a]	0.38	0.27	66.3	246	5.4	5.8	43.9	50.3	1.15
MK3A[a]	0.39	0.34	68.0	200	4.1	0.8	46.5	52.8	1.13
MK3B[a]	0.41	0.36	65.1	181	–	–	–	–	–
Merit-Pila									
MP1L[a]	0.42	0.17	80.4	473	16.2	6.3	45.1	48.6	1.08
MP1M[a]	0.41	0.12	66.0	550	14.4	0.9	48.1	51.0	1.06
MP1U[a]	0.39	0.20	62.3	312	18.1	4.0	45.6	50.5	1.11
MP2L[a]	0.39	0.15	66.5	443	13.3	6.6	52.0	41.4	0.80
MP2U[a]	0.37	0.20	65.6	328	13.4	6.6	52.0	41.4	0.80
MP3L	0.40	0.21	67.3	320	10.6	27.3	43.4	29.3	0.67
MP3M[a]	0.38	0.22	51.6	235	9.4	16.0	54.0	30.1	0.56
MP3U	0.41	0.21	62.0	295	10.3	23.9	42.6	33.5	0.79
MP4L[a]	0.40	0.22	56.7	258	12.3	5.9	51.9	42.2	0.81
MP4M	0.38	0.30	63.3	211	10.3	14.5	46.2	39.3	0.85
MP4U[a]	0.38	0.12	61.7	514	12.1	9.4	49.4	41.3	0.84
MP5L	0.37	0.27	61.4	228	13.9	9.4	48.6	42.1	0.87
MP5M[a]	0.36	0.22	61.9	281	5.7	15.1	47.6	37.3	0.78
MP5U	0.41	0.19	67.8	357	13.8	8.7	48.1	43.2	0.90
MP6L[a]	0.40	0.21	63.2	301	13.5	6.0	48.8	45.1	0.92
MP6M[a]	0.43	0.17	63.2	372	13.4	4.9	46.0	49.1	1.07
MP6U	0.41	0.20	61.5	314	14.1	9.8	50.8	39.3	0.77
MP7L[a]	0.39	0.12	66.7	556	7.7	4.7	51.1	44.3	0.87
MP7M	0.39	0.09	63.1	701	11.2	3.8	50.2	45.9	0.91
MP7U	0.37	0.23	65.1	283	10.6	8.5	47.1	44.4	0.94

M_{ad}, moisture, as received; A_d, ash, dried basis; V_d, volatile matter, dried basis; C_d, fixed carbon, dried basis

[a]Sample selected for principal component analysis (PCA)

generation of gas to mixed condensate oil and gas (Ganz and Kalkreuth 1991; Peters and Cassa 1994). However, the relatively higher hydrogen index (HI) values of the Merit-Pila coals are suggestive of greater hydrocarbon-generating potential. Furthermore, geochemical data (type index > 0.4 and $S2/S3 < 10$) indicate that the coals are dominated by type-III kerogen and terrigenous organic matter with varying inputs of type-II kerogen and marine alga organic matter (Larter and Douglas 1980; Peters and Cassa 1994).

4.2 Proximate analysis

The result of the proximate analysis, which indicates the moisture, fixed carbon, ash, and volatile matter contents of the studied Sarawak Basin coals, is given in Table 2. The total moisture content (as received) of the Sarawak Basin coals varies widely between 3.3 wt% and 42.3 wt% with an average value of 15.0 wt%. The moisture content is relatively higher for the Balingian coals (avg. 22.4 wt%) than for the Mukah (avg. 7.0 wt%) and Merit-Pila (avg. 12.2 wt%) coals (Table 2). The ash content (dried) of the studied samples ranges widely, varying from 0.8 to 37.5 with average values of 7.3, 16.6, and 17.1 for the Balingian, Mukah, and Merit-Pila coals, respectively. Correlation analysis of proximate and vitrinite reflectance data for all the studied Malaysian coals indicates that the ash content correlates moderately ($r = -0.619$) with volatile matter content and strongly ($r = -0.832$) with fixed carbon content.

Volatile matter in coals consists of methane, carbon monoxide and other incombustible gases. Hence, the volatile matter content is a measure of the gaseous fuels present in coals and high values indicate rapid ignition. Measured values of volatile matter (dried basis) vary from 33.3 wt% to 54.2 wt% with average values of 47.4 wt% , 43.0 wt% and 48.4 wt% for the Balingian, Mukah and Merit-Pila coals, respectively (Table 2). Furthermore, the fixed carbon content, which is an imprecise estimate of coal's heating value varies from 29.2 wt% to 53.6 wt% with similar average values of 45.3 wt% , 45.9 wt% and 42.0 wt% for the Balingian, Mukah, and Merit-Pila coals, respectively. Additionally, the fuel ratio, expressed as the ratio of fixed carbon to volatile matter, is a measure of the ease of ignition and burnout. Hence, lower fuel ratios signify rapid ignition capability (Aich et al. 2020). Calculated fuel ratios vary between 0.94 and 1.05 with average ratios of 0.97, 1.09, and 0.87 for the Balingian, Mukah and Merit-Pila coals, respectively.

4.3 Total organic carbon (TOC) and total sulfur (ST) contents

The total organic carbon (TOC) content of sedimentary rocks is a measure of organic richness (Peters and Cassa 1994). TOC values for the analysed Sarawak Basin coals range between 46.9 wt% and 80.4 wt% with an average value of 62.4 wt%. TOC values are generally slightly higher for the Merit-Pila (avg. 63.9 wt%) than the Balingian (avg. 61.1 wt%) and Mukah (avg. 60.6 wt%) coals. Measured total sulfur (S_T) content in the studied coals is mostly low (< 0.5%), ranging from 0.13% to 1.48% (avg. 0.40%), 0.20% to 0.85% (0.39%), and 0.09% to 0.30% (avg. 0.19%), respectively, for the Balingian, Mukah and Merit-Pila coals. The TOC/S_T ratio is a proxy for paleoredox conditions and higher values indicate oxidizing conditions (Algeo and Liu 2020). Ratios for coals are generally highest for the Merit-Pila coals (avg. 367) and lowest for the Mukah coals (avg. 184).

4.4 CHN elemental and bulk isotopic composition

The elemental carbon content of the coals varies broadly over the 24.4 wt%–53.6 wt% range. Average carbon content increases from Mukah coals (avg. 34.9 wt%) to Merit-Pila (avg. 38.0 wt%) and Balingian (avg. 38.7 wt%) coals. The hydrogen content of the Balingian, Mukah and Merit-Pila coals varies widely from 4.7 wt% to 7.1 wt% (avg. 5.6 wt%), 4.8 wt% to 5.8 wt% (avg. 5.2 wt%) and 4.8 wt% to 6.1 wt% (avg. 5.5 wt%), respectively (Table 3). Additionally, the nitrogen content is generally highest for the Mukah coals (0.74 wt%–1.30 wt%) and lowest for the Merit-Pila coals (0.69 wt%–0.97 wt%) whilst the Balingian coals (0.69 wt%–1.42 wt%) show intermediate values. Resultantly, the atomic C/N ratios for the studied coals vary widely between 38.8 wt% and 66.9 wt% with mean ratios of 48.1 wt%, 39.6 wt%, and 55.1 wt% for the Balingian, Mukah and Merit-Pila coals, respectively.

The bulk stable carbon isotopic ($\delta^{13}C$) values for the coals vary between −29.4‰ and −24.2‰, with mean values of −28.0‰, −26.7‰ and −28.3‰ for the Balingian, Mukah, and Merit-Pila coals, respectively (Table 3). These values show that the Mukah coals are mostly isotopically heavier than the Balingian and Merit-Pila Basin coals. Furthermore, the hydrogen isotopic ($\delta\Delta$) values of the analysed samples vary widely between a maximum of −91.0‰ and a minimum of −173.5‰. The Merit-Pila coals are relatively depleted in deuterium with a mean $\delta\Delta$ value of −143.4‰. In contrast, the Balingian and Mukah coals are relatively enriched in deuterium and show more positive $\delta\Delta$ values with a mean of −114.7‰ and −117.9‰, respectively.

4.5 Major and trace elements composition

The concentrations of major and trace elements have been widely applied as proxies for past redox, climatic and depositional conditions in coal environments (Goodarzi and Swaine 1993, 1994; Spears and Tewalt 2009; Spears 2017; Krzeszowska 2019; Li et al. 2019; Lv et al. 2019; Liu et al. 2021; Zhou et al. 2021). Given that coals are only formed

Table 3 Isotopic and atomic composition of the Sarawak Basin coals

Sample/*coalfield*	Isotope ratios (‰)		Atomic abundance (wt%)				
	$\delta^{13}C$	$\delta^{2}H$	C	H	N	O	C/N
Balingian							
B01-1	−28.7	−104.7	34.5	6.4	0.9	44.2	42.8
B03-6	−27.7	−107.8	35.0	6.0	0.9	21.6	46.8
E55-2	−28.7	−104.3	53.6	7.1	1.4	10.6	44.0
L04A-1	−27.9	−103.1	32.0	5.5	0.7	28.2	54.2
ML46A-7	−27.3	−125.3	46.7	4.7	1.2	12.3	46.0
BG1	−28.0	−133.6	37.9	4.8	0.9	47.4	51.1
BG2	−27.4	−123.8	31.5	4.7	0.7	51.3	51.6
Mukah							
046A	−27.6	−130.0	34.4	5.1	1.0	41.9	40.0
M03-2	−26.8	−91.0	24.4	4.8	0.7	30.3	38.8
MK1	−27.6	−110.3	31.3	5.8	0.9	34.9	39.2
MK2	−24.2	−128.5	40.2	5.6	1.2	41.8	40.6
MK3A	−27.4	−129.9	44.0	4.7	1.3	44.8	39.5
Merit-Pila							
MP1L	−26.7	−128.7	39.3	5.6	0.9	32.5	49.3
MP1U	−28.0	−122.4	37.7	4.8	0.9	35.0	49.6
MP2L	−28.6	−145.2	36.7	5.4	0.8	37.9	55.2
MP2U	−29.4	−153.2	33.8	5.5	0.7	40.8	56.6
MP3M	−28.0	−173.5	38.9	5.8	0.7	30.5	65.6
MP4L	−28.2	−154.7	39.6	5.8	0.9	36.0	50.4
MP5M	−29.3	−144.4	37.8	5.3	0.8	35.9	54.2
MP6M	−28.3	−139.0	40.1	5.0	1.0	36.1	48.0
MP7L	−28.0	−129.6	37.9	6.1	0.7	43.2	66.9

C carbon, *H* hydrogen, *O* oxygen, *N* nitrogen. $\%O = 100 - (C + H + N + S_T + Ash)$

in non-marine environments with comparably low detrital inputs, the concentrations of elements in the studied coals are normalized to their global average concentrations, following the method employed by Kombrink et al. (2008):

$$CC = \frac{\sum_{i=1}^{N} \left(\frac{El_{sample}}{El_{average}} \right)}{N} \quad (1)$$

The concentration coefficient (*CC)* is defined as the ratio of abundance of a particular element in a coal sample relative to the reported global average abundance. The concentrations of the major element oxides in studied coals were compared with their reported abundances in Chinese coals by Dai et al. (2012), while the trace elements were compared with global average concentrations reported by Ketris and Yudovich (2009). The *CC*s of major element oxides and trace elements in the coals were calculated, and coefficients < 0.5 and > 5 indicate that the elements are depleted and significantly enriched, respectively. Furthermore, *CC*s over the 0.5–2.0 and 2.0–5.0 ranges indicate normal and slightly enriched abundance, respectively. The *CC* values for the Balingian, Mukah and Merit-Pila coals are shown in Fig. 2.

The abundances of the major oxides in the Malaysian coals are either relatively depleted or comparable to the values reported for Chinese coals by Dai et al. (2012). However, the distributions of major element oxides are dominated by SiO_2, Al_2O_3 and Fe_2O_3 with subordinate abundances of CaO, MgO, and K_2O and low abundances of TiO_2, Na_2O, MnO and Cr_2O_3 (Table 4). The SiO_2/Al_2O_3 ratios vary from 0.18 to 7.30, with relatively higher average ratios in the coals from Balingian (2.84%) than from Merit-Pila (1.96) and Mukah (1.18) coalfields. The average SiO_2/Al_2O_3 ratio of the studied Malaysian coals (2.09) is higher than those of Chinese coals (1.42; Dai et al. 2012) and the theoretical value of kaolinite (1.18; Zhou et al. 2021). Similarly, Fe_2O_3/Al_2O_3 and Na_2O/Al_2O_3 ratios are relatively higher for the Balingian coals (avg. 7.52 and 0.85) than for the Merit-Pila (avg. 3.12 and 0.01) and Mukah (avg. 2.89 and 0.02) coals.

Furthermore, when compared with the global mean abundances reported by Ketris and Yudovich (2009), the Malaysian coals are mostly depleted in trace elements such as U, Mo, V, Pb, Cr, Th, Ga, Rb, Li, As, Ti, Ag, Hf, Zr, Sc and Nb (Fig. 2). However, the Balingian coals show enrichment for B. Elemental ratios have been employed as proxies for past

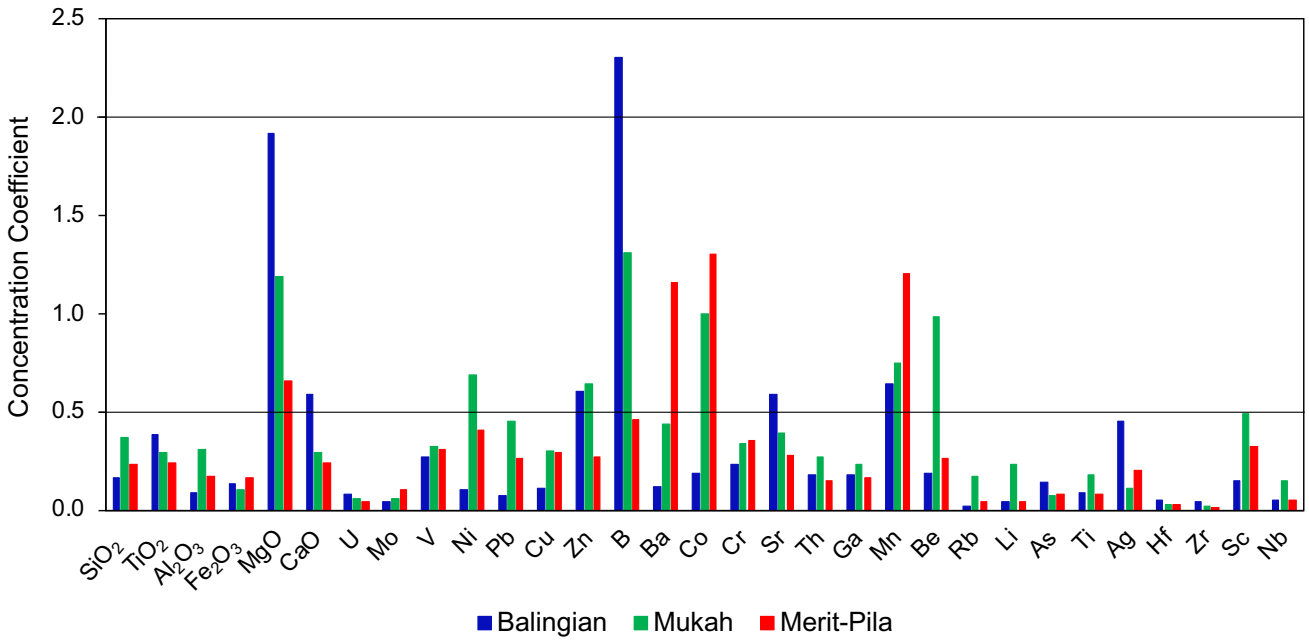

Fig. 2 Correlation coefficients of major oxides and trace elements in the studied Sarawak coals, normalized to their Chinese and global averages reported by Dai et al. (2012) and Ketris and Yudovich (2009), respectively

environmental conditions (Dai et al. 2020). Hence, ratios of elemental abundance in the studied coals are given in Table 5.

4.6 Molecular composition

4.6.1 *n*-Alkanes and isoprenoids

The *m/z* 85 chromatograms of the aliphatic fractions of the coal extracts comprise mainly a series of *n*-C_{15} to *n*-C_{35} *n*-alkanes and are dominated by high molecular weight (MW) homologues (*n*-C_{27} to *n*-C_{33}) with marked odd-over-even predominance. Medium MW *n*-alkanes (*n*-C_{21} to *n*-C_{26}) are present in subordinate abundance in the samples, while low MW alkanes ($\leq$ *n*-C_{20}) are only present in low concentration. Acyclic isoprenoids, pristane (Pr) and Phytane (Ph) are also present in all the studied samples and their relative abundance (Pr/Ph) is widely used to infer redox conditions during sedimentation and diagenesis (Didyk et al. 1978). Whilst the Pr/Ph parameter is affected by thermal maturity (Peters et al. 2005), such an effect is negligible since the studied coals are generally of low rank. Pr/Ph values for the coals range from 0.6 to 14.0 with mean values of 2.3, 4.4 and 6.5 for Balingian, Mukah and Merit-Pila coals, respectively. All the investigated coals (except BG1) show a lower (< 1) relative abundance of Ph over *n*-C_{18}. However, the relative abundance of Pr over *n*-C_{17} is generally higher (> 1) in Mukah and Merit-Pila coals, and relatively lower (< 1) in the Balingian coals (Table 6).

4.6.2 Hopanoids

The distribution of hopanoids for the studied coals is generally similar and characterized by the abundance of neohop-13(18)-enes, hop-17(21)-enes, ββ-hopanes and subordinate abundances of αβ-hopanes ranging from C_{27} to C_{31} without C_{28}. C_{27} β-trinorhopane was observed in most of the samples whilst tricyclic terpanes, βα-moretanes and gammacerane were either absent or present in low abundance. C_{29} neohop-13(18)-ene is the most abundant hopanoid in most of the coal samples, whilst C_{30} ββ-hopane and C_{31} αβ-homohopane (22R) predominate in a few samples. The $(C_{29}+C_{31})/C_{30}$ αβ-hopane parameter, which reflects the relative contributions of terrigenous and marine organic matter, ranges from 2.6 to 23.7 with corresponding average values of 9.9, 8.2, and 11.1 for the Balingian, Mukah, and Merit-Pila coals (Table 6). The relatively lower values for the Mukah coals suggest greater marine algal organic matter (OM) input (Killops et al. 1994).

Table 4 Abundance of elements in the Sarawak Basin coals

Sample/*coalfield*	Major oxides and loss on ignition (LOI; wt%)									Major elements (wt%)							
	SiO_2	TiO_2	Al_2O_3	Fe_2O_3	MgO	CaO	Na_2O	K_2O	LOI	S	Al	Ca	Fe	Mg	K	Na	Ti
Balingian																	
B01-1	0.82	0.03	0.52	0.51	0.59	1.46	0.03	< dl	96.0	0.18	0.11	0.94	0.31	0.32	< dl	0.033	0.011
B03-2	0.33	< dl	0.05	0.78	0.21	0.54	< dl	< dl	98.1	0.09	0.02	0.38	0.56	0.14	< dl	0.010	0.001
E55-2	0.41	< dl	0.11	0.60	0.72	1.17	0.14	< dl	96.8	0.14	0.04	0.74	0.35	0.38	< dl	0.109	0.002
LO4A-1	7.61	0.22	2.74	0.18	0.05	0.03	< dl	0.23	88.9	0.99	0.65	0.02	0.09	< dl	0.01	0.001	0.020
ML46A-7	0.12	< dl	0.12	1.19	0.18	0.29	< dl	< dl	98.4	0.38	0.05	0.19	0.82	0.11	< dl	0.005	0.001
BG-1	0.17	< dl	0.07	0.54	0.65	0.83	0.06	< dl	97.6	0.08	0.02	0.51	0.33	0.34	< dl	0.047	< dl
BG-2	0.09	< dl	0.05	0.61	0.56	0.73	0.06	< dl	97.8	0.09	0.02	0.51	0.43	0.33	0.01	0.055	< dl
Mukah																	
046A	0.18	< dl	0.51	0.12	0.00	0.09	< dl	< dl	99.3	0.42	0.26	0.06	0.1	< dl	< dl		0.001
MK-1	10.80	0.16	5.99	0.48	0.52	0.54	0.05	0.87	80.5	0.14	0.29	0.35	0.17	0.20	0.06	0.023	0.037
MK-2	1.36	0.03	0.94	0.34	0.47	0.71	0.03	0.09	96.0	0.10	0.20	0.51	0.23	0.27	0.02	0.030	0.006
MK-3A	0.10	< dl	0.09	0.98	0.06	0.09	< dl	< dl	98.9	0.17	0.04	0.06	0.66	0.03	< dl	0.003	< dl
Merit-Pila																	
MP-1L	0.04	< dl	0.13	0.61	0.04	0.12	< dl	< dl	99.0	0.06	0.07	0.08	0.43	0.02	< dl	< dl	< dl
MP-1M	0.13	< dl	0.08	0.62	0.04	0.11	< dl	< dl	99.1	0.06	0.04	0.08	0.47	0.03	< dl	< dl	< dl
MP-1U	0.07	< dl	0.38	0.47	0.03	0.13	< dl	< dl	99.1	0.12	0.20	0.09	0.32	0.02	< dl	< dl	< dl
MP-2L	1.46	0.06	0.20	0.84	0.11	0.21	< dl	< dl	97.1	0.09	0.10	0.15	0.59	0.07	< dl	0.003	0.006
MP-2U	1.44	0.10	0.56	0.96	0.09	0.22	< dl	< dl	96.5	0.11	0.26	0.16	0.67	0.06	< dl	0.002	0.006
MP-3M	6.81	0.11	3.31	0.46	0.35	0.42	0.02	0.37	88.0	0.11	0.28	0.29	0.25	0.16	0.04	0.002	0.012
MP-4L	2.73	0.09	1.19	0.69	0.09	0.21	< dl	0.03	94.9	0.11	0.29	0.15	0.46	0.05	< dl	0.001	0.008
MP-4U	2.81	0.05	2.18	0.76	0.09	0.12	< dl	0.04	93.9	0.16	0.37	0.09	0.51	0.05	< dl	0.001	0.008
MP-5M	6.03	0.10	2.80	0.92	0.20	0.45	0.02	0.21	89.2	0.09	0.25	0.32	0.59	0.10	0.01	< dl	0.007
MP-6L	1.15	0.04	0.90	0.76	0.24	0.59	< dl	0.02	96.2	0.10	0.35	0.42	0.53	0.15	< dl	0.001	0.003
MP-6M	0.15	< dl	0.08	1.00	0.32	0.65	< dl	< dl	97.7	0.07	0.03	0.43	0.69	0.19	< dl	< dl	< dl
MP-7L	0.19	< dl	0.32	1.01	0.15	0.35	< dl	0.01	97.9	0.05	0.16	0.23	0.65	0.08	< dl	0.003	0.002

Sample/*coalfield*	Trace elements (ppm)																	
	B	Ba	Be	Co	Cr	Cu	Ga	Mn	Mo	Pb	As	Rb	Ni	Sr	Th	U	V	Zn
Balingian																		
B01-1	248	9	0.3	0.5	2.7	1.3	1.0	48	0.06	0.96	0.4	0.1	1.1	129.3	1.2	0.2	4	0.8
B03-2	89	38	< dl	0.6	1.7	0.6	< dl	81	0.03	0.19	0.2	0.2	0.1	46.7	0.4	< dl	< dl	1.2
E55-2	121	16	< dl	0.4	1.9	0.8	0.2	59	0.02	0.34	0.2	0.1	0.9	84.3	0.4	< dl	< dl	0.7
LO4A-1	47	12	0.2	3.0	13.1	2.3	2.9	7	0.34	1.30	2.7	1.0	6.1	25.4	1.3	0.2	14	88.1
ML46A-7	89	16	0.4	0.4	3.6	0.8	0.1	77	0.03	0.22	3.9	0.2	0.5	22.3	0.4	< dl	2	0.8
BG-1	109	16	< dl	< dl	1.4	2.9	< dl	59	0.05	0.30	0.4	0.1	0.2	70.2	0.2	< dl	< dl	2.5
BG-2	133	19	< dl	< dl	1.9	3.4	< dl	55	0.11	0.38	0.4	0.2	0.2	73.8	0.2	< dl	< dl	2.6
Mukah																		
046A	91	10	2.6	4.4	5.6	2.7	0.9	4	0.18	1.13	1.0	< dl	11.3	4.0	0.4	< dl	2	43.9
MK-1	53	102	1.0	4.2	9.9	8.5	2.6	46	0.13	9.83	0.6	6.0	4.6	65.6	2.4	0.2	17	5.6
MK-2	71	123	1.1	7.9	3.9	2.9	1.7	71	0.06	2.62	< dl	1.2	11.6	91.3	0.6	0.1	5	5.3
MK-3A	57	32	< dl	3.8	2.2	5.2	0.2	137	0.12	0.54	0.1	0.1	8.3	11.3	0.2	< dl	< dl	4.2
Merit-Pila																		
MP-1L	< dl	82	< dl	8.3	2.1	3.6	0.2	42	0.08	0.67	0.8	< dl	5.6	7.4	0.1	< dl	< dl	12.2
MP-1M	24	74	< dl	1.6	3.5	1.0	0.1	49	0.16	0.31	0.6	< dl	3.9	7.0	0.1	< dl	< dl	5.1
MP-1U	< dl	57	0.2	2.6	2.8	6.8	0.7	27	0.94	2.42	1.0	< dl	4.1	7.4	0.2	< dl	2	11.4
MP-2L	< dl	139	0.1	7.8	2.3	4.1	0.2	133	0.34	1.51	0.5	0.1	5.8	17.3	0.3	< dl	1	5.1
MP-2U	< dl	178	1.2	5.8	12.7	4.2	1.6	146	0.23	1.55	0.6	0.1	7.1	18.1	0.6	< dl	8	2.6

Table 4 (continued)

Sample/*coalfield*	Trace elements (ppm)																	
	B	Ba	Be	Co	Cr	Cu	Ga	Mn	Mo	Pb	As	Rb	Ni	Sr	Th	U	V	Zn
MP-3M	< dl	260	0.1	3.6	8.9	11.7	2.0	83	0.21	4.72	0.8	2.7	3.0	48.7	1.1	0.1	14	2.2
MP-4L	< dl	159	0.2	12.8	6.7	2.7	1.0	96	0.08	2.35	0.7	0.3	7.6	20.2	0.7	< dl	7	1.3
MP-4U	< dl	138	0.5	7.7	7.9	5.9	1.6	127	0.21	4.27	0.5	0.4	5.9	9.5	1.0	< dl	16	5.1
MP-5M	< dl	244	0.3	4.9	9.1	9.2	1.8	119	0.14	3.03	0.9	1.1	4.4	48.8	1.0	< dl	14	1.6
MP-6L	< dl	326	1.1	11.1	6.1	2.6	1.0	141	0.18	2.18	1.0	0.3	5.9	79.2	0.5	< dl	6	1.6
MP-6M	< dl	237	< dl	0.5	1.6	2.3	< dl	169	0.01	0.34	0.5	0.1	5.0	65.6	0.1	< dl	< dl	3.4
MP-7L	< dl	199	0.1	12.7	4.2	2.0	0.3	108	0.19	0.94	0.3	0.1	5.7	40.2	0.4	< dl	2	22.3

< dl = below detection limit

4.6.3 Aliphatic terpenoids

Terpenoids represent a vastly broad family of biomarkers. They are derived from higher plants and are well-recognised in petroleum, sediments and coal as chemosystematic markers of palaeoflora and palaeoclimate (Killops et al. 1995; van Aarssen et al. 2000; Otto et al. 2002a, b; Hautevelle et al. 2006; Nakamura et al. 2010; Jiang and George 2018). Aliphatic diterpenoids such as 8β-labdane (βL), 4α-19-*nor*-isoprimarane (19NIP), 8α-labdane (αL), 18-norabietane (NA), 4α-18-*nor*-isoprimarane (18NIP), rimuane (R), C_{19}-17-nortetracyclane (NT), *ent*-beyerane (B), isopimarane (IP), 16β(H)-phyllocladane (βP), abietane (A), and 16α(H)-phyllocladane (αP) were observed in varying abundances in the studied coals. In contrast, *ent*-16β(H)-kaurane (βK) and *ent*-16α(H)-kaurane (αK) were not present in detectable amounts. The aliphatic diterpenoid distributions are generally dominated by 14α-18-*nor*-isoprimarane and 16α(H)-phyllocladane, while 18-norabietane and abietane are only present in minor abundances. The absence of cuparane- and cedrane-class sesquiterpenoids, totarane, phenolic abietanes and most tetracyclic diterpenoids in the Tertiary Sarawak Basin coals suggests a predominantly Pinaceae family origin for the diterpenoids. Furthermore, the distributions of aliphatic triterpenoids in the studied Sarawak Basin coals are characterised by the presence, in varying proportions, of 10β(H)-des-A-oleanane (dO), 10β(H)-des-A-ursane (dU), 10β(H)-des-A-lupane (dL), and 18β(H)-des-E-hopane (dH), indicating the contribution of angiosperms to paleoflora of the Sarawak Basin (Killops et al. 1994). However, the coals are dominated mostly by the C_{24} ring-A degraded ursane derivative (Figs. 3d–f). Additionally, 18α(H)-oleanane (O), a broadly regarded diagnostic indicator of angiosperm contribution to paleoflora, was not detected in all of the samples.

The relative abundances of angiosperm-derived triterpenoid and gymnosperm-derived diterpenoid biomarkers have been widely utilized to reconstruct variations in past vegetation and climate. Killops et al. (1995) proposed and employed the angiosperm/gymnosperm index (AGI) to evaluate flora changes in the Taranaki Basin, New Zealand during the Cretaceous and Paleogene. Similarly, based on the analysis of angiosperm fossils from Japan, Nakamura et al. (2010) proposed the aliphatic angiosperm/gymnosperm index (al-AGI'). In addition, Bechtel et al. (2001, 2008) employed the Di-/Tri-terpenoids and Di-/(Di- + Tri-terpenoids) ratios to determine the contribution of angiosperms and gymnosperms to paleovegetation. The AGI, al-AGI' and Di-/Tri-terpenoids parameters are calculated for the studied Sarawak Basin coals (Table 6). Di-/Tri-terpenoids ratios for the studied samples range from 0.12 to 1.42 with average values of 0.74, 1.00 and 0.65 for the Balingian, Mukah, and Merit-Pila coals, respectively. Additionally, al-AGI' ratios range from 0.41 to 0.89 with average ratios of 0.60, 0.51, and 0.62 for the Balingian, Mukah, and Merit-Pila coals.

4.6.4 Higher plant-derived polycyclic aromatic hydrocarbons

Aromatic biomarkers such as cadalene, retene, and 6-*iso*-propyl-1-*iso*hexyl-2-methylnaphthalene (ip-iHMN) are important constituents of sedimentary rocks that originate from terrestrial plants due to their structural similarities to precursors (Ellis et al. 1996; Otto and Wilde 2001; Otto et al. 2002a). However, the origin of ip-iHMN has also been attributed to non-vascular plants such as bryophytes, which are less affected by climate (Cesar and Grice 2019).

The aromatic distributions of the sesquiterpenoids and diterpenoids in the analysed coals are dominated by cadalene and retene, respectively (Fig. 4). Retene was identified based on mass fragmentograms of *m/z* 219 and *m/z* 234, while cadalene was recognized by the intersecting mass fragmentograms of *m/z* 183 and *m/z* 198. However, ip-iHMN was mostly absent in the *m/z* 197 of the aromatic fractions of the studied Sarawak Basin coals. Other plant-derived aromatic hydrocarbons such as 1,2,3,4-tetrahydroretene, dehydroabietane, totarane and simonellite were either absent in the coal samples or only detected in minor amounts.

Table 5 Elemental parameters for the studied Sarawak Basin coals

Sample/*coalfield*	SiO_2/Al_2O_3	Al_2O_3/TiO_2	TiO_2/Zr	Sr/Ba	Th/U	Fe/S	Fe/Al	Ni/Co	V/Cr	V/Ni	Sr/Cu	C-Value	Ga/Rb	Fe/Mn	Ca/Mg	Ba/Ti
Balingian																
B01-1	1.6	17.3	27.3	13.8	6.0	1.72	2.8	2.2	1.5	3.6	99.0	0.2	10.0	64.6	2.94	0.1
B03-2	6.6	–	–	1.2	–	6.22	28.0	0.2	–	–	79.2	1.1	–	69.1	2.71	3.8
E55-2	3.7	–	–	5.3	–	2.50	8.8	2.3	–	–	108.1	0.3	2.0	59.3	1.95	0.8
L04A-1	2.8	12.5	57.9	2.1	6.5	0.09	0.1	2.0	1.1	2.3	11.1	2.7	2.9	128.6	–	0.1
ML46A-7	1.0	–	–	1.4	–	2.16	16.4	1.3	0.6	4.0	27.5	2.7	0.5	106.5	1.73	1.6
BG1	2.4	–	–	4.3	–	4.13	16.5	–	–	–	24.0	0.4	–	55.9	1.50	–
BG2	1.8	–	–	4.0	–	4.78	21.5	–	–	–	21.8	0.5	–	78.2	1.55	–
Mukah																
046A	0.4	–	–	0.4	–	0.24	0.4	2.6	0.4	0.2	1.5	1.7	–	250.0	–	1.0
MK1	1.8	37.4	57.1	0.6	12.0	1.21	0.6	1.1	1.7	3.7	7.7	0.3	0.4	37.0	1.75	0.3
MK2	1.4	31.3	75.0	0.7	6.0	2.30	1.2	1.5	1.3	0.4	31.9	0.3	1.4	32.4	1.89	2.0
MK3A	1.1	–	–	0.4	–	3.88	16.5	2.2	–	–	2.2	6.9	2.0	48.2	2.00	–
Merit-Pila																
MP1L	0.3	–	–	0.1	–	7.17	6.1	0.7	–	–	2.1	4.0	–	102.4	4.00	–
MP1M	1.6	–	–	0.1		7.83	11.8	2.4	–	–	7.0	4.0	–	95.9	2.67	–
MP1U	0.2	–	–	0.1	–	2.67	1.6	1.6	0.7	0.5	1.1	2.8	–	118.5	4.50	–
MP2L	7.3	3.3	54.5	0.1	–	6.56	5.9	0.7	0.4	0.2	4.3	2.5	2.0	44.4	2.14	2.3
MP2U	2.6	5.6	47.6	0.1	–	6.09	2.6	1.2	0.6	1.1	4.3	2.8	16.0	45.9	2.67	3.0
MP3M	2.1	30.1	55.0	0.2	11.0	2.27	0.9	0.8	1.6	4.7	4.2	0.5	0.7	30.1	1.81	2.2
MP4L	2.3	13.2	60.0	0.1	–	4.18	1.6	0.6	1.0	0.9	7.5	2.2	3.3	47.9	3.00	2.0
MP4U	1.3	43.6	55.6	0.1	–	3.19	1.4	0.8	2.0	2.7	1.6	3.4	4.0	40.2	1.80	1.7
MP5M	2.2	28.0	55.6	0.2	–	6.56	2.4	0.9	1.5	3.2	5.3	1.3	1.6	49.6	3.20	3.5
MP6L	1.3	22.5	44.4	0.2	–	5.30	1.5	0.5	1.0	1.0	30.9	0.9	3.3	37.6	2.80	10.9
MP6M	1.9	–	–	0.3	–	9.86	23.0	10.0	–	–	29.0	1.1	–	40.8	2.26	–
MP7L	0.6	–	–	0.2	–	13.00	4.1	0.5	0.5	0.4	20.3	2.0	3.0	60.2	2.88	10.0

Sample/*coalfield*	Al/(Al + Fe + Mn)	Th/Sc	Zr/Sc	Th/Co	Th/Cr	Zr/Hf	Cr/V	Cr/Ni	Y/Ni	Cu/Ni
Balingian										
B01-1	0.26	1.50	6.75	2.40	0.44	28.4	0.68	2.5	1.58	1.2
B03-2	0.03	1.33	1.67	0.67	0.24	16.7	–	17.0	0.70	5.9
E55-2	0.10	1.33	2.00	1.00	0.21	30.0	–	2.1	0.31	0.9
L04A-1	0.88	0.93	1.21	0.43	0.10	21.3	0.94	2.2	0.65	0.4
ML46A-7	0.06	0.57	1.43	1.00	0.11	33.3	1.80	7.2	1.90	1.6
BG1	0.06	0.67	1.00	–	0.14	–	–	7.0	0.40	14.7
BG2	0.04	1.00	1.50	–	0.11	15.0	–	9.5	0.25	16.9

Table 5 (continued)

Sample/*coalfield*	Al/(Al + Fe + Mn)	Th/Sc	Zr/Sc	Th/Co	Th/Cr	Zr/Hf	Cr/V	Cr/Ni	Y/Ni	Cu/Ni
Mukah										
046A	0.72	0.21	0.32	0.09	0.07	30.0	2.80	0.5	3.60	0.2
MK1	0.62	0.80	0.33	0.57	0.24	20.0	0.58	2.2	0.89	1.8
MK2	0.46	0.25	0.17	0.08	0.15	20.0	0.78	0.3	0.54	0.2
MK3A	0.06	0.67	0.67	0.05	0.09	–	–	0.3	0.04	0.6
Merit-Pila										
MP1L	0.14	0.33	0.67	0.01	0.05	–	–	0.4	0.04	0.6
MP1M	0.08	0.50	1.50	0.06	0.03	–	–	0.9	0.03	0.3
MP1U	0.38	0.33	0.33	0.08	0.07	–	1.40	0.7	0.22	1.7
MP2L	0.14	0.60	1.40	0.04	0.13	17.5	2.30	0.4	0.11	0.7
MP2U	0.28	0.23	0.23	0.10	0.05	15.0	1.59	1.8	1.10	0.6
MP3M	0.52	0.50	0.27	0.31	0.12	20.0	0.64	3.0	0.43	3.9
MP4L	0.38	0.50	0.36	0.05	0.10	12.5	0.96	0.9	0.39	0.4
MP4U	0.41	0.42	0.29	0.13	0.13	17.5	0.49	1.3	0.80	1.0
MP5M	0.29	0.40	0.20	0.20	0.11	25.0	0.65	2.1	0.18	2.1
MP6L	0.39	0.36	0.21	0.05	0.08	–	1.02	1.0	1.48	0.4
MP6M	0.04	0.33	0.33	0.20	0.06	–	–	0.3	0.03	0.5
MP7L	0.19	0.67	0.67	0.03	0.10	20.0	2.10	0.7	0.08	0.3

C-value = (Fe + Mn + Cr + Ni + V + Co)/(Ca + Mg + Sr + Ba + K + Na)

Table 6 Aliphatic hydrocarbon parameters for the Sarawak Basin coals

Sample/*coalfield*	*m/z* 85 *n*-alkanes and isoprenoids										
	C_{max}	Pr/Ph	ACL	P_{aq}	P_{wax}	C_{23}/C_{25}	C_{23}/C_{29}	C_{23}/C_{31}	$C_{23}/(C_{27}+C_{31})$	C_{27}/C_{31}	$(C_{27}+C_{29})/(C_{23}+C_{25}+\cdots+C_{33})$
Balingian											
B01-1	C_{31}	3.7	29.2	0.21	0.84	0.42	0.19	0.14	0.08	0.79	0.43
B01-4	C_{27}	4.0	29.0	0.41	0.71	0.35	0.53	0.27	0.13	1.01	0.35
B01-5	C_{31}	2.0	29.2	0.30	0.77	0.43	0.36	0.20	0.12	0.74	0.39
B02-4	C_{31}	1.8	29.0	0.25	0.82	0.46	0.26	0.18	0.09	0.96	0.43
B03-2	C_{31}	1.0	29.4	0.21	0.83	0.48	0.24	0.14	0.09	0.53	0.34
B03-3	C_{31}	1.0	29.3	0.34	0.73	0.57	0.46	0.31	0.19	0.67	0.34
B03-6	C_{31}	0.7	29.4	0.21	0.84	0.42	0.20	0.13	0.08	0.60	0.37
E55-2	C_{31}	2.8	29.1	0.28	0.79	0.47	0.26	0.24	0.13	0.90	0.44
L04A-1	C_{31}	2.0	29.3	0.15	0.89	0.23	0.09	0.05	0.03	0.67	0.41
L04B-1	C_{31}	–	29.4	0.19	0.85	0.39	0.17	0.10	0.07	0.55	0.35
ML46A-6	C_{31}	2.0	29.1	0.30	0.77	0.53	0.32	0.29	0.15	0.91	0.43
ML46A-7	C_{27}	5.0	29.0	0.32	0.77	0.52	0.35	0.29	0.15	1.02	0.42
BG1	C_{31}	0.9	29.4	0.12	0.91	0.34	0.09	0.06	0.04	0.59	0.42
BG2	C_{27}	2.7	28.8	0.28	0.81	0.35	0.21	0.20	0.09	1.24	0.45
Mukah											
046A	C_{27}	1.2	28.8	0.49	0.63	0.82	0.83	0.91	0.39	1.35	0.39
M03-2	C_{31}	2.3	29.0	0.32	0.77	0.51	0.35	0.28	0.14	0.98	0.44
MK1	C_{27}	4.7	28.9	0.27	0.81	0.31	0.18	0.17	0.08	1.14	0.46
MK2	C_{31}	4.2	29.2	0.26	0.81	0.50	0.33	0.19	0.11	0.75	0.35
MK3A	C_{31}	6.3	29.1	0.43	0.67	0.64	0.68	0.51	0.27	0.88	0.35
MK3B	C_{31}	7.7	29.2	0.35	0.73	0.67	0.53	0.37	0.21	0.76	0.36
Merit-Pila											
MP1L	C_{31}	3.7	29.0	0.32	0.77	0.57	0.43	0.30	0.15	0.99	0.41
MP1M	C_{29}	4.0	28.7	0.27	0.81	0.38	0.16	0.29	0.11	1.59	0.57
MP1U	C_{25}	0.6	28.3	0.69	0.52	0.39	1.52	1.08	0.31	2.47	0.37
MP2L	C_{29}	12.5	29.2	0.31	0.75	0.43	0.27	0.27	0.16	0.75	0.39
MP2U	C_{31}	14.0	29.1	0.35	0.73	0.49	0.38	0.33	0.18	0.88	0.40
MP3L	C_{31}	5.7	29.4	0.23	0.81	0.50	0.26	0.17	0.11	0.55	0.36
MP3M	C_{31}	3.0	29.9	0.17	0.85	0.30	0.19	0.06	0.05	0.25	0.24
MP3U	C_{31}	4.4	29.4	0.22	0.83	0.42	0.21	0.14	0.09	0.59	0.38
MP4L	C_{31}	8.8	29.3	0.32	0.74	0.51	0.42	0.26	0.16	0.63	0.35
MP4M	C_{31}	4.6	29.3	0.36	0.72	0.55	0.52	0.32	0.19	0.64	0.34
MP4U	C_{31}	7.1	29.6	0.22	0.81	0.40	0.22	0.13	0.09	0.37	0.33
MP5L	C_{31}	9.4	29.7	0.17	0.86	0.40	0.15	0.09	0.07	0.34	0.35
MP5M	C_{31}	4.1	29.4	0.26	0.80	0.53	0.35	0.19	0.12	0.58	0.33
MP5U	C_{31}	5.3	29.5	0.21	0.83	0.48	0.21	0.15	0.10	0.50	0.37
MP6L	C_{31}	5.0	29.5	0.19	0.84	0.38	0.16	0.11	0.08	0.46	0.36
MP6M	C_{31}	7.1	29.2	0.41	0.68	0.45	0.61	0.33	0.19	0.72	0.31
MP6U	C_{31}	6.5	29.4	0.24	0.81	0.43	0.24	0.16	0.10	0.60	0.38
MP7L	C_{31}	6.4	30.0	0.16	0.86	0.32	0.21	0.06	0.05	0.23	0.22
MP7M	C_{31}	11.0	29.5	0.26	0.79	0.37	0.26	0.15	0.10	0.48	0.34
MP7U	C_{31}	7.3	29.9	0.14	0.88	0.41	0.17	0.06	0.05	0.25	0.26

Sample/*coalfield*	*m/z* 191 hopanes and triterpenoids				*m/z* 123 diterpenoids		
	$(C_{29}+C_{31})/C_{30}$ αβ	C_{31} ββ/(ββ + αβ)	pH	dL/(dL + dO)	AGI	Al-AGI'	Di/Tri
Balingian							
B01-1	–	0.12	3.7	–	–	0.72	0.38

Table 6 (continued)

Sample/*coalfield*	*m/z* 191 hopanes and triterpenoids				*m/z* 123 diterpenoids		
	$(C_{29}+C_{31})/C_{30}$ αβ	C_{31} ββ/(ββ + αβ)	pH	dL/(dL + dO)	AGI	Al-AGI'	Di/Tri
B01-4	5.0	0.27	4.5	0.25	8.44	0.89	0.12
B01-5	–	0.17	4.0	–	–	0.73	0.37
B02-4	2.6	0.29	4.6	0.40	1.32	0.57	0.76
B03-2	7.4	0.21	4.2	0.87	1.13	0.53	0.89
B03-3	10.1	0.17	4.0	0.84	1.21	0.55	0.82
B03-6	–	0.14	3.9	–	–	0.61	0.65
E55-2	17.9	0.19	4.1	0.78	2.34	0.70	0.43
L04A-1	9.7	0.10	3.7	0.71	2.79	0.74	0.36
L04B-1	–	0.12	3.8	–	–	0.43	1.35
ML46A-6	20.3	0.17	4.0	–	0.73	0.42	1.38
ML46A-7	10.1	0.25	4.4	0.84	0.94	0.48	1.06
BG1	6.1	0.29	4.6	0.80	1.01	0.50	0.99
BG2	–	0.36	5.0	0.67	–	0.56	0.77
Mukah							
046A	20.0	0.12	3.8	0.76	1.24	0.55	0.80
M03-2	7.9	0.17	4.0	–	1.36	0.58	0.73
MK1	7.3	0.27	4.5	0.69	0.74	0.43	1.35
MK2	4.8	0.33	4.9	0.32	0.77	0.43	1.31
MK3A	5.7	0.42	5.3	0.33	1.11	0.53	0.90
MK3B	3.4	0.38	5.1	–	1.14	0.53	0.88
Merit-Pila							
MP1L	5.5	0.28	4.6	0.61	1.95	0.66	0.51
MP1M	5.8	0.35	5.0	0.70	0.97	0.49	1.03
MP1U	–	–	–	–	–	–	–
MP2L	5.9	0.34	4.9	0.11	3.21	0.76	0.31
MP2U	5.3	0.27	4.5	–	3.67	0.79	0.27
MP3L	8.2	0.24	4.3	0.54	1.10	0.52	0.91
MP3M	5.8	0.20	4.1	0.48	–	–	–
MP3U	13.6	0.32	4.8	0.30	0.70	0.41	1.42
MP4L	6.4	0.30	4.7	0.32	1.92	0.66	0.52
MP4M	7.7	0.24	4.3	0.11	0.77	0.44	1.30
MP4U	8.9	0.36	5.0	0.38	2.61	0.72	0.38
MP5L	11.3	0.23	4.3	0.16	1.77	0.64	0.56
MP5M	12.5	0.26	4.5	0.07	1.57	0.61	0.64
MP5U	15.8	0.21	4.2	0.17	3.29	0.77	0.30
MP6L	16.8	0.26	4.5	0.40	1.25	0.56	0.80
MP6M	11.6	0.41	5.2	0.18	3.63	0.78	0.28
MP6U	18.9	0.22	4.3	–	1.53	0.60	0.66
MP7L	10.2	0.19	4.1	–	1.59	0.58	0.63
MP7M	6.8	0.30	4.7	0.37	1.71	0.63	0.59
MP7U	23.7	0.18	4.1	0.82	1.59	0.61	0.63

C_{max}, *n*-alkane maxima; Pr, Pristane; Ph, Phytane; ACL, Average Chain Length = $[(27\times C_{27})+(29\times C_{29})+(31\times C_{31})]/[C_{27}+C_{29}+C_{31}]$; P_{aq}, Proxy Aqueous = $[C_{23}+C_{25}]/[C_{23}+C_{25}+C_{29}+C_{31}]$; P_{wax}, Proxy Wax = $[C_{27}+C_{29}+C_{31}]/[C_{23}+C_{25}+C_{27}+C_{29}+C_{31}]$; αβ-Hopane, 17α(H), 21β(H)-Hopane; ββ-Hopane, 17β(H), 21β(H)-norhopane; pH = $[5.22\times C_{31}$ ββ/(ββ + αβ)] + 3.11; dL, 10β(H)-des-A-lupane; dO, 10β(H)-des-A-oleanane; AGI, angiosperm/gymnosperm index (Killops et al. 1995); al-AGI', aliphatic angiosperm-gymnosperm index (Nakamura et al. 2010); Di/Tri, diterpenoids/triterpenoids (Bechtel et al. 2001)

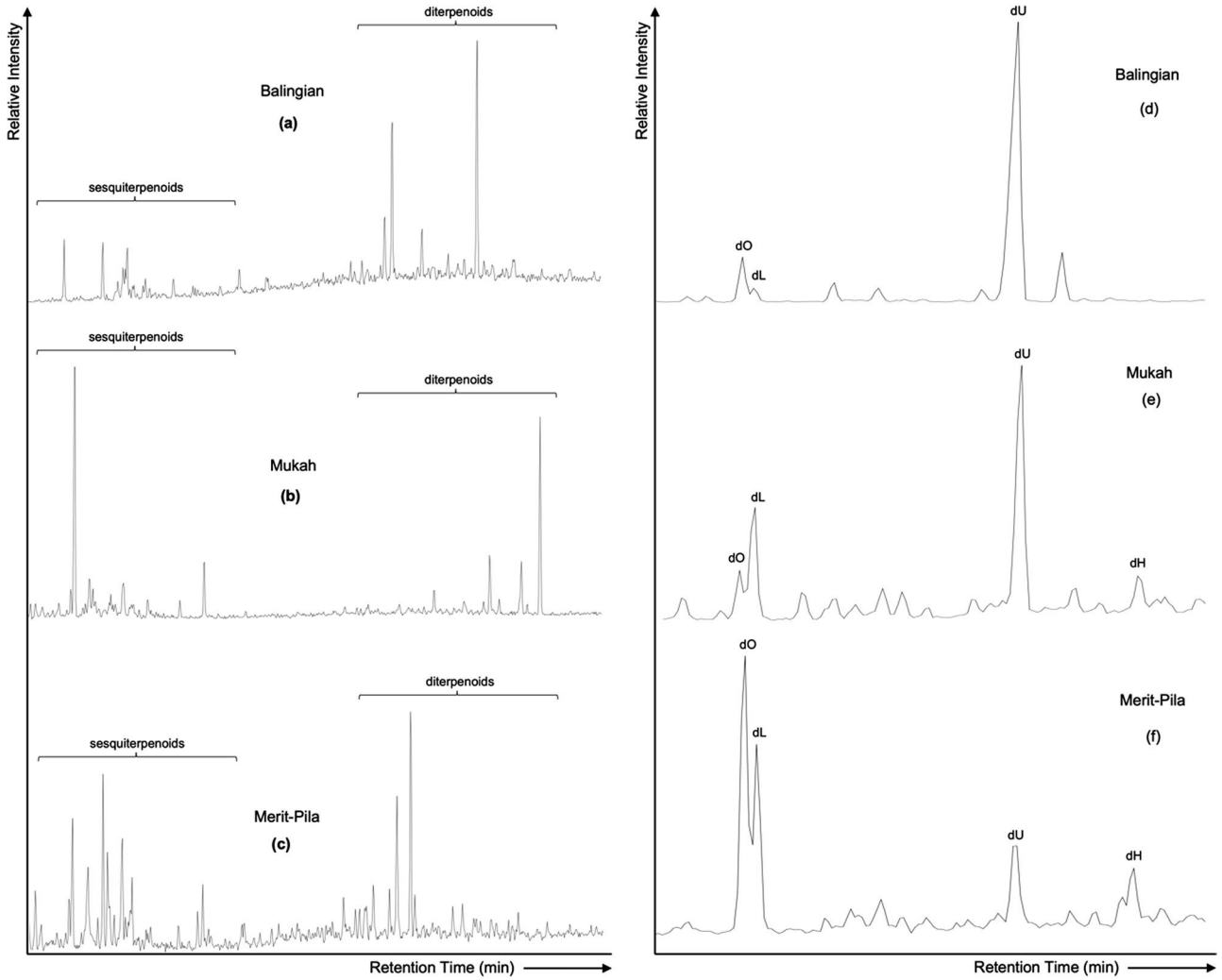

Fig. 3 Partial chromatograms of the aliphatic hydrocarbon fractions showing the distributions of: **a**–**c** Sesquiterpenoids and diterpenoids (*m/z* 123), and **d**–**f** Triterpenoids (*m/z* 191) in representative samples of the Sarawak Basin coals. dO: 10β(H)-des-A-olenane; dL: 10β(H)-des-A-lupane; dU: 10β(H)-des-A-ursane; dH: 18β(H)-des-E-hopane

The changes in abundances of the plant-derived aromatic biomarkers have been employed to track changes in paleoflora due to fluctuating paleoenvironmental conditions (van Aarssen et al. 2000; Romero-Sarmiento et al. 2011; Hautevelle et al. 2006; Marynowski et al. 2013; Grice et al. 2015; Cesar and Grice 2019; Jiang and George 2019; Jiang et al. 2020). The plant-derived biomarker parameters for the studied coals are calculated and recorded in Table 7.

4.6.5 Combustion-derived polycyclic aromatic hydrocarbons

Whereas alkylphenanthrenes and alkylnaphthalenes dominate the total ion chromatograms of the aromatic hydrocarbon fractions of the studied coals, unsubstituted and substituted polycyclic aromatic hydrocarbons (PAHs) with 3–5 rings are also present in relatively low abundances (Fig. 5). Fluoranthene (Fl) and pyrene (Py) were observed in the *m/z* 202 mass chromatograms of the aromatic fractions of the coal extracts, and the abundances of fluoranthene mostly predominate that of pyrene in the analysed samples. Benzo[*a*]anthracene (BaA), chrysene (Ch), and triphenylene (Tph) were detected in the *m/z* 228 mass chromatograms. The co-eluting chrysene and triphenylene are present in all the samples, while benzo[*a*]anthracene is present in some of the samples but particularly absent in the Merit-Pila coals. Additionally, 5-ring PAHs such as benzo[*b,j,k*]fluoranthene (BFl), benzo[*e*]pyrene (BePy), benzo[*a*]pyrene (BaPy), and perylene (Per) were identified in the *m/z* 252 mass chromatograms of some of the coals. However, BFl, BePy, and BaPy are generally absent in the

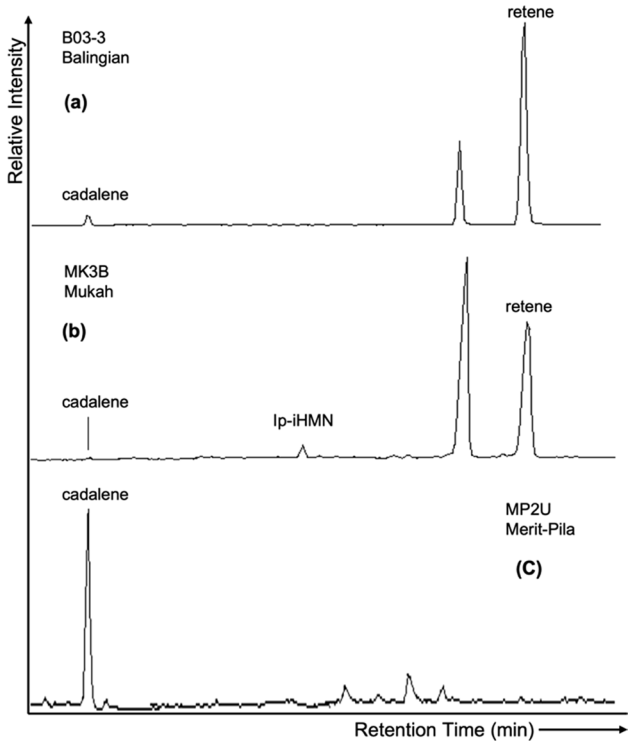

Fig. 4 Summed partial chromatograms of the aromatic hydrocarbon fractions showing the distribution of plant-derived PAHs (*m/z* 183 + 197 + 219), of representative samples. ip-iHMN = 6-*iso*propyl-1-*iso*hexyl-2-methylnaphthalene

Merit-Pila and Mukah coals, while BaPy and Per are mostly absent in the Balingian coals.

5 Discussion

5.1 Paleovegetation, paleohydrology, and paleoclimate

Whereas the abundance of plant-derived biomarkers in sediments is mainly dependent on the original biological source input, it is greatly influenced by prevailing climatic conditions during and after deposition (Jiang et al. 1998; van Aarssen et al. 2000; Hautevelle et al. 2006; Diefendorf and Freimuth 2017). Additionally, other factors such as seasonality, proximity to the coast and soil conditions also influence vegetation type. Hence, plant macrofossils are veritable proxies to reconstruct paleovegetation, paleohydrology, and consequently, paleoclimate. A summary of biomarker proxies for the reconstruction of past vegetation, environment and climate is provided by Naafs et al. (2019).

5.1.1 Bulk isotopes

Higher land plants utilise two main carbon fixation pathways during photosynthesis: C_3 and C_4 pathways. The C_3 pathway developed with the advent of land plants during the Ordovician and thus over 80% of land plant species utilise the C_3 photosynthetic pathway (Rommerskirchen et al. 2006; Cernusak et al. 2013). In contrast, the C_4 pathway evolved during the Tertiary in response to the decline in CO_2 concentration. Recent studies have shown that C_4 plants are favoured by hot, dry conditions, while C_3 plants thrive under cooler, wetter conditions (Bush and McInerney 2015). Hence, temperature and aridity are controlling factors of the proportion of C_3–C_4 plants. The carbon isotopic composition of land plants is widely used to assign plants to the C_3 and C_4 photosynthetic pathways (Meyers 1994; Rommerskirchen et al. 2006; Diefendorf and Freimuth 2017). C_4 plants are isotopically heavier than C_3 plants with mean $\delta^{13}C$ mean bulk values of −14‰ and −27‰, respectively (Meyers 1994). Hence, the bulk $\delta^{13}C$ values for the studied coals signify a C_3 vegetation origin (Fig. 6a).

Furthermore, stable carbon signatures are a proven indicator of major plant groups (i.e. angiosperms and gymnosperms). Plant wax derived from angiosperms are isotopically lighter than those sourced from gymnosperm vegetation (Diefendorf et al. 2011) and in coals, $\delta^{13}C$ values are strongly correlated with the proportion of plant groups (Widodo et al. 2009; Radhwani et al. 2018). The angiosperms-dominated Miocene Embalut lignite and subbituminous, samples from Kutai Basin, Indonesia show $\delta^{13}C$ values between −28.0‰ and −27.0‰ (Widodo et al. 2009) while the gymnosperm-dominated Miocene lignite deposits from Zillingdorf deposit, Austria show $\delta^{13}C$ values between −27.2‰ and −24.6‰ (Bechtel et al. 2007). The $\delta^{13}C$ values for the Tertiary coals from Sarawak vary between −29.4‰ and −24.2‰ with a mean of −28.0‰, −26.7‰, and −28.3‰ for the Balingian, Mukah and Merit-Pila coals, respectively. Additionally, $\delta^{13}C$ values for the studied coals are lower than −26.5‰ except in one Mukah sample (MK2) with an anomalous value of −24.2‰ (Table 3). The studied coals are of different ages and from different localities, and therefore, the varying isotopic composition can be adduced to varying climatic and environmental conditions, and their influences on plant physiology (Bechtel et al. 2008). Hence, the peat-forming vegetation of the Sarawak Basin is considered to be generally dominated by angiosperm taxa but with a significant contribution of conifer vegetation to the Mukah paleopeats.

Similarly, the stable hydrogen isotopic composition of plants and sediments has been employed as a proxy for

Table 7 Aromatic hydrocarbon parameters for the Sarawak Basin coals

Sample/*coalfield*	DBT/P	MDBT/MDBF	A/(A + P)	MP/P	BaA/228	Fl/(Fl + Py)	Py/(Py + Per)	BFl/(BFl + BePy)
Balingian								
B01-1	0.01	0.06	–	0.3	–	0.67	–	–
B01-4	0.03	0.32	–	25.3	0.35	0.57	–	0.74
B01-5	0.04	0.10	0.00	0.3	0.19	0.69	–	0.75
B02-4	0.05	0.34	0.02	0.7	0.41	0.57	–	0.74
B03-2	0.04	0.08	–	0.2	0.22	0.71	–	0.71
B03-3	0.06	0.10	–	10.1	0.22	0.61	–	0.55
B03-6	0.04	0.07	–	0.2	–	0.77	–	0.73
E55-2	0.04	0.12	–	0.7	0.24	0.61	0.95	–
L04A-1	0.06	0.05	–	0.2	0.16	0.77	–	0.71
L04B-1	0.06	0.13	–	0.3	0.20	0.70	–	0.78
ML46A-6	0.03	0.15	–	0.6	0.17	0.62	–	–
ML46A-7	0.03	1.04	0.01	16.5	0.39	0.57	0.88	–
BG1	–	–	0.32	44.0	–	0.58	0.06	–
BG2	0.09	0.30	0.17	14.8	–	0.50	0.10	–
Mukah								
046A	0.05	0.89	0.10	0.4	0.25	0.49	0.67	0.72
M03-2	0.05	0.36	0.08	0.8	0.26	0.59	0.54	0.73
MK1	0.55	0.81	0.14	1.9	0.21	0.62	0.01	–
MK2	0.34	–	0.08	3.0	–	0.57	0.18	–
MK3A	0.36	0.46	–	4.9	0.27	0.59	0.42	–
MK3B	0.27	0.18	–	4.2	0.25	0.46	–	–
Merit-Pila								
MP1L	0.10	0.72	–	4.1	–	0.34	0.86	–
MP1M	0.10	0.33	–	5.5	–	0.20	0.92	–
MP1U	0.04	0.06	0.04	2.5	0.27	0.55	0.80	0.63
MP2L	–	0.64	0.11	4.6	–	0.92	0.27	–
MP2U	–	0.66	–	3.0	0.10	0.82	0.26	–
MP3L	–	0.36	–	3.0	0.12	0.70	0.28	–
MP3M	–	0.13	0.11	1.5	–	0.56	0.52	–
MP3U	–	0.60	–	2.7	–	0.60	0.27	–
MP4L	–	1.46	–	1.6	–	0.84	0.20	–
MP4M	–	0.20	–	5.0	–	0.74	0.22	–
MP4U	–	0.62	–	1.2	–	0.78	0.21	–
MP5L	–	0.55	–	1.2	0.06	0.83	0.56	–
MP5M	–	0.31	–	1.9	–	0.83	0.17	–
MP5U	–	0.27	–	1.1	–	0.60	0.34	–
MP6L	–	0.59	–	4.1	–	–	–	–
MP6M	–	0.94	–	12.3	–	–	–	–
MP6U	–	0.54	–	3.6	–	0.42	0.33	–
MP7L	–	1.84	–	8.0	–	0.81	0.16	–
MP7M	–	0.70	–	17.3	–	0.84	0.13	–
MP7U	–	0.87	–	5.1	–	0.69	0.38	–

Sample/*coalfield*	Ret/Cad	HPP	HPI	mHPI	PAHr
Balingian					
B01-1	5.37	0.84	–	–	0.57
B01-4	–	–	20.4	0.95	0.83
B01-5	11.50	0.92	–	–	0.71

Table 7 (continued)

Sample/*coalfield*	Ret/Cad	HPP	HPI	mHPI	PAHr
B02-4	–	–	9.0	0.90	0.97
B03-2	2.81	0.74	27.6	0.96	0.89
B03-3	25.98	0.96	–	–	0.19
B03-6	2.91	0.74	–	–	0.88
E55-2	0.22	0.18	125.9	0.99	0.35
L04A-1	1.90	0.65	15.7	0.94	0.91
L04B-1	4.64	0.82	31.4	0.97	0.91
ML46A-6	1.77	0.64	–	–	0.64
ML46A-7	–	–	19.6	0.95	0.63
BG1	3.88	0.80	–	–	0.03
BG2	20.66	0.95	–	–	0.23
Mukah					
046A	22.26	0.96	35.4	0.97	0.87
M03-2	2.09	0.68	25.2	0.96	0.83
MK1	4.53	0.82	31.5	0.97	0.84
MK2	23.50	0.96	–	–	0.72
MK3A	31.24	0.97	211.2	1.00	0.16
MK3B	91.79	0.99	463.8	1.00	0.24
Merit-Pila					
MP1L	–	–	9.8	0.91	0.56
MP1M	–	–	46.3	0.98	0.23
MP1U	5.66	0.85	253.5	1.00	0.12
MP2L	0.24	0.19	16.1	0.94	0.67
MP2U	–	–	12.9	0.93	0.75
MP3L	–	–	4.8	0.83	0.88
MP3M	–	–	39.6	0.98	0.41
MP3U	–	–	9.9	0.91	0.79
MP4L	–	–	12.1	0.92	0.69
MP4M	–	–	–	–	0.74
MP4U	–	–	33.3	0.97	0.64
MP5L	–	–	8.8	0.90	0.87
MP5M	–	–	4.4	0.81	0.90
MP5U	–	–	63.4	0.98	0.37
MP6L	–	–	–	–	0.66
MP6M	–	–	–	–	0.30
MP6U	–	–	29.8	0.97	0.37
MP7L	–	–	–	–	0.30
MP7M	0.17	0.14	–	–	0.49
MP7U	–	–	6.1	0.86	0.26

P, Phenanthrene; MP, Methylphenanthrene; MDBF, Methyldibenzofuran; DBT, Dibenzothiophene; MDBT, Methyldibenzothiophene; A, Anthracene; BaA, Benzo[*a*]anthracene; Ch, Chrysene; Tph, Triphenylene; Fl, Fluoranthene; Py, Pyrene; BbFl, Benzo[*b*]fluoranthene; BePy, Benzo[*e*]pyrene; BaPy, Benzo[*a*]pyrene; Per, Perylene; Ret, Retene; Cad, Cadalene; 228 = BaA + Ch + Tph; HPP, Higher Plant Parameter = Ret/(Ret + Cad); HPI, Higher Plant Input = (Ret + Cad + *ip*-iHMN)/1,3,6,7-tetramethylnaphthalene; mHPI, modified HPI = (Ret + Cad + *ip*-iHMN)/(Ret + Cad + *ip*-iHMN + 1,3,6,7-TeMN); PAHr = (P + Py + Fl + Per)/(P + Py + Fl + Per + Ret + Cad)

reconstructing paleoflora and past environmental conditions such as precipitation, temperature and humidity (Dawson et al. 2004; Schimmelmann et al. 2004; Hou et al. 2007; Duan and Xu 2012; Duan et al. 2014; Sessions 2016). Whilst the δD values of meteoric water depend on temperature, length of moisture transport and amount of moisture, the amount of moisture is the most important control on δD values in tropical latitudes such as the study areas (Randlett et al. 2017). Furthermore, δD values mainly reflect continental rainfall fluctuations and, relatively negative δD values

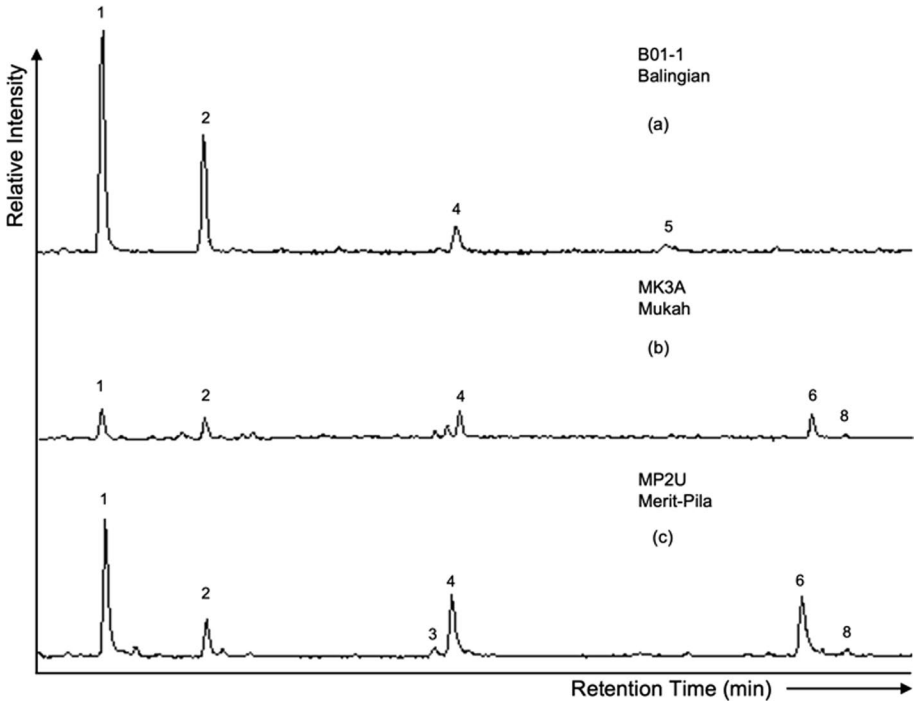

Fig. 5 Summed partial chromatograms of the aromatic hydrocarbon fractions showing the distribution of combustion-derived polycyclic aromatic hydrocarbons (*m/z* 202 + 228 + 252) of representative samples. 1: fluoranthene; 2: pyrene; 3: benzo[*a*]anthracene; 4: chrysene + triphenylene; 5: benzo[*b*]fluoranthene + benzo[*k*]fluoranthene; 6: benzo[*e*]pyrene; 8: perylene

reportedly indicate wetter conditions (Schefuß et al. 2005; Sachse et al. 2012). Paleogeographical and paleoclimatic reconstruction studies have established that the Sarawak Basin was located within the tropical region and under a humid climate throughout the Cenozoic (Friederich et al. 2016). Hence, the observed varying hydrogen isotopic composition can be attributed to past hydrological conditions.

The δD values of the coals are generally higher for the Balingian (− 133.6‰ to − 103.1‰) and Mukah coals (− 130.0‰ to − 91.0‰) than for the Merit-Pila coals (− 173.5‰ to − 122.4‰). The δD values imply relatively warmer, wetter conditions during the accumulation of the Merit-Pila paleopeats in the Late Oligocene to Early Miocene (Fig. 6b). However, the distinct δD values of the Early Miocene Merit-Pila (avg. − 143.4‰) and Mukah (avg. − 117.9‰) coals suggest that isotopic difference is possibly attributable to the distance of the coal seams from the ocean as the Merit-Pila coalfield is further inland. According to Dawson et al. (2004), meteoric water becomes increasingly depleted in deuterium with

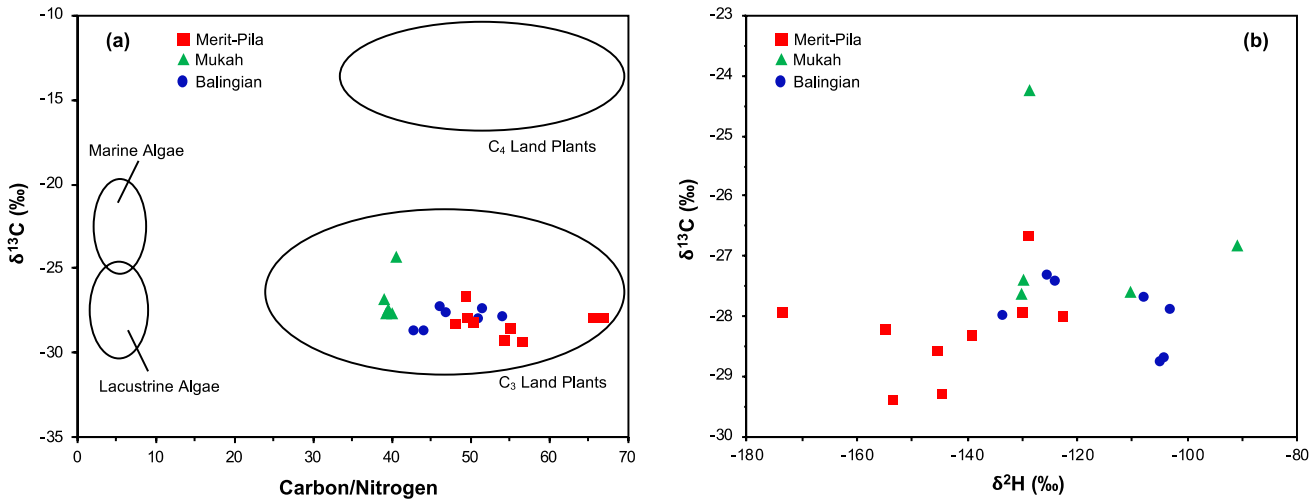

Fig. 6 **a** Source input diagram of atomic ratio versus bulk carbon isotopic value (after Meyers 1994), and **b** Cross plot of bulk carbon and hydrogen isotopic ratios of the studied coals

increasing distance from the ocean due to the 'raining out' of heavier isotopes.

5.1.2 *n*-alkane proxies

Leaf waxes from *Sphagnum* mosses and terrestrial higher plants are correspondingly dominated by medium MW (C_{23} and C_{25}) and high MW (> C_{27}) *n*-alkanes (Baas et al. 2000; Ficken et al. 2000; Nott et al. 2000; Bush and McInerney 2013). In addition, *Sphagnum* mosses and terrestrial higher plants prevail under wetter and drier bog conditions, respectively. Hence, given the abundance of *n*-alkanes and rapidity of GC–MS analysis, various studies have employed *n*-alkane proxies such as P_{wax}, P_{aq}, and average chain length (ACL) to reconstruct past hydrology and accordingly, the vegetation and climate of peatlands (Nichols et al. 2006; Zheng et al. 2007; Andersson et al. 2011). The use of these proxies is based on the established control of hydrology on peatland vegetation and peat decomposition rates (McCabe 1987; Moore 1987; Diessel 1992).

Maximum abundances of *n*-C_{27}, *n*-C_{29}, and *n*-C_{31} are suggestive of the predominant contributions of deciduous trees, conifers, and grasses, respectively, to paleovegetation (Schwark et al. 2002; Ortiz et al. 2013). The relative proportions of the high MW *n*-alkanes in the studied coals show a predominant proportion of C_{31} *n*-alkanes that is suggestive of a predominant contribution of herbaceous vegetation to peat formation (Fig. 7; Ortiz et al. 2013). Furthermore, C_{27}/C_{31} and C_{27+29}/C_{31+33} *n*-alkane ratios are widely used to estimate the relative contribution of woody versus herbaceous inputs to paleovegetation (Schwark et al. 2002; Buggle et al. 2010; López-Días et al. 2013). *n*-C_{27}/*n*-C_{31} and *n*-C_{27+29}/*n*-C_{31+33} values for the Balingian (avg. 0.80 and 1.15), Mukah (avg. 0.98 and 1.21) and Merit-Pila (avg. 0.69 and 1.01) indicate a relatively highest contribution of woody vegetation to the Mukah paleopeats. Similarly, the $(C_{27}+C_{29})/(C_{23}+C_{25}+C_{27}+C_{29}+C_{31}+C_{33})$ *n*-alkane ratio measures the contribution of deciduous trees to paleovegetation (Hanisch et al. 2003). Values of the parameter for the studied Merit-Pila coals (avg. 0.35) are generally slightly lower than in the Balingian (avg. 0.40) and Mukah (avg. 0.39) coals, indicating a higher relative abundance of deciduous trees in the Mukah-Balingian area during the Tertiary (Schwark et al. 2002).

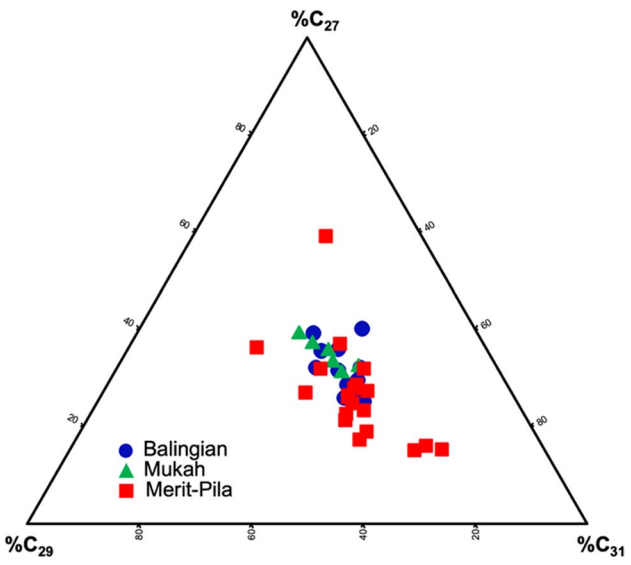

Fig. 7 Ternary diagram of relative abundances of C_{27}, C_{29}, and C_{31} *n*-alkanes in the coals

The ACL measures the average chain length of high MW *n*-alkanes (Poynter and Eglinton 1990). Previous studies have established that plants produce higher MW *n*-alkanes in warmer climates, and non-woody plants produce leaf wax with longer ACL values than woody plants (Rommerskirchen et al. 2006). However, a few studies have noted that ACL is more influenced by precipitation than temperature or vegetation type (Schefuß et al. 2003; Sachse et al. 2006). ACL values > 27 are reportedly indicative of emergent macrophytes and terrestrial plants input (Duan and Xu 2012; Diefendorf and Freimuth 2017) with values generally increasing under warmer and drier conditions (Andersson et al. 2011; Silva et al. 2012; Bush and McInerney 2015). Given these conflicting results, Hoffmann et al. (2013) recommended caution in the use of ACL as a paleoclimate proxy mainly because the parameter can also be affected by vegetational changes. Nevertheless, such concern is not pertinent as the *n*-alkane distributions suggest similar paleovegetation for the studied coals. ACL values for studied coals vary from 28.3 to 30.0, with average values of 29.2, 29.0, and 29.4 for the Balingian, Mukah, and Merit-Pila coals, respectively (Table 6). The higher ACL values for the Merit-Pila samples suggest the paleopeats accumulated under relatively warmer climatic conditions from the Late Oligocene to the earliest Miocene.

The P_{aq} parameter measures the contribution of non-emergent macrophytes to organic matter input (Ficken et al. 2000). Values < 0.1 and > 0.4 correspond to the dominant contribution from terrestrial plants and non-emergent aquatic plants, respectively. P_{aq} values for the studied coals are mostly between 0.1 and 0.4 with average values of 0.26, 0.35 and 0.26 for the Balingian, Mukah, and Merit-Pila coals, which are suggestive of mixed contributions from terrestrial plants and aquatic macrophytes (Ficken et al. 2000). Furthermore, the P_{wax}, parameter estimates the proportion of waxy hydrocarbons derived from terrestrial and emergent aquatic plants (Zheng et al. 2007). P_{wax} values for the studied coals are mostly > 0.7 and with averages of 0.81, 0.74, and 0.78 for the Balingian, Mukah, and Merit-Pila coals, respectively (Table 6). The P_{wax} values indicate the predominant input of land plants (Zheng et al. 2007).

Similarly, the n-C_{23}/n-C_{29} and n-C_{23}/n-C_{31} ratios are proxies to estimate the relative contribution of *Sphagnum* species and vascular plants to peat formation and to reconstruct past mire water-table levels (Nichols et al. 2006). Except for sample MP1U, values of both n-alkane ratios are < 1 for the studied coals (Table 6). In addition, both ratios are higher for the Mukah coals (avg. 0.48 and 0.40) than the Merit-Pila (avg. 0.35 and 0.23) and Balingian (avg. 0.27 and 0.19) coals. The higher n-C_{23}/n-C_{29} and n-C_{23}/n-C_{31} ratios of the Mukah coals indicate a relatively higher contribution of *Sphagnum* to the paleo-peats, which implies relatively higher water table levels.

Following the finding by Sachse et al. (2006) that n-C_{23} can be derived from both aquatic macrophytes and terrestrial plants, Andersson et al. (2011) concluded that the n-C_{23}/n-C_{29} and n-C_{23}/n-C_{31} ratios can be misleading when contributions of *Betula* and *Sphagnum fuscum* to the peat are significant. Consequently, Andersson et al. (2011) proposed the n-C_{23}/(n-C_{27} + n-C_{31}) parameter to accurately reconstruct past water table levels. According to He et al. (2019), n-C_{23}/(n-C_{27} + n-C_{31}) ratios > 0.2 are suggestive of the significant contribution of *Sphagnum* in wetter habitats. Values of the parameter for the Balingian (0.04–0.19), Mukah (0.08–0.39) and Merit-Pila (0.05–0.31) coals indicate that peats accumulated under relatively low water table levels in the Balingian coalfield, high water table level in the Mukah coalfield and intermittent low and high water table levels in the Merit-Pila coalfield.

Overall, n-C_{23}/n-C_{31}, n-C_{23}/(n-C_{27} + n-C_{31}), n-C_{27}/n-C_{31}, and P_{aq} ratios of the investigated Sarawak Basin coals are generally highest for the Mukah coals, and lowest for the Balingian coals. These ratios suggest relatively lower and higher water table levels for paleopeats of the Balingian and Mukah coals, respectively. In addition, the wide-ranging ratios observed for Merit-Pila coals imply intermittent low–high water table levels during peat accumulation.

5.1.3 Plant-derived aromatic hydrocarbons

Aromatic hydrocarbon parameters such as plant fingerprint (PF), higher plant input (HPI) and the modified higher plant input (mHPI) have been employed to evaluate the contribution of land-derived higher plants using the relative distribution of retene, cadalene, *ip*-iHMN and 1,3,6,7-TeMN (van Aarssen et al. 2000; Cesar and Grice 2019; Zakrzewski et al. 2020). Whereas retene, cadalene and *ip*-iHMN are higher plant biomarkers, 1,3,6,7-TeMN is mostly derived from microbial action and thus abundant in both marine and terrestrial sediments (Jiang et al. 1998; van Aarssen et al. 1999). Hence, the HPI is employed to evaluate the contribution of land plants to organic matter (Table 7). The index is calculated from the formula (retene + cadalene + *ip*-iHMN)/1,3,6,7-TeMN. HPI values of all samples are > 1, varying significantly from 4.4 to 463.8 and thus indicative of a varying but predominant input of land plants to organic matter. Similarly, the modified HPI (mHPI), which is calculated from (retene + cadalene + *ip*-iHMN)/(retene + cadalene + *ip*-iHMN + 1,3,6,7-TeMN), ranges from 0.8 to 1.0. The mHPI values are indicative of the dominant proportion of higher plant-derived terrigenous organic matter (Zakrzewski et al. 2020).

Previous studies have found that higher plants that adapt to humid and arid climates are the main sources of retene and cadalene, respectively (Hautevelle et al. 2006; Grice et al. 2015; Xu et al. 2019). Although the abundance of retene has often been associated with gymnosperm contribution to paleoflora, Grice et al. (2007) found no strong association between gymnosperm pollen and the abundance of retene. Additionally, van Aarssen et al. (2000) linked variations in the relative abundances of retene and cadalene to changes in paleoclimate, while Hautevelle et al. (2006) established that the retene/cadalene ratio is unaffected by depositional and diagenetic conditions but by climatic conditions. Cadalene predominated in the earliest Miocene as retene was mostly absent in the Merit-Pila coals. This was perhaps due to the warm and moderately dry climate that prevailed from the Late Oligocene to the earliest Miocene (Jablonski 2005). The Early Miocene Mukah coals are however dominated by retene (avg. 89%) with a subordinate contribution of cadalene (avg. 10%), which coincides with the return of humid climate around 20 Ma (Morley 1998, 2012). The Upper Pliocene Balingian coals are typified by a mostly dominant abundance of retene (avg. 59%) with a significant contribution of cadalene (avg. 41%) and the complete absence of *ip*-iHMN. This finding is supportive of earlier interpretations of seasonal dry conditions in the Sarawak Basin during the Late Pliocene.

5.1.4 Combustion-derived polycyclic aromatic hydrocarbons

The presence of combustion-derived PAHs in sediments is suggestive of past high-temperature events and the consequent reworking of organic matter (Huang et al. 2015). However, PAHs can also be diagenetically derived from algal OM origin (Xu et al. 2019). Nevertheless, the absence of PAHs with 5–7 rings in the studied coals suggests a mostly humid paleoclimate in Sarawak Basin during the Tertiary. The PAHr parameter was proposed by Asiwaju et al. (2023) to measure the abundance of combustion-derived PAHs relative to land plants-derived aromatic biomarkers. Values of the PAHr for the studied Sarawak Basin range broadly from 0.12 to 0.97 and are generally highest for the Pliocene Balingian coals with relatively lower values for the Miocene Merit-Pila and Mukah coals (Table 7).

PAH ratios based on the difference in relative thermodynamic stability have been widely utilized to distinguish between diagenetic/petrogenic and combustion/pyrogenic origins of PAHs in sedimentary rocks and oils (Yunker et al. 2002; Huang et al. 2015; Xu et al. 2019; Zakrzewski et al. 2020). The relative abundance of anthracene (A) to phenanthrene (P) is a widely employed parameter in distinguishing the origins of PAHs, with A/(A + P) ratios > 0.10 indicating a pyrogenic origin (Huang et al. 2015). However, anthracene is mostly absent in the Sarawak Basin, which is indicative of humid paleoclimate. In addition, the ratio of methylphenanthrenes to phenanthrene (MP/P) is another often utilized proxy. MP/P ratios < 1.0 and > 2.0 signify pyrogenic and petrogenic origins, respectively (Yunker et al. 2002; Xu et al. 2019). The calculated MP/P ratios vary broadly from 0.2 to 44.0, 0.4 to 4.2 and 1.1 to 17.3 for the Balingian, Mukah and Merit-Pila coals, respectively (Table 7). These ratios imply a mixed origin of pyrogenic and petrogenic sources for the studied coals. However, the relatively lower (< 1) ratios for most of the Balingian coals imply a predominant pyrogenic origin (Yunker et al. 2002).

The relative abundances of 4-ring PAHs such as Pyrene (Py), fluoranthene (Fl), benzo[a]anthracene (BaA), chrysene (Ch) and triphenylene (Tph), are important combustion markers. According to Yunker et al. (2002), Fl/(Fl + Py) ratios < 0.4 and > 0.5 indicate petrogenic-related and pyrogenic-related sources, respectively. Additionally, Yunker et al. (2002) concluded that BaA/(BaA + Ch + TPh) ratios < 0.20 and > 0.35 imply petrogenic and pyrogenic origins, respectively. The Fl/(Fl + Py) ratios for the Balingian, Mukah and Merit-Pila coals range accordingly from 0.50 to 0.77, 0.46 to 0.62, and 0.20 to 0.92. The ratios are mostly > 0.5, which signifies a dominantly pyrogenic or combustion origin (Fig. 8a). BaA/(BaA + Ch + TPh) ratios are < 0.35 for the Mukah and Merit-Pila coals, signifying petrogenic origins (Table 7). Conversely, BaA/(BaA + Ch + TPh) ratios vary from 0.16 to 0.41 for the Balingian coals, indicating a mixed to pyrogenic origin (Fig. 8b).

5-ring PAHs such as benzopyrenes and benzofluoranthenes are less susceptible to alteration during catagenesis (Jiang et al. 1998). Hence, the relative abundance of summed benzofluoranthenes over benzo[e]pyrene (BFl/(BFl + BePy)) is an effective indicator of the origin of PAHs, with ratios > 0.7 indicating a pyrogenic or combustion origin (Xu et al. 2019). Whilst the 5-ring PAHs are mostly undetected in the Mukah and Merit-Pila coals, BFl/(BFl + BePy) ratios for the Balingian coals vary from 0.55 to 0.78 and thus indicate a mixed to pyrogenic origin. In general, the relatively higher Fl/(Fl + Py), BaA/(BaA + Ch + TPh) and BFl/(BFl + BePy) ratios of the Balingian coals are suggestive of low-temperature fire events, which supports our interpretations of frequent dry episodes during the Pliocene.

5.1.5 Elemental abundance

The abundance of elements in coals provides important information on paleoenvironmental conditions and several studies have documented the effect of paleoclimate on the elemental composition of coals (Bai et al. 2015; Li et al. 2019; Lv et al. 2019; Liu et al. 2021; Zhou et al. 2021). Hence, bimetal ratios such as Sr/Cu, Rb/Sr and Ga/Rb are often employed as paleoclimate proxies (Cao et al. 2012; Krzeszowska 2019).

The low Rb/Sr ratios (< 1) for all the coals generally indicate warmer climatic conditions (Krzeszowska 2019). Furthermore, the relative abundance of strontium over copper (Sr/Cu) has been used to determine climatic conditions. Sr/

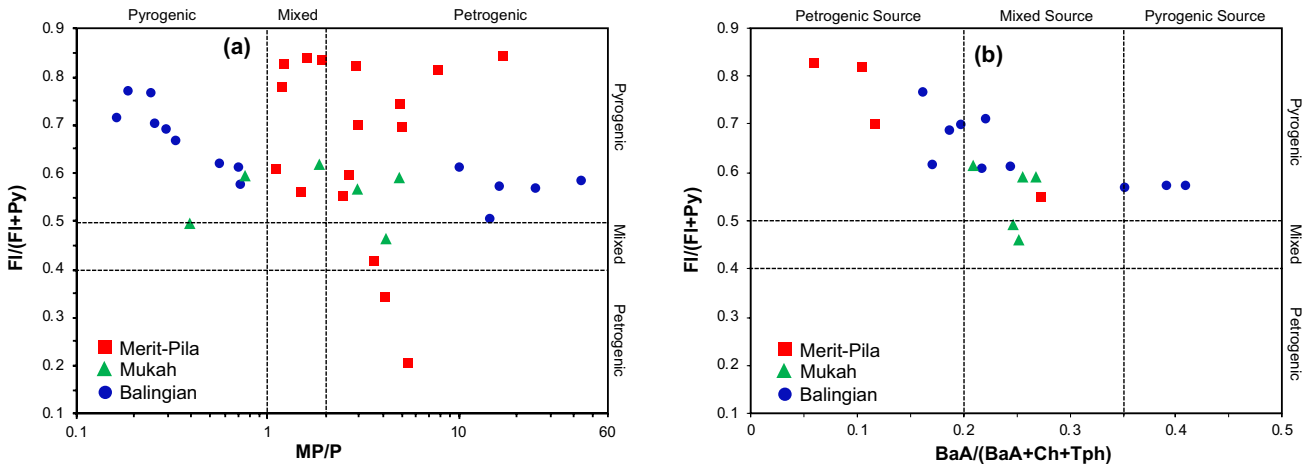

Fig. 8 **a** Cross-plots of MP/P versus Fl/(Fl + Py) and **b** BaA/(BaA + Ch + Tph) versus Fl/(Fl + Py). MP: methylphenanthrenes; P: phenanthrene; Fl: fluoranthene, Py: pyrene; BaA: benzo[*a*]anthracene; Ch: chrysene; Tph: triphenylene

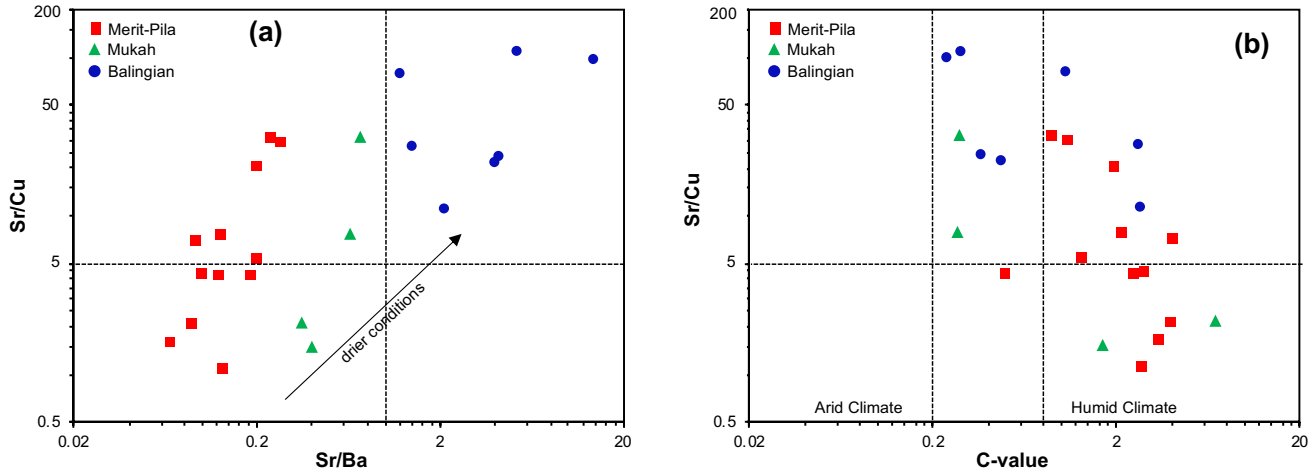

Fig. 9 Cross-plots of **a** Strontium/barium (Sr/Ba) ratio versus strontium/copper (Sr/Cu) ratio, and **b** C-value versus Sr/Cu ratio, showing paleoclimatic conditions

Cu ratios between 1.5 and 5.0 reportedly indicate a humid climate, while ratios > 5.0 indicate an arid climate (Sarki Yandoka et al. 2015; Han et al. 2020). The Sr/Cu ratio ranges from 11.1 to 108.1, 1.5 to 31.9, and 1.1 to 30.9 for the Balingian, Mukah and Merit-Pila coals. The ratios are suggestive of relatively drier climatic conditions for the Balingian coals and fluctuating wet and dry conditions during the accumulation of the Mukah and Merit-Pila paleopeats. The Sr/Ba ratio is another widely utilized bimetal proxy for paleoclimate, and ratios < 1 and > 1 generally imply humid and arid climatic conditions, respectively (Dai et al. 2020). Sr/Ba ratios for the Merit-Pila (avg. 0.15) and Mukah (avg. 0.54) coals are < 1 whilst ratios for the Balingian coals (avg. 4.58) are > 1 (Table 5). The cross-plot of Sr/Ba and Sr/Cu ratios in Fig. 9a shows that the Merit-Pila and Mukah coals were deposited under wetter conditions of a warm and humid climate in the Late Oligocene to Early Miocene, while the Liang Formation coals accumulated under relatively drier conditions in the Late Pliocene.

Furthermore, the *C*-value, defined as [Fe + Mn + Cr + Ni + V + Co]/[Ca + Mg + Sr + Ba + K + Na], is an effective proxy of paleoclimate in mudstones and its values reduce with increasing aridity. According to Cao et al. (2012), ratios of the *C*-value parameter < 0.2 and > 0.8 corresponds, respectively, to arid and humid climate. The *C*-value ratios are > 0.2 for all the studied Sarawak Basin coals, ranging from 0.24 to 6.94 and with averages of 1.12, 2.29, and 2.29, respectively, for the Balingian, Mukah, and Merit-Pila coals (Table 5). The ratios are indicative of peat accumulation in humid climates (Fig. 9b). Additionally, the lower ratios for the Balingian coals corroborate the interpretation of relatively drier conditions in the Late Pliocene.

In a study of coals and shales from Huangxian Basin, China, Lv et al. (2019) established that SiO_2/Al_2O_3 ratios are indicative of redox and climatic conditions during deposition. According to the workers, SiO_2/Al_2O_3 ratios increase with decreasing humidity. Generally, the SiO_2/Al_2O_3 ratios are highest for the Balingian coals (1.0–6.6) and lowest for the Mukah coals (0.4–1.8). These ratios corroborate our interpretation of less humid and more humid conditions during peat accumulation in the Pliocene and Miocene, respectively. Additionally, consistent with previous interpretations, the Merit-Pila coals show varying ratios of SiO_2/Al_2O_3 (0.2–7.3) that are suggestive of fluctuating wet-dry conditions.

The interpretation of considerably drier conditions during the accumulation of the Balingian peats in the Late Pliocene and a warm, tropical wet-dry climate when the Mukah and Merit-Pila peats accumulated in the Late Oligocene to Early Miocene is corroborated by published paleovegetation (Morley 1998; Barry et al. 2002; Widodo et al. 2009) and paleoclimate (Zachos et al. 2001; Jablonski 2005; Morley 2012; Holbourn et al. 2014; Friederich et al. 2016) studies. According to Morley (1998, 2012), plant dispersal in the SE Asia region has been mainly controlled by climate since the Eocene and the climate from Late Oligocene to the earliest Miocene was warm and considerably drier. However, moist climate and tropical rain forests became widespread in the Early Miocene (~ 20 Ma) until the Middle Miocene (~ 15 Ma) when warming peaked. This was followed by a period of gradual cooling, increased aridity, the recession of rain forests and expansion of grasslands from the Middle Miocene to the Early Pliocene (Barry et al. 2002; Chamberlain et al. 2014). In contrast, the Early Pliocene was marked by a subtle warming trend that ended in the Late Pliocene (~ 3.2 Ma) when glaciation resumed with pronounced seasonal climates in the Late Pliocene and Quaternary (Morley 1998; Zachos et al. 2001; Jablonski 2005).

The wide variation in values of *n*-alkane proxies (n-C_{23}/n-C_{29}, ACL, P_{wax}, P_{aq}) for the Merit-Pila and, to a lesser degree in the Mukah coals indicates fluctuating peat hydrological conditions (Zheng et al. 2007). This finding suggests that Merit-Pila coals were deposited under the tropical wet-dry climate that prevailed in the Late Oligocene and earliest Miocene and are probably stratigraphically older than the Mukah coals which accumulated under the relatively stable humid conditions of the Early to Middle Miocene, possibly between 20 and 15 Ma (Morley 1998, 2012; Jablonski 2005). Palynological and sedimentological investigation of the Mukah coals and sediments by Murtaza et al. (2018) showed the occurrence of *Florscheutzia trilobata* and *Florscheutzia levipoli* and based on this finding, the authors assigned an Early to Middle Miocene age. In addition, Hennig-Breitfeld et al. (2019) ascribed Oligocene to Early Miocene, and uppermost Early to Middle Miocene ages to the Nyalau and Balingian Formations, respectively. Hence, the geochemical interpretations of this research support the conclusions by Murtaza et al. (2018) and Hennig-Breitfeld et al. (2019) of the latest Oligocene to Early age for the Merit-Pila coals, and Early to Middle Miocene age for the Mukah coals (Fig. 1b).

Although most studies have ascribed a Pliocene to Pleistocene age to the Balingian coals, the revised stratigraphy proposed by Hennig-Breitfeld et al. (2019) suggests a latest Middle Miocene age. Interpretations of *n*-alkane proxies, bimetal ratios and δD values indicate relatively warmer and drier conditions during the accumulation of the Balingian paleopeats. This interpretation is further corroborated by preliminary results of the oxygen isotopic ($\delta^{18}O$) analysis of the studied coals which show a 2‰ decline in $\delta^{18}O$ values from Mukah to Balingian coals, signifying relatively warmer climatic conditions (Zachos et al. 2001).

The Middle Miocene is generally characterised by cooler climatic conditions (Holbourn et al. 2014). A global climate study by Zachos et al. (2001) established that $\delta^{18}O$ values increased after Middle Miocene Climate Optimum (MMCO) until the Early Pliocene when $\delta^{18}O$ values declined due to warming. Warming events are often accompanied by rising sea levels and decreasing surface productivity, which are accordingly reflected by higher Sr/Ca and lower $\delta^{13}C$ values (Stüben et al. 2003). Average $\delta^{13}C$ values are lower for the Balingian coals (-28.0‰) than the Mukah coals (-26.7‰), while average Sr/Ca ratios are higher for Balingian coals (0.029) than the Mukah coals (0.016). These findings validate relatively warmer depositional conditions for the Balingian coals. Hence the geochemical evidence presented in this research contradicts the latest Middle Miocene age recently assigned by Hennig-Breitfeld et al. (2019).

Nevertheless, the palynological study by Sia et al. (2019) concluded that the Balingian coals were dominated by palynomorphs, and characterized by a strong diversity of species, which according to the authors suggests wet climatic conditions. Additionally, a review of the climate in the Cenozoic by Morley (2012) concluded that the Borneo Island areas have, without interruption, experienced ever-wet climates since the Late Miocene. These petrography and palynology interpretations of ever-wet conditions in the Late Pliocene contradict this research's biomarker and elemental data interpretation of relatively drier conditions. This is possibly due to the highly seasonal climate in the Late Pliocene which limited peat fires and ensured minimal diversity of species (Jablonski 2005).

5.2 Paleodepositional conditions

5.2.1 Paleoenvironments

The relative abundances of aromatic compounds such as phenanthrene (PHE), naphthalene (Np), dibenzofuran (DBF), fluorene (F), and dibenzothiophene (DBT) are effective markers of facies and depositional environments (Pu et al. 1990; Hughes et al. 1995; Radke et al. 2000; Asif and Wenger 2019). In general, the relative abundances of PHE, F and DBF are higher in source rocks from freshwater sedimentary environments than in those from marine environments whilst the abundances of DBT and Np are relatively higher in source rocks from marine environments. Hence, the predominant abundance of PHE over DBT and DBF in the analysed coals signifies non-marine depositional environments (Pu et al. 1990). Although the dominance of methylphenanthrenes (MPs) over methyldibenzofurans (MDBFs) and methyldibenzothiophenes (MDBTs) is less pronounced, the moderately high abundance of MDBFs supports the interpretation of a non-marine depositional environment (Radke et al. 2000).

Hughes et al. (1995) utilized the cross-plot of dibenzothiophene/phenanthrene (DBT/PHE) and pristane/phytane (Pr/Ph) ratios to differentiate five distinct environments and lithologies (Fig. 10a). The studied coals plot across zones C, D and E, which corresponds to lacustrine (sulphate-poor), marine and lacustrine, and fluvio-deltaic depositional environments, respectively. Whilst the Balingian coals plot across zones C, D and E, Mukah coals plot in zones D and E, and the Merit-Pila coals are mostly within zone E (Fig. 10a). Due to the dominant abundance of PHE over DBT in terrestrial sedimentary environments, Radke et al. (2000) modified the Hughes et al. (1995) diagram to differentiate high-rank coals and mature mudstones by plotting Pr/Ph ratios against MDBT/MDBF ratios. Similarly, the studied coals plot in the zones C, D and E of the modified diagram (Fig. 10b), thus corroborating the interpretation of peat accumulation in a lacustrine swamp to fluvial/deltaic depositional environments.

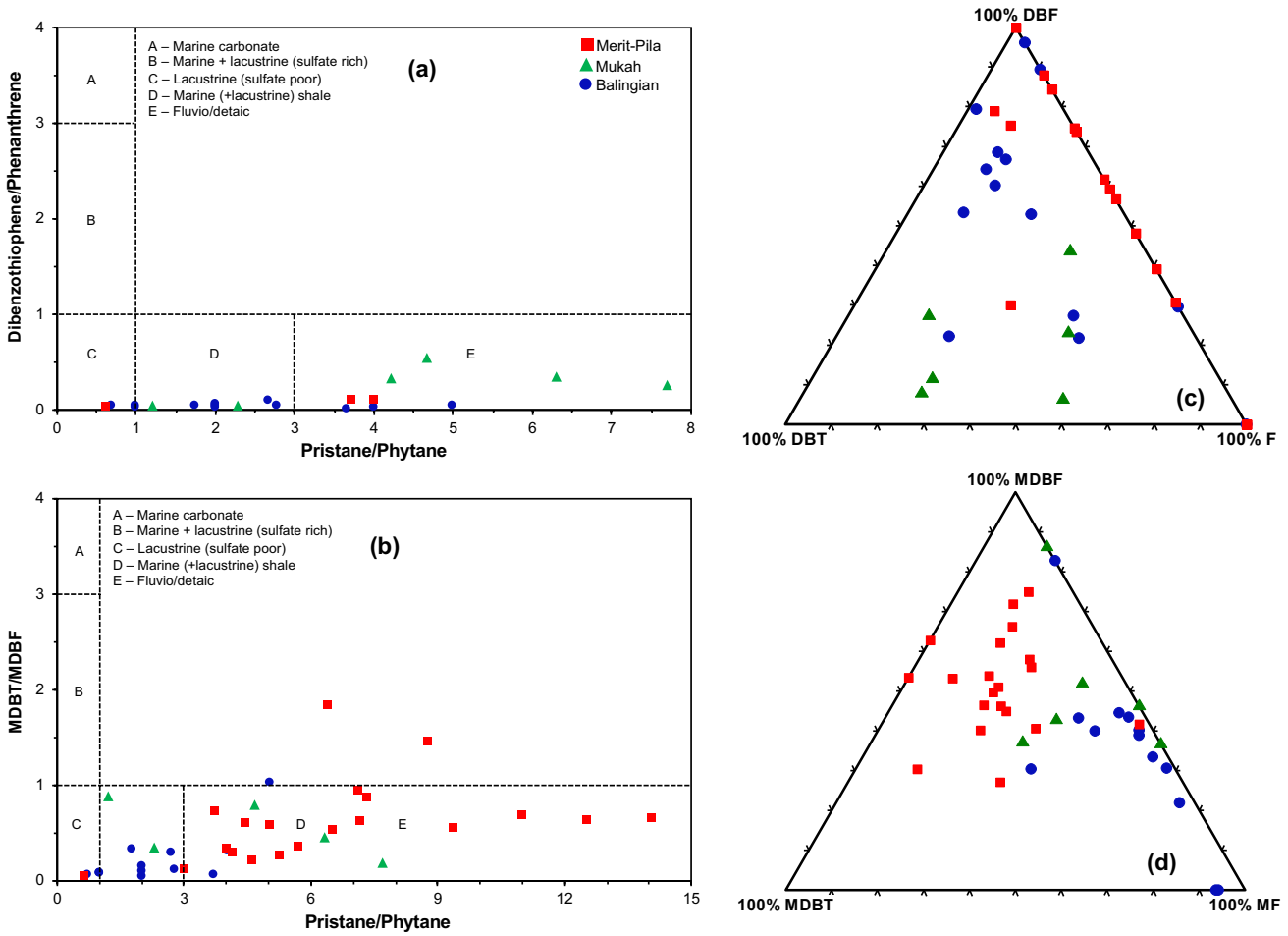

Fig. 10 **a** Cross-plot of pristane/phytane ratios versus dibenzothiophene/phenanthrene ratios (after Hughes et al. 1995) **b** Cross-plot of pristane/phytane ratios vs. methyldibenzothiophenes/methyldibenzofurans (MDBT/MDBF) ratios (after Radke et al. 2000) **c** Ternary plot of the relative abundance of fluorene (F), dibenzofuran (DBF) and dibenzothiophene (DBT) and **d** Ternary plot of the relative abundance of methylfluorenes (MF), methyldibenzofurans (MDBF) and methyldibenzothiophenes (MDBT) for the studied Sarawak Basin coals

Furthermore, Asif and Wenger (2019) utilized the ternary diagram of the relative abundances of F, DBF and DBT to differentiate source facies. The authors reported that freshwater lacustrine-, coaly-, and marine carbonate-sourced oils have the highest abundances of F, DBF and DBT, respectively. The ternary plot of %F, %DBF and %DBT in Fig. 10c shows that the studied coals are generally characterised by the predominant abundance of DBF and F and subordinate abundance of DBT, which is suggestive of terrestrial organic matter deposited in freshwater- to lacustrine-swamp environment (Asif and Wenger 2019). DBF (avg. 52.3%) predominates over F (avg. 28.9%) and DBT (avg. 18.8%) in the Balingian coals, while DBF (avg. 50.1%) and F (avg. 46.7%) predominate over DBT (avg. 3.2%) in the Merit-Pila coals. Conversely, DBT (avg. 44.1%) predominates over F (avg. 35.9%) and DBF (19.9%) in the Mukah coals, which is suggestive of brackish-water influence.

The methylated homologue distributions of the heterocyclic compounds are characterized by the predominant abundances of MDBF and MF, and the subordinate abundance of MDBT (Fig. 10d). However, MDBF/MF ratios vary widely from 0.29 to 6.30 with generally highest and lowest ratios, respectively, for the Merit-Pila (avg. 2.75) and Balingian (avg. 1.00) coals, while the Mukah coals show intermediate ratios (avg. 1.89). The wide range of MDBF/MF ratios supports the finding of varying depositional sub-environments as higher MDBF/MF ratios imply swampy paleoenvironment for Merit-Pila coals, while lower ratios suggest freshwater lacustrine paleoenvironment for the Balingian coals (Asif and Wenger 2019).

5.2.2 Paleoredox conditions

The pristane-to-phytane ratio is an important indicator of paleoenvironmental conditions (Didyk et al. 1978). Pr/Ph values < 0.8 indicate saline to hypersaline conditions, while values > 3 suggest terrigenous organic matter deposited under oxic conditions (Peters et al. 2005). The Pr/Ph ratios for the Balingian coals are mostly > 1, with an average value of 2.3 which is indicative of deposition under suboxic to dysoxic paleoenvironmental conditions. In contrast, Pr/Ph ratios for the Mukah and Merit-Pila coals are mostly > 3, with average values of 4.4 and 6.5, respectively (Table 6). The ratios for the Mukah and Merit-Pila coals are indicative of peat accumulation under fully oxidizing conditions.

The abundances of trace elements and bimetal proxies such as V/Cr, V/Ni and Ni/Co have been widely used to infer paleoredox conditions (Jones and Manning 1994; Algeo and Maynard 2004; Tribovillard et al. 2006; Kombrink et al. 2008; Bennett and Canfield 2020). For instance, the concentrations of Mo, U and V have been found to increase under reducing conditions (Tribovillard et al. 2006), while V and Ni are more abundant in minerotrophic than ombrotrophic peats (Shotyk 1988). However, a recent study by Algeo and Liu (2020) re-examined the thresholds for bimetal proxies established by Jones and Manning (1994). The authors noted that the universal adoption of proxy thresholds established for sediments of specific formations and ages is problematic, and concluded that thresholds must be applied cautiously. Although these paleoredox proxy thresholds may not be suitable for determining the specific redox conditions in coal depositional environments, the parameters are nonetheless useful for a comparative evaluation of the degree of varying redox conditions.

The low concentrations of Mo (< 1 ppm), U (< 0.2 ppm), V (< 20 ppm), and Ni (< 20 ppm) in the studied coals indicate oxic to suboxic depositional conditions (Tribovillard et al. 2006; Galarraga et al. 2008). However, the relatively higher Zn abundance in the Balingian and Mukah coals suggests intermittent less oxidizing reducing conditions (Algeo and Maynard 2004; Kombrink et al. 2008). Furthermore, V/Cr and Ni/Co ratios are widely utilized proxies for reconstructing redox conditions in argillaceous rocks. Ni/Co and V/Cr ratios < 5 and < 2, respectively, indicate oxic conditions, while ratios > 5 and > 2 reflect reducing conditions (Jones and Manning 1994). V/Cr ratios for the studied coals vary from 0.36 to 2.03 whilst Ni/Co ratios (except MP6M) are < 5.0 (Table 5). Hence, the V/Cr and Ni/Co ratios generally indicate oxic depositional conditions (Fig. 11). The Fe/Al ratio is another indicator of paleoredox condition as Fe enrichment is favoured by reducing conditions (Tribovillard et al. 2006; Algeo and Liu 2020). The Fe/Al ratios range

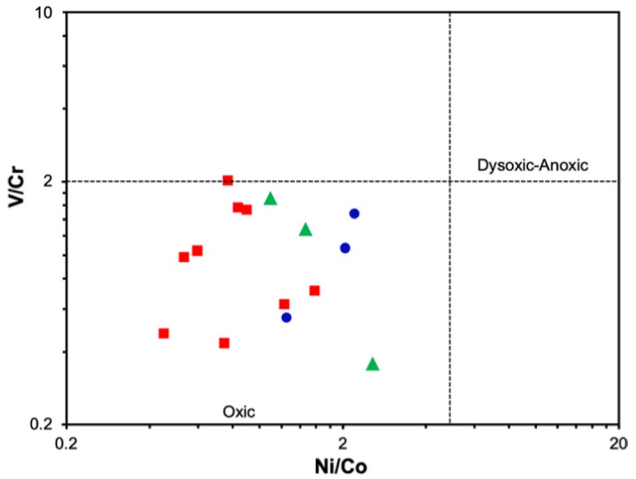

Fig. 11 Cross-plot of nickel/cobalt (Ni/Co) and vanadium/chromium (V/Cr) ratios, showing paleoredox conditions

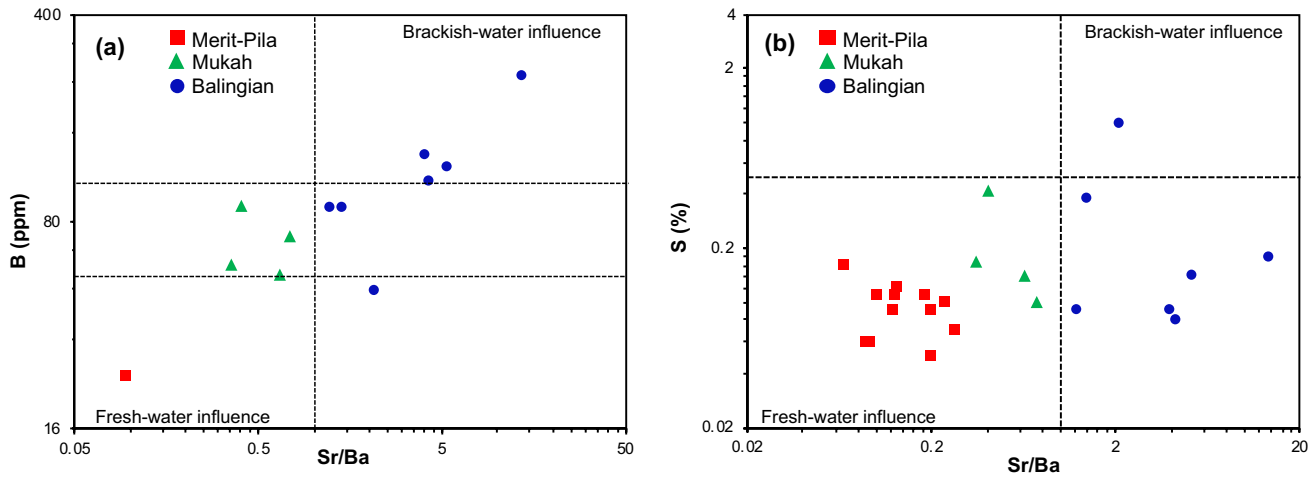

Fig. 12 Plots of strontium/barium (Sr/Ba) ratio versus **a** Boron concentration and **b** Sulphur content in the studied coals

from 0.1 to 28.0 with mean values of 13.4, 4.7 and 5.2 for the Balingian, Mukah and Merit-Pila, respectively. These ratios suggest the Balingian coals were deposited under relatively less-oxidizing conditions (Tribovillard et al. 2006).

5.2.3 Paleosalinity and marine influence

The Sr/Ba ratio could be a useful indicator of freshwater and seawater influence in depositional environments, and ratios > 1 and < 1 are indicative of marine-influenced and freshwater-influenced environments, respectively (Gayer et al. 1999; Dai et al. 2020). The Sr/Ba ratios are > 1 for the Balingian (1.4–13.8) coals and < 1 for the Mukah (0.4–0.7) and Merit-Pila (0.1–0.3) coals, suggesting some marine influence on the Balingian coals (Fig. 12). Furthermore, the total abundance of B can indicate paleosalinity (Diessel 1992; Dai et al. 2020). According to Goodarzi and Swaine (1994), B concentrations in coals < 50 ppm and > 110 ppm, respectively, indicate freshwater and brackish water influence, while concentrations between 50 and 110 ppm indicate mildly brackish water influence. The concentration of B in the Merit-Pila coals is generally below the detection limit of 20 ppm. However, B concentration ranges from 47 to 248 (avg. 119 ppm) and 53 to 91 (avg. 68 ppm), respectively, for the Balingian and Mukah coals (Table 4). Hence, the low (< 50 ppm) concentration of boron in the Merit-Pila coals is suggestive of low salinity typical of a freshwater depositional environment, while higher concentrations (> 50 ppm) in the Balingian and Mukah coals infer mildly brackish-water influenced depositional environments (Fig. 12a).

The incursion of sulfate-rich karstic aquifer support into freshwater paleomires has resulted in elevated S_T content (Siavalas et al. 2009; Oskay et al. 2016). Nevertheless, the S_T content of coals is a widely utilised indicator of marine influence on coal seams (Casagrande 1987; Chou 2012; Dai et al. 2020). According to Sykes et al. (2014), S_T content > 0.5 wt% indicates some degree of seawater influence, with S_T contents in the 0.5 wt%–1.5 wt%, and > 1.5 wt% range regarded as indicating slight and strong marine influence, respectively. S_T contents vary from 0.13 wt% to 1.48 wt%, 0.20 wt% to 0.85 wt%, and 0.09 wt% to 0.30 wt% for the Balingian, Mukah, and Merit-Pila coals, respectively (Table 2). The S_T contents generally indicate freshwater conditions with possible slight seawater influence on the Balingian and Mukah coals (Fig. 12b).

This finding is supported by the reported presence of cleat-filling pyrite in the Balingian coals, and framboidal pyrite in some of the Mukah coals (Sia and Abdullah 2012; Sia et al. 2014). The epigenetic pyrites found in the Balingian coals are indicative of the post-depositional influence of percolating sulfate-rich waters. In contrast, the observed syngenetic, framboidal pyrites in the Mukah coals are suggestive of brackish conditions during peat accumulation (Widodo et al. 2010). The Mukah paleopeats were possibly inundated by sulfate-rich lake waters or sulfate-rich groundwater but increased precipitation in the Early Miocene ensured that peat accumulation continued (Diessel 1992, pg. 15). This postulation is supported by the substantially lower terrigenous OM input in the Mukah coals (avg. 6.0) when compared with Balingian and Merit-Pila coals (avg. 19.1 and 16.6).

The Fe content of coals has been closely related to the abundance of pyritic sulfur (Kombrink et al. 2008; Spears and Tewalt 2009; Widodo et al. 2010). The correlation coefficient ($r = -0.40$) between Fe and S content of the studied Sarawak Basin coals is negative and weak. Conversely, strong and positive relationships ($r = 0.86$ and 0.92) were reported by Widodo et al. (2010) for some Indonesian coals, and by Spears and Tewalt (2009) for the marine-influenced British Parkgate coals. Hence, the weak, negative correlation between Fe and S corroborates the near absence of pyritic sulfur and the finding of slight or no seawater influence.

Pyrite formation is enhanced by the combination of sulfate-rich groundwater and Fe-rich mire waters (Dellwig et al. 2001). However, the supply of sulfate-rich groundwater must be greater than Fe-rich mire waters to create a system that is Fe-deficient and thus with excess sulfur. According to Marshall et al. (2015), all available sulfur in peats with Fe/S ratios > 0.87 is presumably sequestered as pyrite and the excess iron deposited as Fe-carbonates. The additional supply of sulphate-rich groundwater, however, reduces the Fe/S ratio below 0.87, creating excess sulfur that ultimately forms organosulfur compounds (Sinninghe Damste and De Leeuw 1990; Marshall et al. 2015). Calculated Fe/S ratios range from 0.1 to 13.0 with averages of 3.1, 1.9, and 6.2 for the Balingian, Mukah, and Merit-Pila coals (Table 5). These ratios mostly suggest the absence of excess S required to form organosulfur compounds in the paleopeats. Nonetheless, the Fe/S ratios also indicate a relatively higher supply of sulfate-rich sea water into the Mukah mires, which corroborates the finding of minor marine influence.

The S_T content of coals has also been associated with the pH conditions of peat-forming mires (Cecil et al. 1985; Casagrande 1987; Bechtel et al. 2003). Additionally, the acidity of peatlands is negatively correlated with the abundance of pyritic sulfur (Diessel 1992). Therefore, the generally low sulfur content of the studied Sarawak Basin coals signifies mostly low pH (< 4) conditions during peat formation as the high acidity of mire waters inhibits sulfur fixation (Cecil et al. 1985). This interpretation is supported by the predominant abundance of the stable geological C_{31} αβ-22R-homohopane (C_{31}αβR) over its less stable, biological C_{31} ββ-hopane. According to Inglis et al. (2018), αβ-hopanes are products of the acid-catalyzed oxidation and decarboxylation reactions of bacteriohopanetetrol, and thus, the presence of C_{31}αβR in peats has been observed to be strongly dependent

on pH (Dehmer 1995; Bechtel et al. 2003). Additionally, Inglis et al. (2018) established a significant, positive correlation between the C_{31} ββ/(αβ + ββ) ratio and pH. Values of the C_{31} ββ/(αβ + ββ) ratio for the studied coals vary from 0.10 to 0.42 whilst the corresponding calibrated pH values vary from 3.7 to 5.3 (Table 6). The estimated pH values are mostly > 4, indicating less acidic conditions that are typical of planar peat deposits (Cecil et al. 1985). Nevertheless, the average pH value for the Balingian (4.2), Mukah (4.6), and Merit-Pila (4.5) coals is corroborative of relatively less acidic conditions in the Mukah paleopeats.

Elevated U concentrations and low Th/U ratios in coals have been linked to sea-water influence (Gayer et al. 1999). Therefore, the low U concentration (< 0.1 ppm) and high Th/U ratios (> 4.8) for the studied coals signify little or no seawater influence (Gayer et al. 1999; Kombrink et al. 2008). Whereas the generally low S and U abundances and high Th/U ratios for the Balingian coals suggest no marine influence, high boron concentration and Sr/Ba ratios suggest a brackish-water influence on the coals (Fig. 12). These contradictory interpretations highlight the drawbacks of elemental paleosalinity proxies as the concentrations of elements can be affected by physicochemical processes in source areas (Dai et al. 2020). For example, Moore et al. (2005) attributed the high B concentration (up to 7000 ppm) in some coals from Waikato, New Zealand to precipitation from hydrothermal solutions. Similarly, Gürdal and Bozcu (2011) attributed the high S_T content (up to 12.2 wt%) in some Çan Basin coals from Turkey to regional volcanic activity. Nevertheless, the average B concentration (1838 ppm) for the Waikato coals investigated by Moore et al. (2005) is two orders of magnitude higher than the global average value (52 ppm) reported by Ketris and Yudovich (2009). In contrast, B concentrations (< 248 ppm) in the studied Balingian coals are significantly lower and can thus be plausibly explained by the post-burial influence of seawater or saline lacustrine water (Dai et al. 2020). First, this hypothesis is supported by the positive correlations of B with CaO ($r = 0.822$) and MgO (0.614), and negative correlations with ash yield ($r = -0.196$) and K_2O ($r = -0.435$), which are suggestive of a mixed organic/inorganic association (Spears 2017). This hypothesis is corroborated by the presence of cleat-filling pyrites that were incorporated after compaction/partial consolidation of the Balingian paleopeats (Widodo et al. 2010; Sia and Abdullah 2012).

The ash content of coals correlates strongly and positively with mineral and sulfur contents (Widodo et al. 2010). Ombrotrophic peats are typified by low S_T and mineral contents, while rheotrophic peats which are subjected to regular flooding are characterized by high ash content (Anderson 1964; Dehmer 1993). Hence, the generally low S_T and low to moderately high ash contents of the studied coals indicate the presence of ombrotrophic and rheotrophic peat deposits,

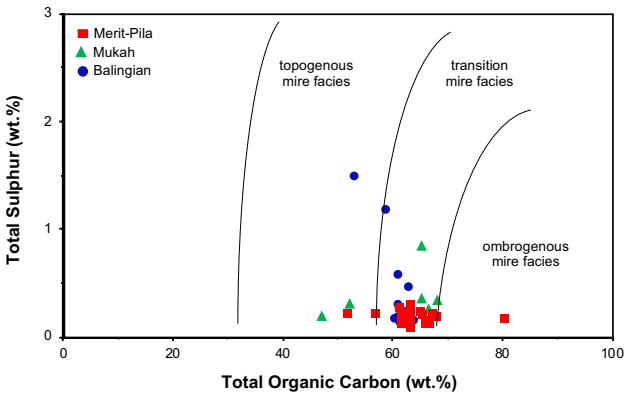

Fig. 13 Cross-plot of total organic carbon vs. total sulphur (after Jasper et al. 2010)

and their proportion connotes the evolutionary development of the Sarawak paleopeats. Lower ash contents in the basal layers of the Merit-Pila coals suggest that peat accumulation in the coalfield possibly originated under ombrotrophic mire settings but morphed into rheotrophic mire settings with the observed higher ash contents in samples of the upper coal zone. Similarly, the Mukah coals are characterised by varying ash content (0.8 wt%–37.5 wt%) which also suggests the presence of multiple mire facies (Fig. 13). This finding is corroborated by Zainal Abidin et al. (2022), which found that due to rising water table levels, peat accumulated originally in ombrotrophic mires but ultimately in rheotrophic mires. In contrast, the Balingian coals generally contain low ash (avg. 7.3 wt%) and S_T (avg. 0.40 wt%) contents, typical of ombrogenous peats (Anderson 1964; Moore 1987; Dehmer 1993). This interpretation is corroborated by the observed absence of non-coal epiclastic partings in the seams (Sia and Abdullah 2012). However, given the established dry-seasonal tropical climate in the Late Pliocene, the Balingian paleopeats possibly originated in rheotrophic mires that were protected from detrital inputs (Cecil et al. 1985; Fikri et al. 2022). This theory is supported by the TOC and S_T contents, which suggest that the Balingian paleopeats developed within ombrogenous to topogenous mire facies (Fig. 13).

5.3 Controlling factors on hydrocarbon potential

The oil-generating capacity of humic coals depends primarily on the volume and type of mire petrofacies (Sykes et al. 2014). Petrofacies are mainly classified based on the association of plant tissues and matrix types, and rheotrophic, planar mire facies have been shown to possess higher oil-generating potential than ombrotrophic, raised mire facies. (Sykes 1994; Sykes et al. 2014). Furthermore, whilst biomass production is markedly aided by warm and

humid climates, humification generally proceeds faster under cooler climates and in low-nutrient, highly acidic environments with less fluctuating hydrologic conditions (McCabe 1987; Moore 1987; Dehmer 1993). In addition, Moore and Shearer (2003) investigated four New Zealand peat bogs and found no direct relationship between depositional environment, tectonic setting, climatic condition, and peat types. In summary, humification and the liquid hydrocarbon generation capacity of coals are dependent on factors such as stratigraphic age, paleobotany, paleoclimate, and depositional conditions (Collinson et al. 1994; Isaksen et al 1998; Wilkins and George 2002; Petersen and Nytoft 2006).

The studied Cenozoic Sarawak Basin coals are of similar thermal maturity, OM input, and paleoflora. However, the paleopeats accumulated under varying sub-environmental conditions that could contribute to the varying hydrocarbon-generating potential. Hence, multivariate statistical analyses of several geochemical proxies were used to provide insight into the controlling influence(s) on the distribution of hydrocarbons in the coals. The examined probable influences include kerogen type and organic matter input, paleoflora, paleoclimate, paleohydrology, and depositional conditions. For each probable controlling influence, two runs of principal component analysis (PCA) were carried out. The first run compared the geochemical proxies, identifying correlations among the proxies while the second run compared proxies of hydrocarbon-generating potential and the probable controlling factor. The result of the correlation analysis of over 100 geochemical parameters is presented in Supplementary Table A.3.

Vitrinite reflectance values ranged from 0.27 to 0.43 (Table 2), indicating that the studied are thermally immature for hydrocarbon generation (Peters et al. 2005). Furthermore, vitrinite reflectance shows weak correlations with hydrogen index ($r = 0.209$), genetic potential ($r = 0.303$), A-factor ($r = -0.318$), and bitumen yield ($r = 0.305$), thus implying that the slight variation in the rank of the studied coals did not impact their petroleum potential.

Organic matter of marine-algal and terrigenous origin are generally regarded as oil- and gas-prone, respectively.

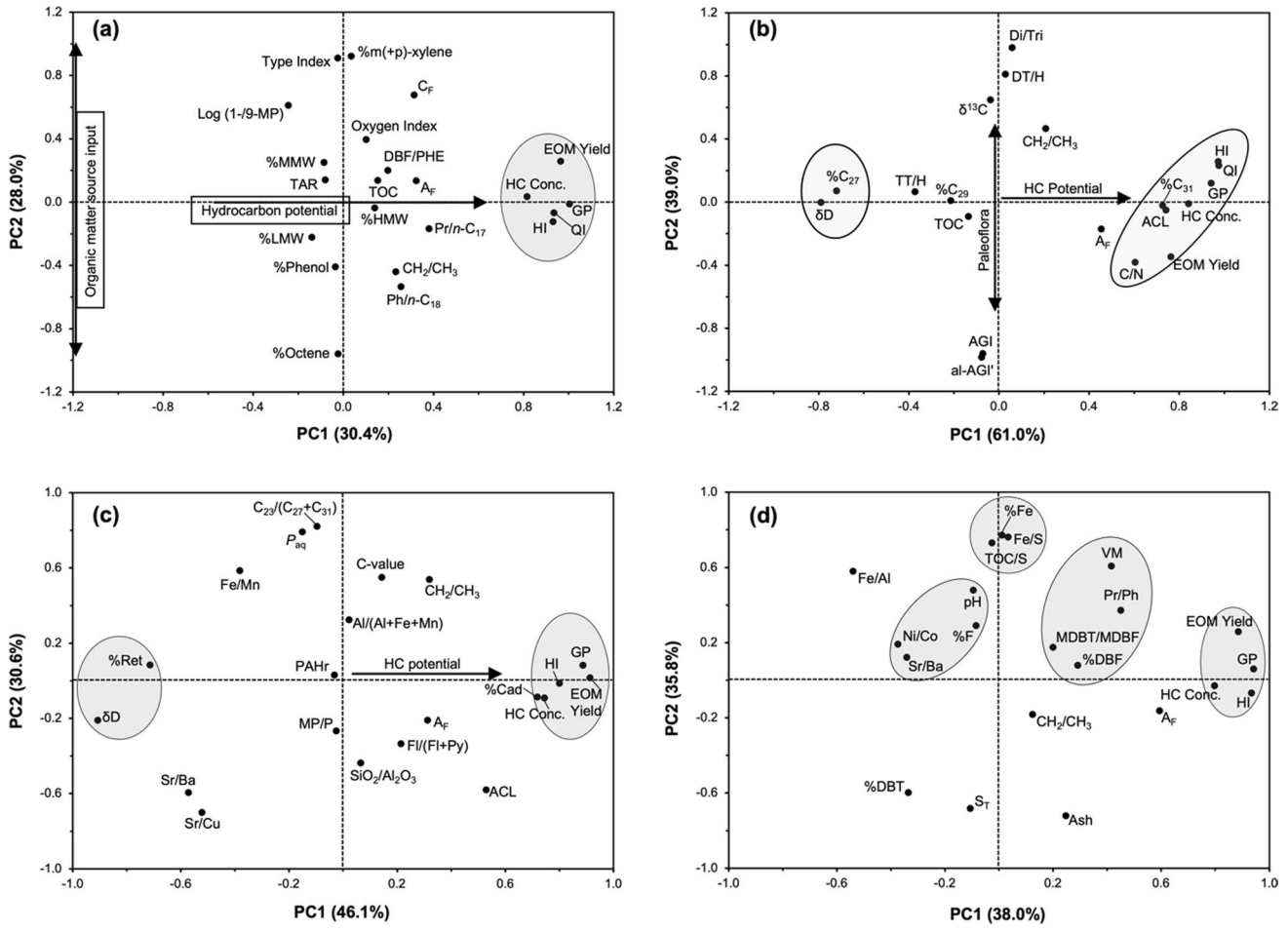

Fig. 14 Rotated loadings of parameters of petroleum potential and: **a** Organic matter source input **b** Paleoflora **c** Paleohydrological and paleoclimate and **d** Depositional environments. Refer to Tables 1, 2, 3, 4, 5, 6, 7 for parameter abbreviations

Hence, the amount and type of kerogens in source rocks are directly related to the oil-generating potential. Principal component analysis of the petroleum-potential and source input parameters indicates that the first two components account for 58.4% of the total variance, with the variance slightly higher for PC1 (30.4%) than PC2 (28.0%). The source input and petroleum potential parameters are mostly loaded on PC2 and PC1, respectively, thus indicating little correlation (Fig. 14a). However, there appear to be moderate correlations between DBF/P and organic richness parameters such as TOC and A-factor.

The increasing contribution of angiosperm flora is associated with higher petroleum source potential (Isaksen et al. 1998; Newman et al. 1999). In addition, the concentrations of long-chain *n*-alkanes in angiosperms are significantly higher than in gymnosperms (Diefendorf et al. 2011, 2015; Lane 2017). Whilst the paleoflora of the Sarawak Basin was dominated by angiosperms, the contribution of gymnosperms varies and is highest in the Mukah coals. The PCA result of petroleum potential and paleoflora proxies is shown in Fig. 14b. The rotated components account for 100.0% of the variance (PC1, 61.0%; PC2, 39.0%). Additionally, as shown on the loadings cross-plot, paleoflora proxies such as the angiosperm-gymnosperm ratios load strongly on PC1, while petroleum potential parameters load positively and strongly on PC2, indicating no correlation between paleoflora and petroleum potential for the studied coals. However, *n*-alkane proxies such as $\%C_{27}$, $\%C_{31}$, and ACL, which are also affected by environmental conditions are weakly correlated with petroleum potential parameters.

Warm and humid climates in tropical latitudes favour plant growth and peat accumulation whilst humification is enhanced by the introduction of oxygen into the peat during drier periods (Nichols et al. 2006; Morley 2013). Hence, hydrological and climatic conditions are possible controls on the oil-generating potential of humic coals. PCA result indicates that hydrocarbon potential proxies are positively loaded on PC1, while paleohydrology and paleoclimate proxies are mostly loaded on PC2 (Fig. 14c). The plotted rotated components account for 76.7% of the total variation around the PCs. *n*-Alkane paleohydrology proxies such as P_{aq} and $C_{23}/(C_{27}+C_{31})$ are positively loaded on PC2, thus indicating no correlation between paleohydrological conditions and the hydrocarbon potential of the Sarawak Basin coals. However, some paleoclimate proxies such as %ret, Sr/Ba and Sr/Cu are partly loaded on both PC1 and PC2, suggesting slight climatic control on the petroleum potential of the coals.

Furthermore, paleodepositional conditions such as marine influence and redox setting have been established to influence the petroleum-generating capacity of humic coals (Flores and Sykes 1996; Sykes et al. 2014). PCA

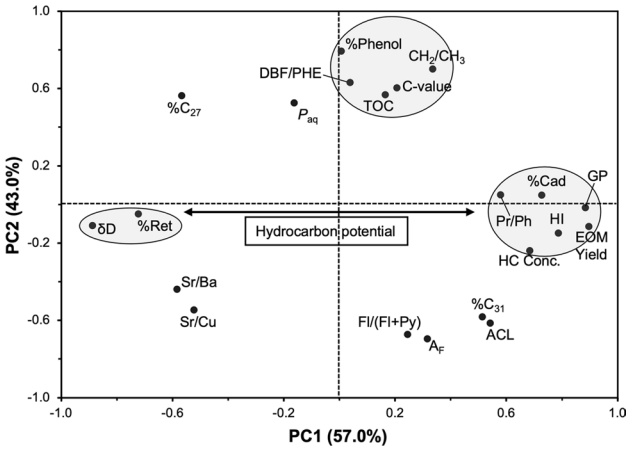

Fig. 15 Rotated bulk and molecular geochemical parameter loadings for the analysed Sarawak Basin coals. TOC: Total Organic Carbon; DBF/PHE: Dibenzofuran/Phenanthrene; EOM: Extractable Organic Matter; HC Conc.: Hydrocarbon Concentration; %Ret = [retene/(retene + cadalene) × 100]; %Cad = [cadalene/(retene + cadalene) × 100]; %Phenol = [Phenol/(*n*-1-octene + m(+ p)-xylene + Phenol) × 100]; $\%C_{27} = [n\text{-}C_{27}/(n\text{-}C_{27}+n\text{-}C_{29}+n\text{-}C_{31}) \times 100]$; $\%C_{31} = [n\text{-}C_{31}/(n\text{-}C_{27}+n\text{-}C_{29}+n\text{-}C_{31}) \times 100]$; Fl(Fl + Py) = Fluoranthene/(Fluoranthene + Pyrene); Pr/Ph: Pristane/Phytane; A_F: A-factor; P_{aq}: Proxy Aqueous = $(n\text{-}C_{23}+n\text{-}C_{25})/(n\text{-}C_{23}+n\text{-}C_{25}+n\text{-}C_{29}+n\text{-}C_{31})$; ACL: Average Chain Length = $[(27 \times n\text{-}C_{27})+(29 \times n\text{-}C_{29})+(31 \times n\text{-}C_{31})]/(n\text{-}C_{27}+n\text{-}C_{29}+n\text{-}C_{31})$; GP: Genetic Potential = *S*1 + *S*2; HI: Hydrogen Index = [(*S*2/TOC) × 100]; Sr/Ba: Strontium/Barium; Sr/Cu: Strontium/Copper; C-value = (Fe + Mn + Cr + Ni + V + Co)/(Ca + Mg + Sr + Ba + K + Na)

study of 21 parameters of depositional environment and petroleum potential showed that 73.8% of the total variance is accounted for by the first two PCs (PC1, 38.0%; RC2, 35.8%). Whilst petroleum potential indicators are positively, and strongly loaded on PC1, proxies of seawater influence such as S_T, Fe/S, %DBT, and TOC/S are strongly loaded on PC2, thus implying that seawater incursions did not affect the petroleum potential of the Sarawak coals (Fig. 14d). This finding supports the enhanced preservation model postulated by Sykes et al. (2014), which argued that the inherent HI and petroleum potential of freshwater-sourced OM is not increased by sulfurization. Conversely, sulfurization significantly enhances the bio-resistance of peat biomass, reducing its biodegradation and thus preserving organic richness. Additionally, Fig. 14d shows that redox and lithology/environment proxies are weakly loaded on PC1, which suggests weak correlations with petroleum potential parameters.

Based on the PCA results discussed above, geochemical parameters with strong coefficients (> 0.5) were selected for another PCA run. The PCA result of the selected geochemical parameters indicates that the total variance in the data is fully explained by the two PC (PC1, 57.0%; RC2, 43.0%). The loadings plot of the PCs shows that petroleum potential parameters such as HI, GP, and extract yield are strongly

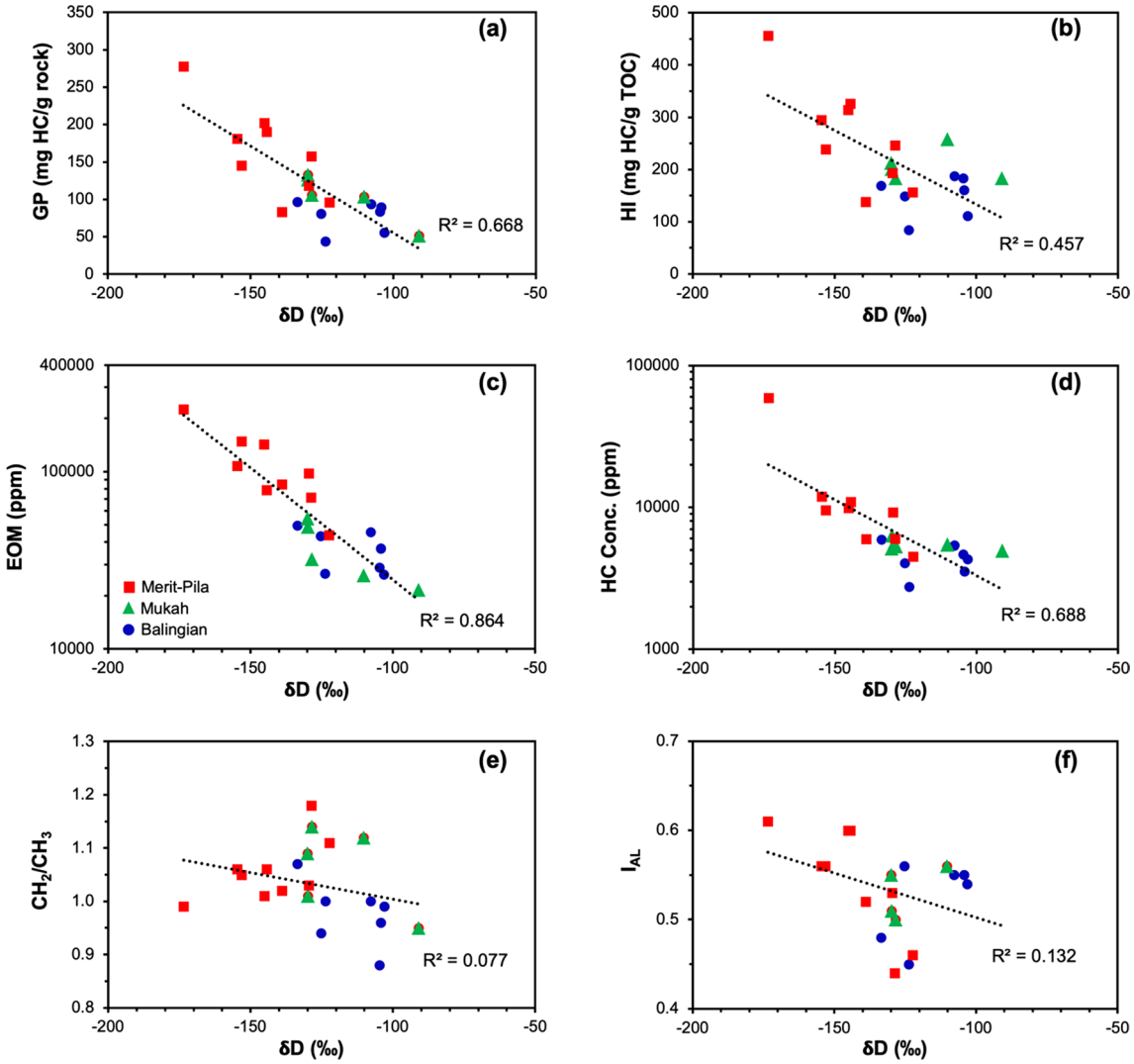

Fig. 16 Cross plots of δD versus **a** Genetic potential (GP) **b** Hydrogen index (HI) **c** Extractable organic matter (EOM) yield **d** Hydrocarbon concentration **e** Aliphatic chain length and **f** Aliphaticity index (I_{AL})

and positively loaded on PC1 (Fig. 15; Supplementary Table A.4). Additionally, paleoclimate and paleoredox proxies such as Pr/Ph, %retene, and δD are strongly correlated with PC1, indicating some degree of climatic and depositional controls on the total petroleum potential. Conversely, %Phenol and FTIR's A-factor and aliphatic chain length parameter (CH_2/CH_3) are strongly loaded on PC2, thus showing no correlation with petroleum potential parameters that are loaded on PC1 (Fig. 15).

The PCA result suggests that the total petroleum potential is considerably influenced by a combination of climate, redox and depositional factors. For example, δD, which reflects the isotopic composition of meteoric water during plant growth, is moderately to strongly correlated with total petroleum potential parameters such as EOM yield, *S*2, GP, I_{HG}, HI, and hydrocarbon concentration (Figs. 16a–d; Supplementary Table A.3). However, the oil-generating potential of coals depends mainly on the length and type of aliphatic chains in their structures (Ganz and Kalkreuth 1991; Petersen 2005). Hence, the very weak correlations between δD values and FTIR parameters such as the aliphatic chain length and aliphaticity index (I_{AL}) suggest no controlling environmental and depositional influence on the liquid hydrocarbon generation potential of the coals (Figs. 16e–f).

Paleoclimatic changes influence the geochemistry and morphology of peat-forming environments (Cecil et al. 1985). Peat humification, which is a measure of the decomposition of organic matter, is influenced both by peat botanical composition and mire hydrological conditions (Yeloff and Mauquoy 2006). According to Davis et al. (2007), the greater the degree of degradation, the greater the petroleum potential of coals. Additionally, humification is accelerated in the zones

of frequent water table fluctuations due to the presence of a permanent zone of aeration (Moore and Shearer 2003). The wide variation in the δD values of the Merit-Pila coals possibly reflects the warm, wet-dry conditions of the Late Oligocene to the earliest Miocene. Hence, the high degree of water table fluctuations in the Merit-Pila paleopeats possibly aided microbial degradation of plant tissue, and consequently, the generative potential of the Merit-Pila coals.

6 Conclusions

Low-rank Tertiary humic coals from Mukah-Balingian and Merit-Pila coalfields of the Sarawak Basin, Malaysia were analysed using organic geochemical techniques to determine the paleoflora, paleoclimate, and paleodepositional conditions. Additionally, the distributions of hydrocarbons and non-hydrocarbon compounds coals were compared and using statistical analytical tools, the major geochemical controls on petroleum potential were determined.

Proximate analysis of the coals indicates widely-varying moisture and ash contents. The varying ash content in the Mukah and Merit-Pila coals is indicative of the presence of multiple mire facies, while the low ash content of the Balingian coals is typical of ombrogenous peats. Results of the elemental analysis of the coals show that when compared with the published global average concentrations, the studied coals are mostly depleted in major oxides and trace elements. This reflects low input of detrital materials during peat accumulation. Furthermore, sulfur content and some bimetal proxies suggest little or no marine influence in freshwater-dominated environments. However, B concentrations and Sr/Ba ratios indicate marine influence, particularly, on the Balingian coals. Whilst this contradiction may be explained post by secondary enrichment, it does underline the limitations of elemental proxies of paleosalinity. Additionally, DBT/P and Pr/Ph ratios of the studied coals indicate deposition under sub-oxic to oxic and moderately acidic conditions of a deltaic system. The relative abundances of heterocyclic aromatic hydrocarbon imply freshwater- to lacustrine-swamp environments of deposition.

Stable bulk carbon isotopic ratios and the distribution of aliphatic and aromatic terpenoid biomarkers in the coals both indicate that paleovegetation of the Sarawak Basin was dominated by angiosperms. The distribution of combustion-derived polycyclic aromatic hydrocarbons (PAHs) signifies a mixed to dominant pyrogenic origin. Nevertheless, the absence of ≥ 6-ring PAHs, which are products of high-temperature events, signifies a mostly humid paleoclimate. Additionally, *n*-alkane and elemental paleoclimate proxies indicate that the Merit-Pila and Mukah coals were deposited under humid and warm paleoclimate with wet-dry conditions in the Early Miocene, while the Balingian coals were deposited under humid but strongly seasonal paleoclimate in the Late Pliocene.

Principal component analysis result of over 100 geochemical proxies of source input, paleoflora, paleoclimate and paleoredox indicates that organic matter input, marine incursions, peat hydrology and paleoflora are not principal controls on the petroleum potential of the studied coals. However, the fluctuating paleoclimatic conditions and distinct sub-environments appear to be the controlling influence on their hydrocarbon-generating capacity. Water table fluctuations in the Merit-Pila paleopeats due to the wet-dry conditions that prevailed during Late Oligocene and earliest Miocene likely enhanced the microbial degradation of plant tissues, and thus the petroleum potential of the Merit-Pila coals.

Supplementary Information The online version contains supplementary material available at https://doi.org/10.1007/s40789-024-00690-0.

Acknowledgements The authors are grateful to the Department of Geology, University of Malaya for providing laboratory facilities to carry out this research. In addition, the authors appreciate Professor Shimin Liu, the Editor-in-Chief, and the two anonymous reviewers for their invaluable contributions, which have significantly improved the manuscript.

Author contributions All authors contributed to the study's conception and design. Material preparation, data collection and analysis were performed by LA. The first draft of the manuscript was written by LA and all authors commented on previous versions of the manuscript. All authors read and approved the final manuscript.

Funding Lanre Asiwaju received a scholarship for doctorate study from the Nigerian Government through the Petroleum Technology Development Fund (PTDF). Prof. Wan Hasiah Abdullah, Dr Khairul Azlan Mustapha, Dr Say-Gee Sia, and Dr Mohammed Hail Hakimi did not receive support from any organization for the submitted work.

Declarations

Competing interests The authors have no relevant financial or non-financial interests to disclose.

References

Abdullah WH (1997) Common Iiptinitic constituents of Tertiary coals from the Bintulu and Merit-Pila coalfield, Sarawak and their relation to oil generation from coal. Bull Geol Soc Malays 41:85–94. https://doi.org/10.7186/bgsm41199708

Ahmed M, Volk H, George SC et al (2009) Generation and expulsion of oils from Permian coals of the Sydney Basin, Australia. Org Geochem 40:810–831. https://doi.org/10.1016/j.orggeochem.2009.04.003

Aich S, Behera D, Nandi BK, Bhattacharya S (2020) Relationship between proximate analysis parameters and combustion behaviour of high ash Indian coal. Int J Coal Sci Technol 7:766–777. https://doi.org/10.1007/s40789-020-00312-5

Algeo TJ, Liu J (2020) A re-assessment of elemental proxies for paleoredox analysis. Chem Geol 540:119549. https://doi.org/10.1016/j.chemgeo.2020.119549

Algeo TJ, Maynard JB (2004) Trace-element behavior and redox facies in core shales of Upper Pennsylvanian Kansas-type cyclothems. Chem Geol 206:289–318. https://doi.org/10.1016/j.chemgeo.2003.12.009

Amir Hassan MH, Johnson HD, Allison PA, Abdullah WH (2017) Sedimentology and stratigraphic architecture of a Miocene retrogradational, tide-dominated delta system: Balingian Province, offshore Sarawak, Malaysia. Geol Soc Lond Spec Publ 444:215–250. https://doi.org/10.1144/SP444.12

Anderson JAR (1964) Peat swamps of Sarawak and Brunei. J Trop Geogr 18:7–16

Andersson RA, Kuhry P, Meyers P et al (2011) Impacts of paleohydrological changes on n-alkane biomarker compositions of a Holocene peat sequence in the eastern European Russian Arctic. Org Geochem 42:1065–1075. https://doi.org/10.1016/j.orggeochem.2011.06.020

Asif M, Wenger LM (2019) Heterocyclic aromatic hydrocarbon distributions in petroleum: a source facies assessment tool. Org Geochem 137:103896. https://doi.org/10.1016/j.orggeochem.2019.07.005

Asiwaju L, Mustapha KA, Abdullah WH et al (2023) Organic matter input, paleovegetation and paleoclimate of Upper Cretaceous lignite from Maiganga coalfield, Upper Benue Trough, Nigeria: Insights from biomarkers and stable isotopes. J Afr Earth Sci 205:105010. https://doi.org/10.1016/j.jafrearsci.2023.105010

Awang Jamil AS, Anwar ML, Seah EPK (1991) Geochemistry of selected crude oils from Sabah and Sarawak. Bull Geol Soc Malays 28:123–149. https://doi.org/10.7186/bgsm28199107

Baas M, Pancost R, Van Geel B, Sinninghe Damsté JS (2000) A comparative study of lipids in Sphagnum species. Org Geochem 31:535–541. https://doi.org/10.1016/S0146-6380(00)00037-1

Bai Y, Liu Z, Sun P et al (2015) Rare earth and major element geochemistry of Eocene fine-grained sediments in oil shale- and coal-bearing layers of the Meihe Basin, Northeast China. J Asian Earth Sci 97:89–101. https://doi.org/10.1016/j.jseaes.2014.10.008

Barry JC, Morgan ME, Flynn LJ et al (2002) Faunal and environmental change in the late Miocene Siwaliks of northern Pakistan. Paleobiology 28:1–71. https://doi.org/10.1666/0094-8373(2002)28[1:faecit]2.0.co;2

Bechtel A, Gruber W, Sachsenhofer RF et al (2001) Organic geochemical and stable carbon isotopic investigation of coals formed in low-lying and raised mires within the Eastern Alps (Austria). Org Geochem 32:1289–1310. https://doi.org/10.1016/S0146-6380(01)00101-2

Bechtel A, Gruber W, Sachsenhofer RF et al (2003) Depositional environment of the Late Miocene Hausruck lignite (Alpine Foreland Basin): insights from petrography, organic geochemistry, and stable carbon isotopes. Int J Coal Geol 53:153–180. https://doi.org/10.1016/S0166-5162(02)00194-5

Bechtel A, Reischenbacher D, Sachsenhofer RF et al (2007) Paleogeography and paleoecology of the upper Miocene Zillingdorf lignite deposit (Austria). Int J Coal Geol 69:119–143. https://doi.org/10.1016/j.coal.2006.03.001

Bechtel A, Gratzer R, Sachsenhofer RF et al (2008) Biomarker and carbon isotope variation in coal and fossil wood of Central Europe through the Cenozoic. Palaeogeogr Palaeoclimatol Palaeoecol 262:166–175. https://doi.org/10.1016/j.palaeo.2008.03.005

Bennett WW, Canfield DE (2020) Redox-sensitive trace metals as paleoredox proxies: a review and analysis of data from modern sediments. Earth-Science Rev 204:103175. https://doi.org/10.1016/j.earscirev.2020.103175

Breitfeld HT, Hennig-Breitfeld J, BouDagher-Fadel MK et al (2020) Oligocene-Miocene drainage evolution of NW Borneo: stratigraphy, sedimentology and provenance of Tatau-Nyalau province sediments. J Asian Earth Sci 195:104331. https://doi.org/10.1016/j.jseaes.2020.104331

Buggle B, Wiesenberg GLB, Glaser B (2010) Is there a possibility to correct fossil n-alkane data for postsedimentary alteration effects? Appl Geochem 25:947–957. https://doi.org/10.1016/j.apgeochem.2010.04.003

Bush RT, McInerney FA (2013) Leaf wax n-alkane distributions in and across modern plants: implications for paleoecology and chemotaxonomy. Geochim Cosmochim Acta 117:161–179. https://doi.org/10.1016/j.gca.2013.04.016

Bush RT, McInerney FA (2015) Influence of temperature and C4 abundance on n-alkane chain length distributions across the central USA. Org Geochem 79:65–73. https://doi.org/10.1016/j.orggeochem.2014.12.003

Cao J, Wu M, Chen Y et al (2012) Trace and rare earth element geochemistry of Jurassic mudstones in the northern Qaidam Basin, northwest China. Chem Erde 72:245–252. https://doi.org/10.1016/j.chemer.2011.12.002

Casagrande DJ (1987) Sulphur in peat and coal. Geol Soc Spec Publ 32:87–105. https://doi.org/10.1144/GSL.SP.1987.032.01.07

Cecil CB, Stanton RW, Neuzil SG et al (1985) Paleoclimate controls on late paleozoic sedimentation and peat formation in the central appalachian basin (U.S.A.). Int J Coal Geol 5:195–230. https://doi.org/10.1016/0166-5162(85)90014-X

Cernusak LA, Ubierna N, Winter K et al (2013) Environmental and physiological determinants of carbon isotope discrimination in terrestrial plants. New Phytol 200:950–965. https://doi.org/10.1111/nph.12423

Cesar J, Grice K (2019) Molecular fingerprint from plant biomarkers in Triassic-Jurassic petroleum source rocks from the Dampier sub-Basin, Northwest Shelf of Australia. Mar Pet Geol 110:189–197. https://doi.org/10.1016/j.marpetgeo.2019.07.024

Chamberlain CP, Winnick MJ, Mix HT et al (2014) The impact of neogene grassland expansion and aridification on the isotopic composition of continental precipitation. Glob Biogeochem Cycles 28:992–1004. https://doi.org/10.1002/2014GB004822

Chou C-L (2012) Sulfur in coals: a review of geochemistry and origins. Int J Coal Geol 100:1–13. https://doi.org/10.1016/j.coal.2012.05.009

Collinson ME, Van Bergen PF, Scott AC, De Leeuw JW (1994) The oil-generating potential of plants from coal and coal-bearing strata through time: a review with new evidence from Carboniferous plants. Geol Soc Lond Spec Publ 77:31–70. https://doi.org/10.1144/GSL.SP.1994.077.01.03

Dai S, Ren D, Chou CL et al (2012) Geochemistry of trace elements in Chinese coals: a review of abundances, genetic types, impacts on human health, and industrial utilization. Int J Coal Geol 94:3–21. https://doi.org/10.1016/j.coal.2011.02.003

Dai S, Bechtel A, Eble CF et al (2020) Recognition of peat depositional environments in coal: a review. Int J Coal Geol 219:103383. https://doi.org/10.1016/j.coal.2019.103383

Davis RC, Noon SW, Harrington J (2007) The petroleum potential of Tertiary coals from Western Indonesia: relationship to mire type and sequence stratigraphic setting. Int J Coal Geol 70:35–52. https://doi.org/10.1016/j.coal.2006.02.008

Dawson D, Grice K, Wang SX et al (2004) Stable hydrogen isotopic composition of hydrocarbons in torbanites (Late Carboniferous to Late Permian) deposited under various climatic conditions. Org Geochem 35:189–197. https://doi.org/10.1016/j.orggeochem.2003.09.004

Dehmer J (1993) Petrology and organic geochemistry of peat samples from a raised bog in Kalimantan (Borneo). Org Geochem 20:349–362. https://doi.org/10.1016/0146-6380(93)90125-U

Dehmer J (1995) Petrological and organic geochemical investigation of recent peats with known environments of deposition. Int J Coal Geol 28:111–138. https://doi.org/10.1016/0166-5162(95)00016-X

Dellwig O, Watermann F, Brumsack HJ et al (2001) Sulphur and iron geochemistry of Holocene coastal peats (NW Germany): a tool for palaeoenvironmental reconstruction. Palaeogeogr Palaeoclimatol Palaeoecol 167:359–379. https://doi.org/10.1016/S0031-0182(00)00247-9

Didyk BM, Simoneit BRT, Brassell SC, Eglinton G (1978) Organic geochemical indicators of palaeoenvironmental conditions of sedimentation. Nature 272:216–222. https://doi.org/10.1038/272216a0

Diefendorf AF, Freimuth EJ (2017) Extracting the most from terrestrial plant-derived n-alkyl lipids and their carbon isotopes from the sedimentary record: a review. Org Geochem 103:1–21. https://doi.org/10.1016/j.orggeochem.2016.10.016

Diefendorf AF, Freeman KH, Wing SL, Graham HV (2011) Production of n-alkyl lipids in living plants and implications for the geologic past. Geochim Cosmochim Acta 75:7472–7485. https://doi.org/10.1016/j.gca.2011.09.028

Diefendorf AF, Leslie AB, Wing SL (2015) Leaf wax composition and carbon isotopes vary among major conifer groups. Geochim Cosmochim Acta 170:145–156. https://doi.org/10.1016/j.gca.2015.08.018

Diessel CFK (1992) Coal-bearing depositional systems, 1st edn. Springer, Berlin

Donahue CJ, Rais EA (2009) Proximate analysis of coal. J Chem Educ 86:222. https://doi.org/10.1021/ed086p222

Duan Y, Xu L (2012) Distributions of n-alkanes and their hydrogen isotopic composition in plants from Lake Qinghai (China) and the surrounding area. Appl Geochem 27:806–814. https://doi.org/10.1016/j.apgeochem.2011.12.008

Duan Y, Wu Y, Cao X et al (2014) Hydrogen isotope ratios of individual n-alkanes in plants from Gannan Gahai Lake (China) and surrounding area. Org Geochem 77:96–105. https://doi.org/10.1016/j.orggeochem.2014.10.005

Ellis L, Singh RK, Alexander R, Kagi RI (1996) Formation of isohexyl alkylaromatic hydrocarbons from aromatization-rearrangement of terpenoids in the sedimentary environment: a new class of biomarker. Geochim Cosmochim Acta 60:4747–4763. https://doi.org/10.1016/S0016-7037(96)00281-5

Escobar M, Márquez G, Suárez-Ruiz I et al (2016) Source-rock potential of the lowest coal seams of the Marcelina Formation at the Paso Diablo mine in the Venezuelan Guasare Basin: evidence for the correlation of Amana oils with these Paleocene coals. Int J Coal Geol 163:149–165. https://doi.org/10.1016/j.coal.2016.07.003

Ficken KJ, Li B, Swain DL, Eglinton G (2000) An n-alkane proxy for the sedimentary input of submerged/floating freshwater aquatic macrophytes. Org Geochem 31:745–749. https://doi.org/10.1016/S0146-6380(00)00081-4

Fikri HN, Sachsenhofer RF, Bechtel A, Gross D (2022) Coal deposition in the Barito Basin (Southeast Borneo): the Eocene Tanjung formation compared to the Miocene Warukin formation. Int J Coal Geol 263:104117. https://doi.org/10.1016/j.coal.2022.104117

Flores RM, Sykes R (1996) Depositional controls on coal distribution and quality in the Eocene Brunner Coal Measures, Buller Coalfield, South Island, New Zealand. Int J Coal Geol 29:291–336. https://doi.org/10.1016/0166-5162(95)00028-3

Friederich MC, Moore TA, Flores RM (2016) A regional review and new insights into SE Asian Cenozoic coal-bearing sediments: why does Indonesia have such extensive coal deposits? Int J Coal Geol 166:2–35. https://doi.org/10.1016/j.coal.2016.06.013

Galarraga F, Reategui K, Martïnez A et al (2008) V/Ni ratio as a parameter in palaeoenvironmental characterisation of nonmature medium-crude oils from several Latin American basins. J Pet Sci Eng 61:9–14. https://doi.org/10.1016/j.petrol.2007.10.001

Ganz HH, Kalkreuth W (1991) IR classification of kerogen type, thermal maturation, hydrocarbon potential and lithological characteristics. J Southeast Asian Earth Sci 5:19–28. https://doi.org/10.1016/0743-9547(91)90007-K

Gayer RA, Rose M, Dehmer J, Shao LY (1999) Impact of sulphur and trace element geochemistry on the utilization of a marine-influenced coal-case study from the South Wales Variscan foreland basin. Int J Coal Geol 40:151–174. https://doi.org/10.1016/S0166-5162(98)00066-4

Goodarzi F, Swaine DJ (1993) Chalcophile elements in western Canadian coals. Int J Coal Geol 24:281–292. https://doi.org/10.1016/0166-5162(93)90015-3

Goodarzi F, Swaine DJ (1994) The influence of geological factors on the concentration of boron in Australian and Canadian coals. Chem Geol 118:301–318. https://doi.org/10.1016/0009-2541(94)90183-X

Grice K, Nabbefeld B, Maslen E (2007) Source and significance of selected polycyclic aromatic hydrocarbons in sediments (Hovea-3 well Perth Basin Western Australia) spanning the Permian–Triassic boundary. Org Geochem 38(11):1795–1803. https://doi.org/10.1016/j.orggeochem.2007.07.001

Grice K, Riding JB, Foster CB et al (2015) Vascular plant biomarker distributions and stable carbon isotopic signatures from the Middle and Upper Jurassic (Callovian–Kimmeridgian) strata of Staffin Bay, Isle of Skye, northwest Scotland. Palaeogeogr Palaeoclimatol Palaeoecol 440:307–315. https://doi.org/10.1016/j.palaeo.2015.08.036

Gürdal G, Bozcu M (2011) Petrographic characteristics and depositional environment of Miocene Çan coals, Çanakkale-Turkey. Int J Coal Geol 85:143–160. https://doi.org/10.1016/j.coal.2010.11.001

Hageman H (1987) Palaeobathymetrical changes in NW Sarawak during the Oligocene to Pliocene. Bull Geol Soc Malays 21:91–102. https://doi.org/10.7186/bgsm21198705

Hakimi MH, Abdullah WH, Sia S-G, Makeen YM (2013) Organic geochemical and petrographic characteristics of Tertiary coals in the northwest Sarawak, Malaysia: implications for palaeoenvironmental conditions and hydrocarbon generation potential. Mar Pet Geol 48:31–46. https://doi.org/10.1016/j.marpetgeo.2013.07.009

Han S, Zhang Y, Huang J et al (2020) Elemental geochemical characterization of sedimentary conditions and organic matter enrichment for lower cambrian shale formations in northern guizhou, south china. Minerals 10:793. https://doi.org/10.3390/min10090793

Hanisch S, Ariztegui D, Püttmann W (2003) The biomarker record of Lake Albano, central Italy—implications for Holocene aquatic system response to environmental change. Org Geochem 34:1223–1235. https://doi.org/10.1016/S0146-6380(03)00118-9

Hautevelle Y, Michels R, Malartre F, Trouiller A (2006) Vascular plant biomarkers as proxies for palaeoflora and palaeoclimatic changes at the Dogger/Malm transition of the Paris Basin (France). Org Geochem 37:610–625. https://doi.org/10.1016/j.orggeochem.2005.12.010

He D, Huang H, Arismendi GG (2019) n-Alkane distribution in ombrotrophic peatlands from the northeastern Alberta, Canada, and its paleoclimatic implications. Palaeogeogr Palaeoclimatol Palaeoecol 528:247–257. https://doi.org/10.1016/j.palaeo.2019.05.018

Hennig-Breitfeld J, Breitfeld HT, Hall R et al (2019) A new upper Paleogene to Neogene stratigraphy for Sarawak and Labuan in northwestern Borneo: paleogeography of the eastern Sundaland margin. Earth-Science Rev 190:1–32. https://doi.org/10.1016/j.earscirev.2018.12.006

Ho KF (1978) Stratigraphic framework for oil exploration in Sarawak. Bull Geol Soc Malays 10:1–13. https://doi.org/10.7186/bgsm10197801

Hoffmann B, Kahmen A, Cernusak LA et al (2013) Abundance and distribution of leaf wax n-alkanes in leaves of acacia and eucalyptus trees along a strong humidity gradient in Northern Australia. Org Geochem 62:62–67. https://doi.org/10.1016/j.orggeochem.2013.07.003

Holbourn A, Kuhnt W, Lyle M et al (2014) Middle Miocene climate cooling linked to intensification of eastern equatorial Pacific upwelling. Geology 42:19–22. https://doi.org/10.1130/G34890.1

Hou J, D'Andrea WJ, MacDonald D, Huang Y (2007) Hydrogen isotopic variability in leaf waxes among terrestrial and aquatic plants around Blood Pond, Massachusetts (USA). Org Geochem 38:977–984. https://doi.org/10.1016/j.orggeochem.2006.12.009

Huang H, Zhang S, Su J (2015) Pyrolytically derived polycyclic aromatic hydrocarbons in marine oils from the Tarim Basin, NW China. Energy Fuels 29:5578–5586. https://doi.org/10.1021/acs.energyfuels.5b01007

Hughes WB, Holba AG, Dzou LIP (1995) The ratios of dibenzothiophene to phenanthrene and pristane to phytane as indicators of depositional environment and lithology of petroleum source rocks. Geochim Cosmochim Acta 59:3581–3598. https://doi.org/10.1016/0016-7037(95)00225-O

Inglis GN, Naafs BDA, Zheng Y et al (2018) Distributions of geohopanoids in peat: implications for the use of hopanoid-based proxies in natural archives. Geochim Cosmochim Acta 224:249–261. https://doi.org/10.1016/j.gca.2017.12.029

Isaksen GH, Curry DJ, Yeakel JD, Jenssen AI (1998) Controls on the oil and gas potential of humic coals. Org Geochem 29:23–44. https://doi.org/10.1016/S0146-6380(98)00042-4

Jablonski NG (2005) Primate homeland: forests and the evolution of primates during the Tertiary and Quaternary in Asia. Anthropol Sci 113:117–122. https://doi.org/10.1537/ase.04S016

Jasper K, Hartkopf-Fröder C, Flajs G, Littke R (2010) Evolution of Pennsylvanian (Late Carboniferous) peat swamps of the Ruhr Basin, Germany: comparison of palynological, coal petrographical and organic geochemical data. Int J Coal Geol 83:346–365. https://doi.org/10.1016/j.coal.2010.05.008

Jiang L, George SC (2018) Biomarker signatures of Upper Cretaceous Latrobe Group hydrocarbon source rocks, Gippsland Basin, Australia: distribution and palaeoenvironment significance of aliphatic hydrocarbons. Int J Coal Geol 196:29–42. https://doi.org/10.1016/j.coal.2018.06.025

Jiang L, George SC (2019) Biomarker signatures of Upper Cretaceous Latrobe Group petroleum source rocks, Gippsland Basin, Australia: distribution and geological significance of aromatic hydrocarbons. Org Geochem 138:103905. https://doi.org/10.1016/j.orggeochem.2019.103905

Jiang C, Alexander R, Kagi RI, Murray AP (1998) Polycyclic aromatic hydrocarbons in ancient sediments and their relationships to palaeoclimate. Org Geochem 29:1721–1735. https://doi.org/10.1016/S0146-6380(98)00083-7

Jiang L, Ding W, George SC (2020) Late Cretaceous-Paleogene palaeoclimate reconstruction of the Gippsland Basin, SE Australia. Palaeogeogr Palaeoclimatol Palaeoecol 556:109885. https://doi.org/10.1016/j.palaeo.2020.109885

Johari D, Kiat LK, Pei CS, et al (1994) Economic Geology Bulletin 4: evaluation of the Coal Resources of the Tebulan Block Merit-Pila Coalfield, Sarawak. Sarawak

Jones B, Manning DAC (1994) Comparison of geochemical indices used for the interpretation of palaeoredox conditions in ancient mudstones. Chem Geol 111:111–129. https://doi.org/10.1016/0009-2541(94)90085-X

Ketris MP, Yudovich YE (2009) Estimations of Clarkes for Carbonaceous biolithes: world averages for trace element contents in black shales and coals. Int J Coal Geol 78:135–148. https://doi.org/10.1016/j.coal.2009.01.002

Kiat LK, Pei CS, Johari D et al (1987) Economic Geology Bulletin 3: evaluation of the coal resources of the Merit Block Merit Pila Coal Field, Sarawak. Sarawak

Killops SD, Woolhouse AD, Weston RJ, Cook RA (1994) A geochemical appraisal of oil generation in the Taranaki Basin, New Zealand. Am Assoc Pet Geol Bull 78:1560–1584. https://doi.org/10.1306/a25ff21f-171b-11d7-8645000102c1865d

Killops SD, Raine JI, Woolhouse AD, Weston RJ (1995) Chemostratigraphic evidence of higher-plant evolution in the Taranaki Basin, New Zealand. Org Geochem 23:429–445. https://doi.org/10.1016/0146-6380(95)00019-B

Kombrink H, van Os BJH, van der Zwan CJ, Wong TE (2008) Geochemistry of marine and lacustrine bands in the Upper Carboniferous of the Netherlands. Neth J Geosci 87:309–322. https://doi.org/10.1017/S0016774600023374

Krzeszowska E (2019) Geochemistry of the Lublin Formation from the Lublin Coal Basin: implications for weathering intensity, palaeoclimate and provenance. Int J Coal Geol 216:103306. https://doi.org/10.1016/j.coal.2019.103306

Lane CS (2017) Modern n-alkane abundances and isotopic composition of vegetation in a gymnosperm-dominated ecosystem of the southeastern U.S. coastal plain. Org Geochem 105:33–36. https://doi.org/10.1016/j.orggeochem.2016.12.003

Larter SR, Douglas AG (1980) A pyrolysis-gas chromatographic method for kerogen typing. Phys Chem Earth 12:579–583. https://doi.org/10.1016/0079-1946(79)90139-3

Li B, Zhuang X, Querol X et al (2019) The mode of occurrence and origin of minerals in the Early Permian high-rank coals of the Jimunai depression, Xinjiang Uygur Autonomous Region, NW China. Int J Coal Geol 205:58–74. https://doi.org/10.1016/j.coal.2019.03.002

Liu J, Dai S, Song H et al (2021) Geological factors controlling variations in the mineralogical and elemental compositions of Late Permian coals from the Zhijin-Nayong Coalfield, western Guizhou. China Int J Coal Geol 247:103855. https://doi.org/10.1016/j.coal.2021.103855

López-Días V, Urbanczyk J, Blanco CG, Borrego AG (2013) Biomarkers as paleoclimate proxies in peatlands in coastal high plains in Asturias, N Spain. Int J Coal Geol 116–117:270–280. https://doi.org/10.1016/j.coal.2013.04.006

Lunt P (2020) Discussion on: A new upper Paleogene to Neogene stratigraphy for Sarawak and Labuan in northwestern Borneo: paleogeography of the eastern Sundaland margin. Earth Sci Rev 202:102980. https://doi.org/10.1016/j.earscirev.2019.102980

Lunt P, Madon M (2017) A review of the Sarawak Cycles: history and modern application. Bull Geol Soc Malays 63:77–101. https://doi.org/10.7186/bgsm63201704

Lv D, Li Z, Wang D et al (2019) Sedimentary model of coal and shale in the Paleogene Lijiaya formation of the Huangxian Basin: insight from petrological and geochemical characteristics of coal and shale. Energy Fuels 33:10442–10456. https://doi.org/10.1021/acs.energyfuels.9b01299

Macgregor DS (1994) Coal-bearing strata as source rocks: a global overview. Geol Soc Lond Spec Publ 77:107–116. https://doi.org/10.1144/GSL.SP.1994.077.01.06

Madon M, Kim CL, Wong R (2013) The structure and stratigraphy of deepwater Sarawak, Malaysia: implications for tectonic evolution. J Asian Earth Sci 76:312–333. https://doi.org/10.1016/j.jseaes.2013.04.040

Madon M, Abolins P (1999) Balingian Province. In: The petroleum geology and resources of Malaysia, pp 345–367

Madon M (1999a) Geological setting of Sarawak. In: The petroleum geology and resources of Malaysia, pp 273–290

Madon M (1999b) Basin types, tectono-stratigraphic provinces, and structural styles. In: The petroleum geology and resources of Malaysia, pp 77–90

Marshall C, Large DJ, Meredith W et al (2015) Geochemistry and petrology of Palaeocene coals from Spitsbergen—part 1: oil potential and depositional environment. Int J Coal Geol 143:22–33. https://doi.org/10.1016/j.coal.2015.03.006

Marynowski L, Smolarek J, Bechtel A et al (2013) Perylene as an indicator of conifer fossil wood degradation by wood-degrading fungi. Org Geochem 59:143–151. https://doi.org/10.1016/j.orggeochem.2013.04.006

Mat-Zin IC, Swarbrick RE (1997) The tectonic evolution and associated sedimentation history of Sarawak Basin, eastern Malaysia: a guide for future hydrocarbon exploration. Geol Soc Lond Spec Publ 126:237–245

Mat-Zin IC, Tucker ME (1999) An alternative stratigraphic scheme for the Sarawak Basin. J Asian Earth Sci 17:215–232. https://doi.org/10.1016/S0743-9547(98)00042-7

McCabe PJ (1987) Facies studies of coal and coal-bearing strata. Geol Soc Spec Publ 32:51–66. https://doi.org/10.1144/GSL.SP.1987.032.01.05

Meyers PA (1994) Preservation of elemental and isotopic source identification of sedimentary organic matter. Chem Geol 114:289–302. https://doi.org/10.1016/0009-2541(94)90059-0

Moore PD (1987) Ecological and hydrological aspects of peat formation. Geol Soc Lond Spec Publ 32:7–15. https://doi.org/10.1144/GSL.SP.1987.032.01.02

Moore TA, Shearer JC (2003) Peat/coal type and depositional environment: are they related? Int J Coal Geol 56:233–252. https://doi.org/10.1016/S0166-5162(03)00114-9

Moore TA, Li Z, Nelson CM et al (2005) Concentration of trace elements in coal beds. In: Metal contaminants in New Zealand, pp 81–113

Morley RJ (1998) Palynological evidence for Tertiary plant dispersals in the SE Asian region in relation to plate tectonics and climate. Biogeogr Geol Evol SE Asia 1:211–234

Morley RJ (2013) Cenozoic ecological history of South East Asian peat mires based on the comparison of coals with present day and Late Quaternary peats. J Limnol 72:36–59. https://doi.org/10.4081/jlimnol.2013.s2.e3

Morley RJ (2012) A review of the Cenozoic palaeoclimate history of Southeast Asia. In: Gower D et al (eds) Biotic evolution and environmental change in Southeast Asia. Cambridge University Press, Cambridge, pp 79–114

Murtaza M, Rahman AHA, Sum CW, Konjing Z (2018) Facies associations, depositional environments and stratigraphic framework of the Early Miocene-Pleistocene successions of the Mukah-Balingian Area, Sarawak, Malaysia. J Asian Earth Sci 152:23–38. https://doi.org/10.1016/j.jseaes.2017.11.033

Naafs BDA, Inglis GN, Blewett J et al (2019) The potential of biomarker proxies to trace climate, vegetation, and biogeochemical processes in peat: a review. Glob Planet Change 179:57–79

Nakamura H, Sawada K, Takahashi M (2010) Aliphatic and aromatic terpenoid biomarkers in Cretaceous and Paleogene angiosperm fossils from Japan. Org Geochem 41:975–980. https://doi.org/10.1016/j.orggeochem.2010.03.007

Newman J, Boreham CJ, Ward SD et al (1999) Floral influences on the petroleum source potential of New Zealand Coals. In: Mastalerz M et al (eds) Coalbed Methane: scientific, environmental and economic evaluation. Springer, Dordrecht, pp 461–492

Nichols JE, Booth RK, Jackson ST et al (2006) Paleohydrologic reconstruction based on n-alkane distributions in ombrotrophic peat. Org Geochem 37:1505–1513. https://doi.org/10.1016/j.orggeochem.2006.06.020

Noble RA, Alexander R, Kagi RI, Nox JK (1986) Identification of some diterpenoid hydrocarbons in petroleum. Org Geochem 10:825–829. https://doi.org/10.1016/S0146-6380(86)80019-5

Nott CJ, Xie S, Avsejs LA et al (2000) n-Alkane distributions in ombrotrophic mires as indicators of vegetation change related to climatic variation. Org Geochem 31:231–235. https://doi.org/10.1016/S0146-6380(99)00153-9

Ortiz JE, Moreno L, Torres T et al (2013) A 220 ka palaeoenvironmental reconstruction of the Fuentillejo maar lake record (Central Spain) using biomarker analysis. Org Geochem 55:85–97. https://doi.org/10.1016/j.orggeochem.2012.11.012

Oskay RG, Christanis K, Inaner H et al (2016) Palaeoenvironmental reconstruction of the eastern part of the Karapınar-Ayrancı coal deposit (Central Turkey). Int J Coal Geol 163:100–111. https://doi.org/10.1016/j.coal.2016.06.022

Otto A, Wilde V (2001) Sesqui-, di-, and triterpenoids as chemosystematic markers in extant conifers: a review. Bot Rev 67:141–238. https://doi.org/10.1007/BF02858076

Otto A, Simoneit BRT, Wilde V et al (2002a) Terpenoid composition of three fossil resins from Cretaceous and Tertiary conifers. Rev Palaeobot Palynol 120:203–215. https://doi.org/10.1016/S0034-6667(02)00072-6

Otto A, White JD, Simoneit BRT (2002b) Natural product terpenoids in Eocene and Miocene conifer fossils. Science (80-) 297:1543–1545. https://doi.org/10.1126/science.1074225

Peters KE, Cassa MR (1994) Applied source rock geochemistry. In: Magoon LB, Dow WG (eds) The petroleum system: from source to trap. American Association of Petroleum Geologists, Tulsa, pp 93–120

Peters KE, Walters CC, Moldowan JM (2005) The biomarker guide, 2nd edn. Cambridge University Press, Cambridge

Petersen HI (2005) Oil generation from coal source rocks: the influence of depositional conditions and stratigraphic age. Geol Surv Den Greenl Bull 7:9–12

Petersen HI, Nytoft HP (2006) Oil generation capacity of coals as a function of coal age and aliphatic structure. Org Geochem 37:558–583

Poynter J, Eglinton G (1990) Molecular composition of three sediments from hole 717C: The Bengal Fan. In: Proceedings of the ocean drilling program, 116 Scientific Results. Ocean Drilling Program, pp 155–161

Pu F, Philip RP, Zhenxi L, Guangguo Y (1990) Geochemical characteristics of aromatic hydrocarbons of crude oils and source rocks from different sedimentary environments. Org Geochem 16:427–435. https://doi.org/10.1016/0146-6380(90)90059-9

Radhwani M, Bechtel A, Singh VP et al (2018) Petrographic, palynofacies and geochemical characteristics of organic matter in the Saouef Formation (NE Tunisia): origin, paleoenvironment, and economic significance. Int J Coal Geol 187:114–130. https://doi.org/10.1016/j.coal.2018.01.010

Radke M, Vriend SP, Ramanampisoa LR (2000) Alkyldibenzofurans in terrestrial rocks: influence of organic facies and maturation. Geochim Cosmochim Acta 64:275–286. https://doi.org/10.1016/S0016-7037(99)00287-2

Randlett ME, Bechtel A, van der Meer MTJ et al (2017) Biomarkers in Lake Van sediments reveal dry conditions in eastern Anatolia during 110.000–10.000 years B.P. Geochem Geophys Geosyst 18:571–583. https://doi.org/10.1002/2016GC006621

Romero-Sarmiento MF, Riboulleau A, Vecoli M et al (2011) Aliphatic and aromatic biomarkers from Carboniferous coal deposits at Dunbar (East Lothian, Scotland): palaeobotanical and palaeoenvironmental significance. Palaeogeogr Palaeoclimatol Palaeoecol 309:309–326. https://doi.org/10.1016/j.palaeo.2011.06.015

Rommerskirchen F, Plader A, Eglinton G et al (2006) Chemotaxonomic significance of distribution and stable carbon isotopic composition of long-chain alkanes and alkan-1-ols in C4 grass waxes. Org Geochem 37:1303–1332. https://doi.org/10.1016/j.orggeochem.2005.12.013

Sachse D, Radke J, Gleixner G (2006) δD values of individual n-alkanes from terrestrial plants along a climatic gradient: Implications for the sedimentary biomarker record. Org Geochem 37:469–483. https://doi.org/10.1016/j.orggeochem.2005.12.003

Sachse D, Billault I, Bowen GJ et al (2012) Molecular paleohydrology: interpreting the hydrogen-isotopic composition of lipid biomarkers from photosynthesizing organisms. Annu Rev Earth Planet Sci 40:221–249. https://doi.org/10.1146/annurev-earth-042711-105535

Sarki Yandoka BM, Abdullah WH, Abubakar MB et al (2015) Geochemical characterisation of Early Cretaceous lacustrine sediments of Bima Formation, Yola Sub-basin, Northern Benue Trough, NE Nigeria: organic matter input, preservation, paleoenvironment and palaeoclimatic conditions. Mar Pet Geol 61:82–94. https://doi.org/10.1016/j.marpetgeo.2014.12.010

Schefuß E, Ratmeyer V, Stuut JBW et al (2003) Carbon isotope analyses of n-alkanes in dust from the lower atmosphere over the central eastern Atlantic. Geochim Cosmochim Acta 67:1757–1767. https://doi.org/10.1016/S0016-7037(02)01414-X

Schefuß E, Schouten S, Schneider RR (2005) Climatic controls on central African hydrology during the past 20,000 years. Nature 437:1003–1006. https://doi.org/10.1038/nature03945

Schimmelmann A, Sessions AL, Boreham CJ et al (2004) D/H ratios in terrestrially sourced petroleum systems. Org Geochem 35:1169–1195. https://doi.org/10.1016/j.orggeochem.2004.05.006

Schwark L, Zink K, Lechterbeck J (2002) Reconstruction of postglacial to early Holocene vegetation history in terrestrial Central Europe via cuticular lipid biomarkers and pollen records from lake sediments. Geology 30:463. https://doi.org/10.1130/0091-7613(2002)030%3c0463:ROPTEH%3e2.0.CO;2

Sen S, Naskar S, Das S (2016) Discussion on the concepts in paleoenvironmental reconstruction from coal macerals and petrographic indices. Mar Pet Geol 73:371–391. https://doi.org/10.1016/j.marpetgeo.2016.03.015

Sessions AL (2016) Factors controlling the deuterium contents of sedimentary hydrocarbons. Org Geochem 96:43–64. https://doi.org/10.1016/j.orggeochem.2016.02.012

Shotyk W (1988) Review of the inorganic geochemistry of peats and peatland waters. Earth Sci Rev 25:95–176. https://doi.org/10.1016/0012-8252(88)90067-0

Sia SG, Abdullah WH (2012) Geochemical and petrographical characteristics of low-rank Balingian coal from Sarawak, Malaysia: its implications on depositional conditions and thermal maturity. Int J Coal Geol 96–97:22–38. https://doi.org/10.1016/j.coal.2012.03.002

Sia SG, Abdullah WH, Konjing Z, Koraini AM (2014) The age, palaeoclimate, palaeovegetation, coal seam architecture/mire types, paleodepositional environments and thermal maturity of syn-collision paralic coal from Mukah, Sarawak, Malaysia. J Asian Earth Sci 81:1–19. https://doi.org/10.1016/j.jseaes.2013.11.014

Sia SG, Abdullah WH, Konjing Z, John J (2019) Floristic and climatic changes at the Balingian Province of the Sarawak Basin, Malaysia, in response to Neogene global cooling, aridification and grassland expansion. CATENA 173:445–455. https://doi.org/10.1016/j.catena.2018.10.044

Siavalas G, Linou M, Chatziapostolou A et al (2009) Palaeoenvironment of Seam I in the Marathousa Lignite Mine, Megalopolis Basin (Southern Greece). Int J Coal Geol 78:233–248. https://doi.org/10.1016/j.coal.2009.03.003

Silva TR, Lopes SRP, Spörl G et al (2012) Source characterization using molecular distribution and stable carbon isotopic composition of n-alkanes in sediment cores from the tropical Mundaú-Manguaba estuarine-lagoon system, Brazil. Org Geochem 53:25–33. https://doi.org/10.1016/j.orggeochem.2012.05.009

Sinninghe Damste JS, De Leeuw JW (1990) Analysis, structure and geochemical significance of organically-bound sulphur in the geosphere: state of the art and future research. Org Geochem 16:1077–1101. https://doi.org/10.1016/0146-6380(90)90145-P

Spears D (2017) The role of seawater on the trace element geochemistry of some UK coals and a tribute to Goldschmidt. Minerals 7:148. https://doi.org/10.3390/min7080148

Spears DA, Tewalt SJ (2009) The geochemistry of environmentally important trace elements in UK coals, with special reference to the Parkgate coal in the Yorkshire-Nottinghamshire Coalfield, UK. Int J Coal Geol 80:157–166. https://doi.org/10.1016/j.coal.2009.08.010

Stojanović K, Životić D (2013) Comparative study of Serbian Miocene coals: insights from biomarker composition. Int J Coal Geol 107:3–23. https://doi.org/10.1016/j.coal.2012.09.009

Stüben D, Kramar U, Berner ZA et al (2003) Late Maastrichtian paleoclimatic and paleoceanographic changes inferred from Sr/Ca ratio and stable isotopes. Palaeogeogr Palaeoclimatol Palaeoecol 199:107–127. https://doi.org/10.1016/S0031-0182(03)00499-1

Sykes R, Volk H, George SC et al (2014) Marine influence helps preserve the oil potential of coaly source rocks: Eocene Mangahewa Formation, Taranaki Basin, New Zealand. Org Geochem 66:140–163. https://doi.org/10.1016/j.orggeochem.2013.11.005

Sykes R (1994) Coal seams and peat-forming environments. In: Edbrooke SW, Sykes R, Pocknall DT (eds) Geology of the Waikato coal measures, Waikato Coal Region, New Zealand. pp 102–175

Thompson S, Cooper BS, Barnard PC (1994) Some examples and possible explanations for oil generation from coals and coaly sequences. Geol Soc Spec Publ 77:119–137. https://doi.org/10.1144/GSL.SP.1994.077.01.07

Tribovillard N, Algeo TJ, Lyons T, Riboulleau A (2006) Trace metals as paleoredox and paleoproductivity proxies: an update. Chem Geol 232:12–32. https://doi.org/10.1016/j.chemgeo.2006.02.012

van Aarssen BGK, Bastow TP, Alexander R, Kagi RI (1999) Distributions of methylated naphthalenes in crude oils: indicators of maturity, biodegradation and mixing. Org Geochem 30:1213–1227. https://doi.org/10.1016/S0146-6380(99)00097-2

van Aarssen BGK, Alexander R, Kagi RI (2000) Higher plant biomarkers reflect palaeovegetation changes during Jurassic times. Geochim Cosmochim Acta 64:1417–1424. https://doi.org/10.1016/S0016-7037(99)00432-9

Weiss HM, Wilhelms A, Mills N et al (2000) NIGOGA: the Norwegian Industry Guide to Organic Geochemical Analyses [online]. Edition 4.0

Weston RJ, Philp RP, Sheppard CM, Woolhouse AD (1989) Sesquiterpanes, diterpanes and other higher terpanes in oils from the Taranaki basin of New Zealand. Org Geochem 14:405–421. https://doi.org/10.1016/0146-6380(89)90006-5

Widodo S, Bechtel A, Anggayana K, Püttmann W (2009) Reconstruction of floral changes during deposition of the Miocene Embalut coal from Kutai Basin, Mahakam Delta, East Kalimantan, Indonesia by use of aromatic hydrocarbon composition and stable carbon isotope ratios of organic matter. Org Geochem 40:206–218. https://doi.org/10.1016/j.orggeochem.2008.10.008

Widodo S, Oschmann W, Bechtel A et al (2010) Distribution of sulfur and pyrite in coal seams from Kutai Basin (East Kalimantan, Indonesia): implications for paleoenvironmental conditions. Int J Coal Geol 81:151–162. https://doi.org/10.1016/j.coal.2009.12.003

Wilkins RWT, George SC (2002) Coal as a source rock for oil: a review. Int J Coal Geol 50:317–361. https://doi.org/10.1016/S0166-5162(02)00134-9

Xu H, George SC, Hou D (2019) Algal-derived polycyclic aromatic hydrocarbons in Paleogene lacustrine sediments from the Dongying Depression, Bohai Bay Basin, China. Mar Pet Geol 102:402–425. https://doi.org/10.1016/j.marpetgeo.2019.01.004

Yan G, Xu Y-H, Liu Y et al (2019) Evolution and organic geochemical significance of bicyclic sesquiterpanes in pyrolysis simulation experiments on immature organic-rich mudstone. Pet Sci 16:502–512. https://doi.org/10.1007/s12182-019-0326-6

Yeloff D, Mauquoy D (2006) The influence of vegetation composition on peat humification: implications for palaeoclimatic studies. Boreas 35:662–673. https://doi.org/10.1111/j.1502-3885.2006.tb01172.x

Yunker MB, Macdonald RW, Vingarzan R et al (2002) PAHs in the Fraser River basin: a critical appraisal of PAH ratios as indicators of PAH source and composition. Org Geochem 33:489–515. https://doi.org/10.1016/S0146-6380(02)00002-5

Zachos J, Pagani H, Sloan L et al (2001) Trends, rhythms, and aberrations in global climate 65 Ma to present. Science (80-) 292:686–693. https://doi.org/10.1126/science.1059412

Zainal Abidin NS, Mustapha KA, Abdullah WH, Konjing Z (2022) Paleoenvironment reconstruction and peat-forming conditions of Neogene paralic coal sequences from Mukah, Sarawak. Malays Sci Rep 12:8870. https://doi.org/10.1038/s41598-022-12668-6

Zakrzewski A, Kosakowski P, Waliczek M, Kowalski A (2020) Polycyclic aromatic hydrocarbons in Middle Jurassic sediments of the Polish Basin provide evidence for high-temperature palaeowildfires. Org Geochem 145:104037. https://doi.org/10.1016/j.orggeochem.2020.104037

Zheng Y, Zhou W, Meyers PA, Xie S (2007) Lipid biomarkers in the Zoigê-Hongyuan peat deposit: indicators of Holocene climate changes in West China. Org Geochem 38:1927–1940. https://doi.org/10.1016/j.orggeochem.2007.06.012

Zhou M, Zhao L, Wang X et al (2021) Mineralogy and geochemistry of the Late Triassic coal from the Caotang mine, northeastern Sichuan Basin, China, with emphasis on the enrichment of the critical element lithium. Ore Geol Rev 139:104582. https://doi.org/10.1016/j.oregeorev.2021.104582